

5-2017

Development of Novel Chemical Strategies to Modulate Biological Function

Diya M. Uthappa
College of William and Mary

Follow this and additional works at: <https://scholarworks.wm.edu/honorstheses>

 Part of the [Chemistry Commons](#)

Recommended Citation

Uthappa, Diya M., "Development of Novel Chemical Strategies to Modulate Biological Function" (2017). *Undergraduate Honors Theses*. Paper 1119.

<https://scholarworks.wm.edu/honorstheses/1119>

This Honors Thesis is brought to you for free and open access by the Theses, Dissertations, & Master Projects at W&M ScholarWorks. It has been accepted for inclusion in Undergraduate Honors Theses by an authorized administrator of W&M ScholarWorks. For more information, please contact scholarworks@wm.edu.

**DEVELOPMENT OF NOVEL CHEMICAL STRATEGIES TO MODULATE
BIOLOGICAL FUNCTION**

Diya Mapangada Uthappa
East Brunswick, New Jersey

A Thesis presented to
The College of William and Mary in Candidacy for the Degree of
Bachelor of Science

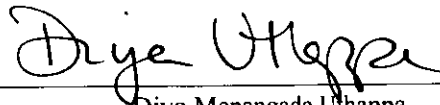
Department of Chemistry

The College of William and Mary
May 2017

APPROVAL PAGE

This Thesis is submitted in partial fulfillment of
the requirements for the degree of

Bachelor of Science



Diya Mapangada Uthappa

Approved by the Committee, April 2017



Committee Chair

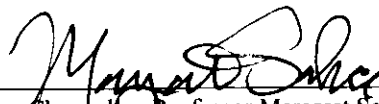
Assistant Professor Douglas Young, Chemistry
The College of William and Mary



Professor Paul Heideman, Biology
The College of William and Mary



Associate Professor Randolph Coleman, Chemistry
The College of William and Mary



Chancellor Professor Margaret Saha, Biology
The College of William and Mary

ABSTRACT

This research involves the development of novel chemical strategies to modulate biological function. This approach has taken multiple forms. First, the site-specific incorporation of unnatural amino acids (UAAs) was utilized to develop a novel labeling strategy. Further, the site-specific incorporation of a photocaged UAA was used to control protein activity. Next, solid-supported Glaser-Hay couplings were utilized to efficiently synthesize natural products and to create a library of polyynes, which are molecules containing multiple conjugated acetylenic units. These synthesized molecules were then screened for biological activities. Overall, this thesis discusses the development of these chemical strategies, which contribute additional levels of sophistication to proffer control over biological function. Studying mechanisms to control biological function is critical, as they have potential downstream medical applications in diagnosis, disease prevention, and disease treatment.

TABLE OF CONTENTS

Acknowledgements	ii
List of Figures	iii
List of Schemes	vi
List of Tables	vii
Chapter 1. Introduction to the Development of Bioconjugates	1
Chapter 2. Introduction to Unnatural Amino Acids and Site-Specific Unnatural Amino Acid Incorporation	7
Chapter 3. Site-Specific Incorporation of a Fluorescent Terphenyl Unnatural Amino Acid	16
Chapter 4. Photoregulation of Protein Arginine Methyltransferase 1 (PRMT1)	32
Chapter 5. Introduction to the Synthesis and Biological Significance of Asymmetric Polyynes	51
Chapter 6. Application of the Solid-Supported Glaser-Hay Reaction to Natural Product Synthesis	58
Chapter 7. Exploring the Properties of Polyynes	79

ACKNOWLEDGEMENTS

First, I would like to thank Dr. Doug Young for providing me with the incredible opportunity to do research in his lab. The experience gained has been extremely valuable to my development as a scientist. Thank you for guiding me through the Beckman Scholars program and for attending the Beckman Symposium with me for both years. Thank you for always being available to answer my questions and reassuring me that my results are “promising.” Thank you for your beautiful snapchats and daily dose of sarcasm. Overall, thank you for playing such an integral role in my college career and providing the best lab experience possible.

I would like to thank Johnathan Maza for introducing me to Young Lab in my sophomore year and for training me. Thank you for being a constant mentor and always being willing to help.

I would also like to thank Jess Lampkowski for laying the foundation for many of the projects I worked on during my undergraduate research career.

Additionally, I would like to thank Rachael Carlberg for her valuable assistance on the PRMT1 project.

Lastly, I would like to thank Chris Travis for reading, rereading, and editing my thesis. Your comma usage is superb and greatly appreciated. In addition, thank you for sitting through numerous practices of my astounding oral defense (and for teaching me that the word astounding is better written than spoken).

LIST OF FIGURES

1.1	Examples of Biocojugate Systems	1
1.2	Unnatural Amino Acids Involved in Bioconjugates	4
2.1	Twenty Canonical Amino Acids	7
2.2	Unnatural Amino Acids	9
2.3	The Genetic Code	10
2.4	Mechanism for Genetic Incorporation of Unnatural Amino Acids	12
2.5	Selection of an Aminoacyl-tRNA Synthetase that Recognizes and Incorporates a Specific Unnatural Amino Acid	14
3.1	Structures of Common Fluorophores Used in Biology	16
3.2	Structures of Fluorescent Unnatural Amino Acids	18
3.3	Aminoacyl-tRNA Synthetase Screen to Identify Previously Evolved Synthetases Capable of Recognizing the Terphenyl Unnatural Amino Acid	21
3.4	SDS-PAGE of GFP Expression with Cultures Containing the Terphenyl Unnatural Amino Acid	22
3.5	Crystal Structure of GFP with Key Residues Indicated	22
3.6	Emission Spectra of GFP Mutants Using a Wavelength of Excitation of 395 nm	23
3.7	Emission Spectra of GFP Mutants Using a Wavelength of Excitation of 300 nm	24
4.1	Structure and Function of PRMT1	33
4.2	Residues within the Catalytic Core of PRMT1	35

4.3	Mechanism of Photocaging	37
4.4	Structure of <i>Ortho</i> -nitrobenzyl Tyrosine (ONBY)	37
4.5	Photoregulation of PRMT1 Using a Photocaged UAA	38
4.6	SDS-PAGE of PRMT1 Expression with ONBY	40
4.7	General Schematic of G-Biosciences SAM 510 nm Methyltransferase Assay	41
4.8	Preliminary Absorbance Data Comparing the Activity of Wild Type PRMT1 and ONBY-Incorporated PRMT1	44
4.9	Comparison of Change between Irradiated and Non-Irradiated Wild Type PRMT1 and ONBY-Incorporated PRMT1	45
5.1	Natural Products Possessing Conjugated Acetylenic Units with Asymmetrical Terminal Groups	52
5.2	Glaser-Hay Coupling of Terminal Alkynes	53
6.1	High Density <i>E. coli</i> Viability Assay for Each Natural Product	63
6.2	Low Density <i>E. coli</i> Viability Assay for Each Natural Product	64
6.3	Summary of <i>E. coli</i> screens with Natural Products Prepared via the Solid-Supported Glaser–Hay Methodology	65
6.4	¹ H NMR of Dodeca-2,4-diyn-1-ol in CDCl ₃	69
6.5	GC trace of Dodeca-2,4-diyn-1-ol	69
6.6	¹ H NMR of Montiporic Acid A in CDCl ₃	70
6.7	GC trace of Montiporic Acid A	71
6.8	¹ H NMR of Octatriyn-1-ol in CDCl ₃	72
6.9	GC trace of Octatriyn-1-ol	72

6.10	¹ H NMR of Phenylhepta-2,4,6-triynyl Acetate in CDCl ₃	74
6.11	GC trace of Phenylhepta-2,4,6-triynyl Acetate	74
7.1	Initial Screening: Absolute Change in Cell Density Relative to Initial Absorbance	82
7.2	Time Course Tracking Change in Absorbance of the Top Hit Compounds	83
7.3	Specified Polyne Screen: Absolute Change in Cell Density Relative to Initial Absorbance	84
7.4	Polyynes with Nitrogenous Terminal Functionalities: Absolute Change in Cell Density Relative to Initial Absorbance	88
7.5	Growth Curve Comparisons for Non-Clinical Yeast Strains in Low Density Plates	90
7.6	Regrowth Curve Comparisons for Non-Clinical Yeast Strains	91
7.7	Growth Curve Comparisons for Clinical Yeast Strains in Low Density Plates	92

LIST OF SCHEMES

3.1	Synthesis of 4-biphenyl-L-phenylalanine	20
4.1	Synthesis of Protected ONBY	39
4.2	Deprotection of ONBY	39
5.1	Cadiot-Chodkiewicz Coupling Reaction	53
6.1	Synthesis of Montiporic Acid A	59
6.2	Synthesis of Octatriyn-1-ol	61
6.3	Synthesis of Phenylhepta-2,4,6-triynyl Acetate	62
7.1	Immobilization of Propargyl Amine onto Trityl Chloride Resin	85
7.2	Synthetic Route to Elongation of the Acetylenic Scaffold	86

LIST OF TABLES

4.1	List of Testing Conditions Employed Using G-Biosciences SAM 510 nm Methyltransferase Assay	42
7.1	Structures of Tested Polyynes	81
7.2	Series Containing Nitrogenous Terminal Functionality to be Synthesized	85
7.3	Percent Yield of Polyynes with Nitrogenous Terminal Functionality	87

CHAPTER 1: INTRODUCTION TO THE DEVELOPMENT OF BIOCONJUGATES

The preparation of well-defined bioconjugates is an emerging field that requires the integration of chemical tools into biological systems. The term bioconjugate encompasses a wide range of molecules; however, broadly defined, it is a covalent linkage between two molecules in which at least one of the linked molecules is a biomacromolecule (e.g. protein, DNA, RNA, etc.). Commonly, a bioconjugate system links a biomacromolecule with a secondary component (e.g. surface, small molecule, labeled probe, etc.) in order to confer novel functionalities on the system that facilitate in isolating or identifying the biomolecule (see Figure 1.1).^{1,2} Overall, the preparation of bioconjugate systems often leads to enhanced properties of the biomolecule. Therefore, bioconjugates have found utility in a wide range of applications including therapeutics, diagnostics, and materials.³⁻⁷ Consequently, the optimization of bioconjugation reactions remains at the forefront of science.

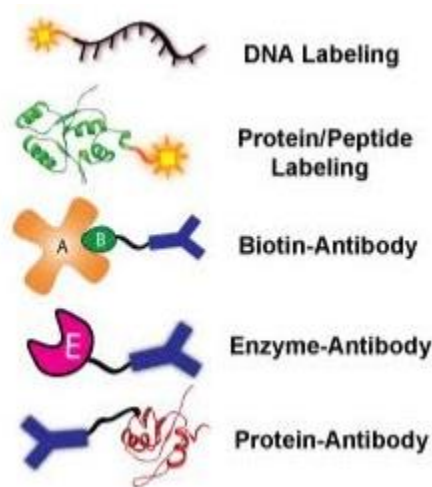


Figure 1.1 Examples of bioconjugate systems. The top three examples display bioconjugate systems in which a biomacromolecule is covalently linked to a secondary component, while the bottom two examples display bioconjugate systems consisting of two covalently linked biomacromolecules.

The design of a bioconjugate is intrinsically tied to its function, and many methodologies have been developed to prepare a variety of conjugates.⁸ Though covalent linkages form a robust connection between molecules, regulating the precise location of the covalent linkage is challenging as multiple sites within one molecule are often capable of binding covalently to multiple sites on the other molecule. Therefore, the ability to generate well-defined conjugates by regulating the bioconjugation site for covalent linkage is crucial to the development of functional bioconjugate systems. Regulating the site of covalent linkage allows for enhanced stability, increased sample homogeneity, and minimized perturbation of biological function of the biomacromolecule.⁸⁻¹³ However, due to the complex nature of many biomacromolecules, site-specific conjugations are often challenging and require additional manipulation of the biological system. First, the conjugation reaction must be compatible with physiological conditions (37 °C, pH ~7.2 to prevent degradation, which results in a loss of function. Second, due to the wide range of chemical functionality of biomolecules, especially proteins, the reaction must be bioorthogonal to maintain specificity.¹⁴ Finally, a mechanism must be established to control the location of the conjugation in order to prevent inactivation of the protein active site. All of these requirements have been overcome by bioorthogonal modifications. In particular, site-specific incorporation of a bioorthogonal unnatural amino acid (UAA) affords the researcher a greater degree of control over the precise location of the reaction within the protein.¹⁵

In addition to the site-specificity possible with their use, UAAs can be employed in a variety of chemical reactions in order to form covalent linkages with a secondary reaction partner (Figure 1.2). This versatility is enabled through the synthesis of UAAs with reactive functional groups capable of participating in a host of chemical reactions that result in the formation of a novel covalent bond. Therefore, site-specific incorporation of UAAs not only ensures a precise

location of the covalent linkage between binding partners, but also allows for versatility in the chemical reaction used to catalyze the covalent linkage.

Reaction	UAA	Linkage ^a	Rate ^b (M·s) ⁻¹
cycloaddition (CuAAC/SPAAC)			10–200
cycloaddition (CuAAC/SPAAC)			10 ⁻² –1
cycloaddition (SPIEDAC)			10 ³ –10
cycloaddition (SPIEDAC)			10 ³ –10
Claser-Hay			n.t. ^c

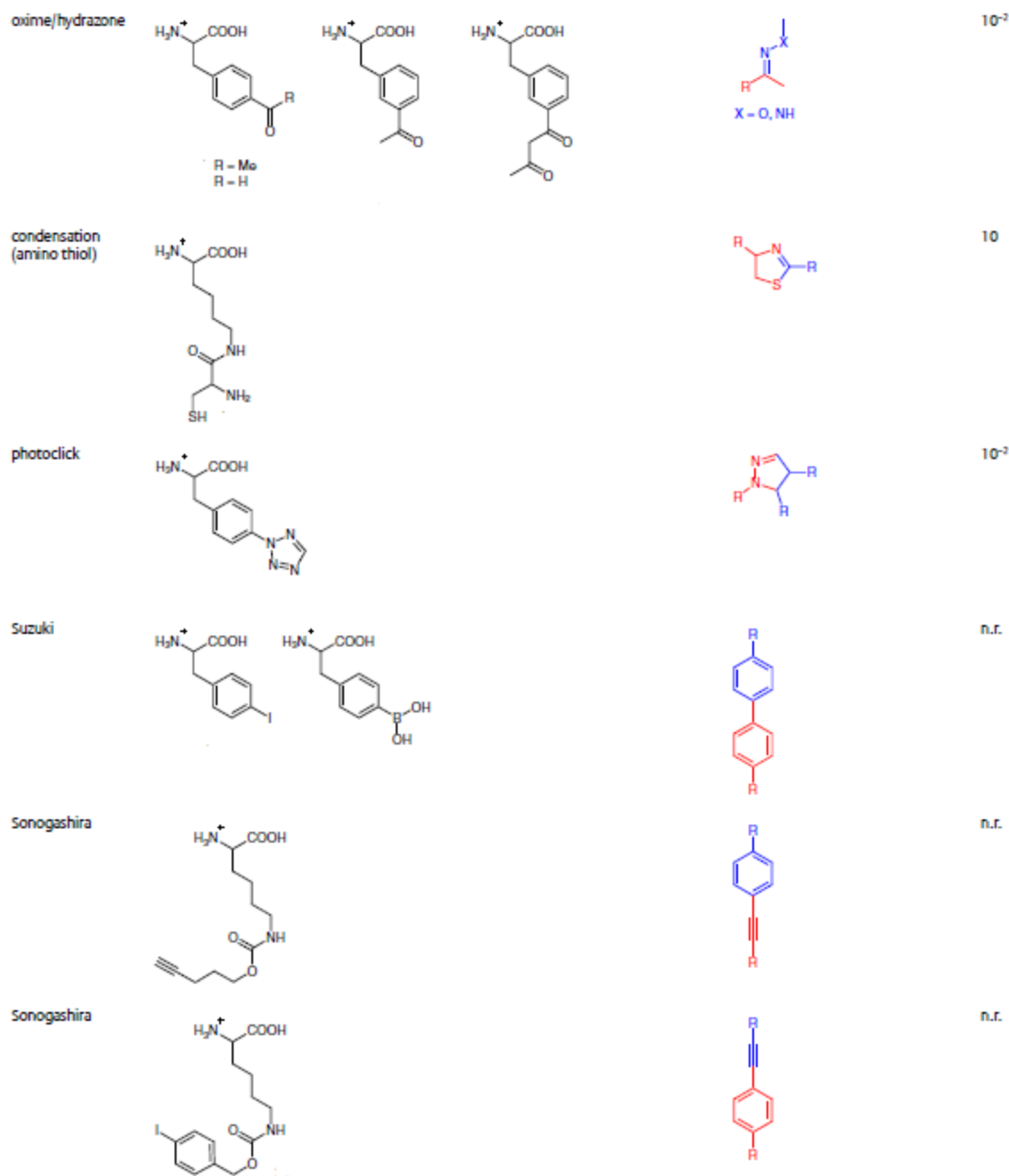


Figure 1.2 Unnatural amino acids involved in bioconjugates. The UAA components are shown in red and the reaction partner's components are shown in blue.

Herein, I will discuss the development of novel bioconjugate systems and their application to medicinal chemistry. Beginning with a discussion of site-specific incorporation of UAAs, I will highlight the use of UAAs in creating novel labeling strategies as well as the use of a photocaged

UAA in regulating protein activity. Next, I will move to discuss Glaser-Hay coupling of terminal alkynes. Though I will discuss the use of the solid-supported Glaser-Hay methodology in a non-protein context, study of the coupling of terminal alkynes is of use as it represents one of the key ways to successfully form a covalent linkage between bioconjugates. Here, the solid supported Glaser-Hay methodology has been employed to facilitate the synthesis of natural products as well as to create a library of polyynes, which are molecules containing multiple conjugated acetylenic units. Lastly, I will discuss the biological properties of the synthesized polyne compounds.

References

1. Hermanson GT. *Bioconjugate Techniques*. Academic Press; London; **1996**. 3rd ed.
2. Lang K, Chin J. *Chem. Rev.* **2014**; 114: 4764
3. Pasut G, Veronese F. *Polymer Therapeutics I. In Advances in Polymer Science*. Vol. 192. Satchi-Fainaro R, Duncan R. Springer; Heidelberg; 2006: 95
4. Boeneman K, Deschamps J, Buckhout-White S, Prasuhn D, Blanco-Canosa J, Dawson P, Stewart M, Susumu K, Goldman E, Ancona M, Medintz I. *ACS Nano*. **2010**; 4: 7253.
5. Thomas K, Sherman D, Amis T, Andaluz S, Pitner J. *Diabetes Technol. Ther.* **2006**; 8: 261.
6. Niemeyer C. *Angew. Chem. Int. Ed.* **2001**; 40: 4128
7. Allen T. *Nat. Rev. Cancer* **2002**; 2: 750
8. Stephanopoulos N, Francis M. *Nat. Chem. Biol.* **2011**; 7: 876
9. Ghosh S, Kao P, Mccue A, Chappelle H. *Bioconjugate Chem.* **1990**; 1: 71
10. Annunziato ME, Patel US, Ranade M, Palumbo PS. *Bioconjugate Chem.* **1993**; 4: 212
11. Johnson I. *Histochem. J.* **1998**; 30: 123
12. Lo K, Lau J, Ng D, Zhu N. *J. Chem. Soc., Dalton Trans.* **2002**; 1753
13. Gauthier MA, Klok HA. *Chem. Commun.* **2008**; 2591
14. Sletten E, Bertozzi C. *Angew. Chem. Int. Ed.* **2009**; 48: 6974
15. Kim CH, Axup JY, Schultz PG. *Curr. Opin. Chem. Biol.* **2013**; 17: 412

CHAPTER 2. INTRODUCTION TO UNNATURAL AMINO ACIDS AND SITE-SPECIFIC UNNATURAL AMINO ACID INCORPORATION

The diversity of processes catalyzed by proteins is astounding, leading to their designation as the workhorses of the cell.¹ Though the chemical capabilities of proteins are vast, the chemical functionalities of their building blocks are limited. The 20 endogenous, or canonical, amino acids represent only a few chemical functionalities and utilize just five of the 118 elements found on the periodic table (Figure 2.1).^{2,3} Within these confines, the multitude of functions and activities performed by proteins is incredible.

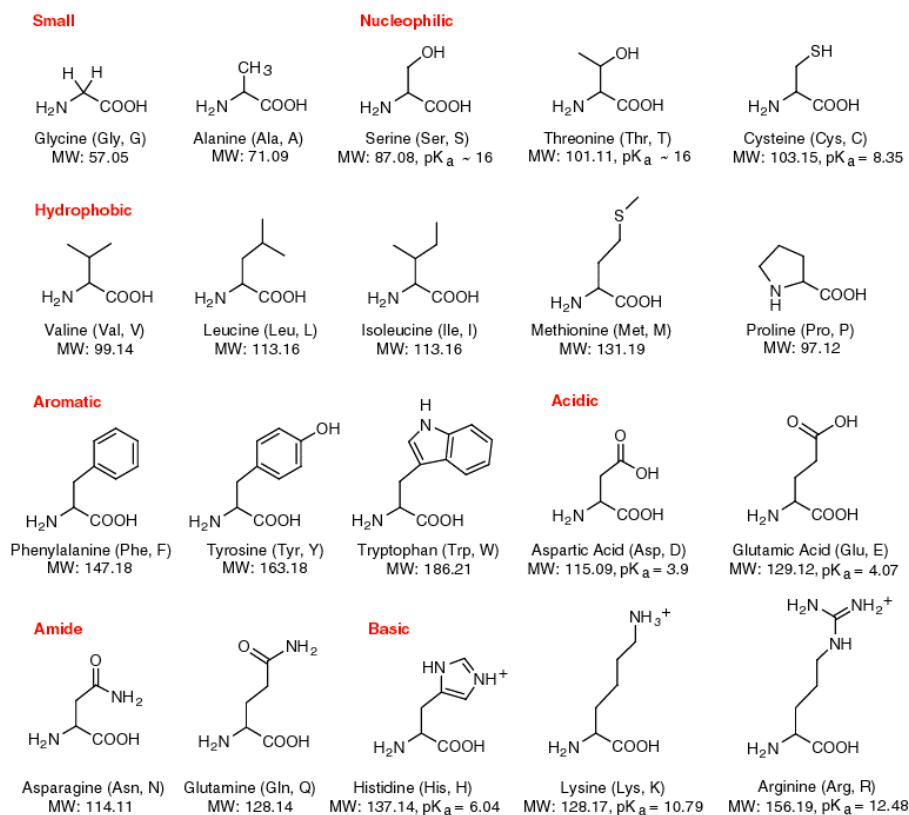


Figure 2.1 There are 20 naturally occurring amino acids. The canonical amino acids possess limited chemical functionality and contain just five of the elements. Adapted from chemwiki.ucdavis.edu

Unnatural Amino Acids

Unnatural amino acids (UAAs) provide a counter to the limited functionalities of the canonical amino acids and can be used to introduce novel chemistries into biological systems, thus expanding the scope of protein function.^{2,4} R-group modification of a standard AA residue ultimately allows for the synthesis of a UAA with a chemical functional group not found within the 20 standard AAs.

UAA synthesis can be easily accomplished as protecting groups can mask the carboxyl and amino ends, leaving only the R-group to be chemically modified. The research presented here modulated the phenol functionality of tyrosine in order to create novel derivatives. To do so, the phenol functionality of the amino acid was activated by the addition of a base, leaving the deprotonated hydroxyl group to participate in nucleophilic substitution reactions with molecules possessing good leaving groups. In this way, UAAs can be designed to possess unique functional moieties including, but not limited to, alkynes, azides, fluorophores, and photocleavable groups (Figure 2.2). Overall, UAAs offer a unique way to introduce novel biochemical functionalities into proteins.

is used in place of thymine (T). A gene is a sequence of DNA nucleotides that encodes a gene product, such as protein. The DNA nucleotides are grouped into sets of three, with each unique set of three nucleotides (a codon) corresponding to a specific AA. The genetic code specifies the AA that corresponds to a specific codon (Figure 2.3).

		SECOND POSITION				
		U	C	A	G	
FIRST POSITION (5' END)	U	Phe	Ser	Tyr	Cys	U
		Phe	Ser	Tyr	Cys	C
		Leu	Ser	Stop	Stop	A
		Leu	Ser	Stop	Trp	G
	C	Leu	Pro	His	Arg	U
		Leu	Pro	His	Arg	C
		Leu	Pro	Gln	Arg	A
		Leu (Met)*	Pro	Gln	Arg	G
	A	Ile	Thr	Asn	Ser	U
		Ile	Thr	Asn	Ser	C
		Ile	Thr	Lys	Arg	A
		Met (Start)	Thr	Lys	Arg	G
	G	Val	Ala	Asp	Gly	U
		Val	Ala	Asp	Gly	C
		Val	Ala	Glu	Gly	A
		Val (Met)*	Ala	Glu	Gly	G

Figure 2.3 The genetic code indicates which codons code for specific amino acids or stop codons.

The genetic code is both redundant and specific. There are 64 codons but only 20 endogenous AAs. Each AA may correspond to multiple codons, but each codon is specific to only one amino acid. Of the 64 codons, three are denoted stop codons. These three codons, TAG, TGA, and TAA, do not code for an AA but rather signal the end of translation. Redundancy within the stop codons can be exploited for use in site-specific UAA incorporation.

Site-Specific UAA Incorporation

UAAs can be incorporated into proteins by utilizing and hijacking the endogenous mechanism of protein synthesis. Use of the Schultz methodology for site-specific UAA

incorporation requires three components: an orthogonal aminoacyl-tRNA synthetase (aaRS), an orthogonal tRNA-codon pair, and an unnatural amino acid.⁴ This method of site-specific UAA incorporation capitalizes on the degeneracy of the genetic code, specifically the multiplicity of stop codons.

Since they do not code for AAs, stop codons can be manipulated to code for the UAA of interest. To do so, the gene of a protein must be mutated to change a specific preexisting codon to a stop codon at the precise location where the UAA is to be incorporated.^{5,6} However, in order for translational readthrough to be successful and for a UAA to be incorporated at the suppressed stop codon, there must exist an aaRS/tRNA pair capable of recognizing the UAA and the suppressed codon.

aaRSs catalyze the linkage of an AA to the appropriate tRNA, and each of the 20 aaRSs is responsible for charging one specific AA to all the tRNAs that encode it.¹ There is no cross-reactivity between synthetases. Therefore, endogenous synthetases will not recognize the UAA. UAA incorporation requires access to an additional aaRS/tRNA pair outside of those which occur endogenously. This is accomplished by importing and evolving an aaRS/tRNA pair from another organism, in this case the archaea *Methanocaldococcus jannaschii*.⁷ The orthogonal aaRS/tRNA pair is analogous in structure and function to those that occur endogenously but does not interfere with the endogenous machinery. Rather, the pair aids in accomplishing translational readthrough of the suppressed amber stop codon and the subsequent site specific incorporation of the UAA (Figure 2.4).^{3,8}

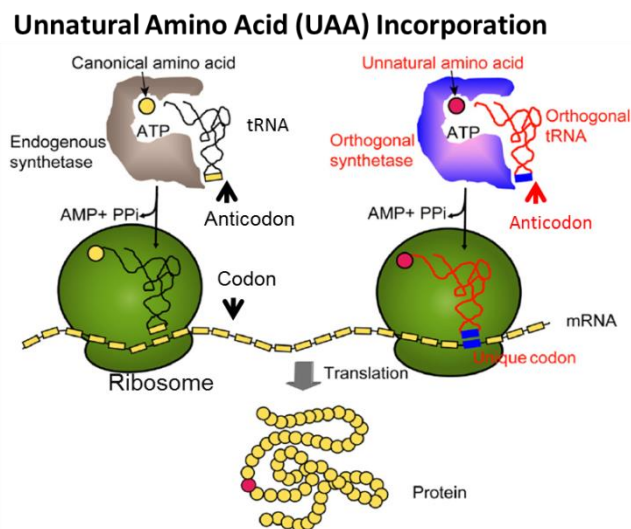


Figure 2.4 UAA Incorporation provides a mechanism to introduce novel chemistry not found in the 20 canonical amino acids into biological systems. Unnatural amino acids can be synthesized in a lab and incorporated into a protein site-specifically through the use of the amber stop codon TAG. Adapted from *Chem. Biol.* **2009**, *16*, 323-336.

The specificity of the evolved aaRS for the UAA was achieved through a double-sieve selection. First, using the *M. jannaschii* tyrosine aaRS, a library of 10^6 to 10^7 mutant aaRSs are created through genetic mutations which change five to six residues within the binding pocket.⁹ Changing the binding pocket residues alters its chemical environment and subsequently changes the aaRS's substrate binding affinity. Next, a series of positive and negative selections are performed in order to elucidate an aaRS suitable to selectively bind and incorporate only the UAA of interest. With the library in hand, a cycle of positive selection can be completed. To do so, *E. coli* are co-transformed with the library of mutated aaRSs and a chloramphenicol-degrading enzyme mutated to possess a TAG mutation. Following transformation, the cells are plated in the presence of both the UAA of interest and chloramphenicol. Though any cell growth indicates proper translation of the chloramphenicol-degrading enzyme, this cannot be solely attributed to incorporation of the UAA, as mutations in the aaRS binding site could have enabled charging a

canonical amino acid to the suppressor tRNA. Therefore, a series of negative selection, selection done in the absence of the UAA, must be performed to eliminate aaRSs which do not selectively bind the UAA. To do so, the plasmids from the cells grown during positive selection are isolated and purified and then transformed for negative selection. Additionally, negative selection necessitates co-transformation of the previously isolated plasmids with the toxic barnase gene, mutated to possess three TAG codons. Barnase is a bacterial ribonuclease that causes cell death by inhibiting protein synthesis through degradation of cellular RNA. Since the transformed cells are grown in the absence of the UAA, cells that are still able to suppress the TAG codons within the mutated barnase gene must be doing so through aaRSs that pair endogenous amino acids to the suppressor tRNA. Such cells successfully translate the barnase protein and die, allowing researchers to use this negative selection to eliminate aaRS which are able to successfully suppress TAG codons through the use of an endogenous amino acid. Multiple rounds of positive and negative selection are performed in order to ensure the identification of an aaRS/tRNA pair that selectively incorporates the UAA (Figure 2.5).

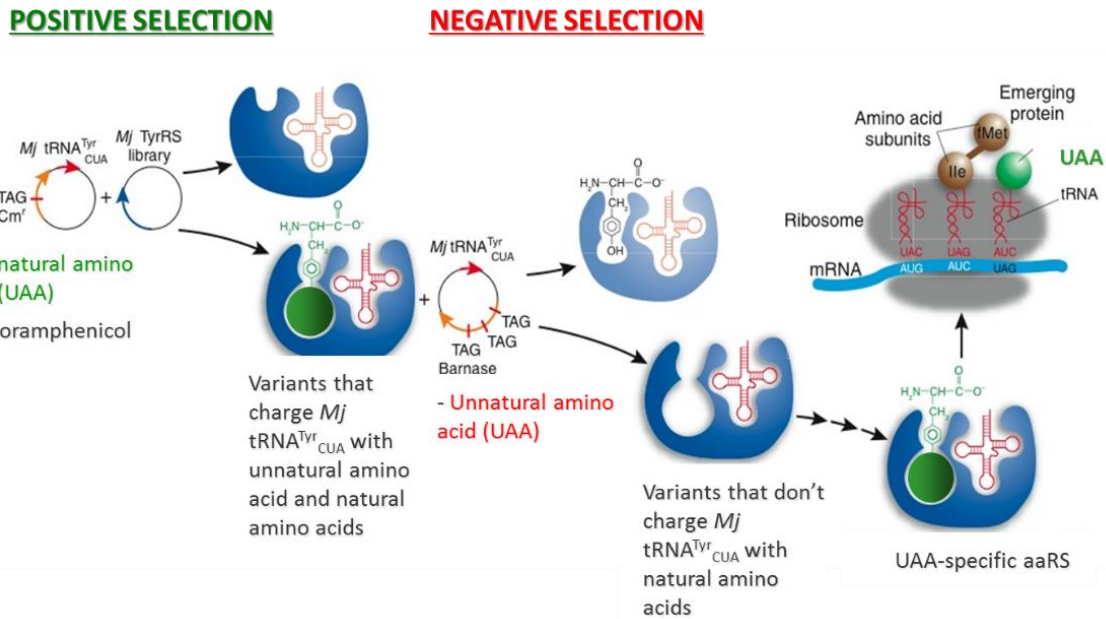


Figure 2.5 Double-sieve selection is employed to evolve an aminoacyl-tRNA synthetase selective for an UAA.

Site-specific incorporation of an UAA can be readily accomplished through this clever methodology that capitalizes on the endogenous protein synthesis mechanism and its involved machinery. Through site-specific UAA incorporation, proteins can be modified in highly specific ways that allow for the addition of novel chemical functionalities with limited disruption of the protein's normal function. In the next few sections, site-specific UAA incorporation will be employed in the creation of novel labeling strategies as well as in the controlled-regulation of protein activity.

References

1. Lodish. Molecular cell biology. 7th ed. Mac Higher; 2013
2. Liu, C. C. & Schultz, P. G. Adding new chemistries to the genetic code. *Annu. Rev. Biochem.* **79**, 413–444 (2010).
3. Young, T. S. & Schultz, P. G. Beyond the canonical 20 amino acids: Expanding the genetic lexicon. *J. Biol. Chem.* **285**, 11039–11044 (2010).
4. Wang, L., Xie, J. & Schultz, P. G. Expanding the genetic code. *Annu. Rev. Biophys. Biomol. Struct.* **35**, 225–249 (2006).
5. Cornish, V. W. & Schultz, P. G. Mutagenesis an. (1995).
6. Martin, a B. & Schultz, P. G. Opportunities at the interface of chemistry and biology. *Trends Cell Biol.* **9**, M24–M28 (1999).
7. Wang, L., Brock, A., Hererich, B. & Schultz, P. G. Expanding the genetic code of E. Coli. *Science* **292**, 498–500 (2001).
8. Mehl, R. a. *et al.* Generation of a bacterium with a 21 amino acid genetic code. *J. Am. Chem. Soc.* **125**, 935–939 (2003).
9. Wang, L. & Schultz, P. G. A general approach for the generation of orthogonal tRNAs. *Chem. Biol.* **8**, 883–890 (2001).

CHAPTER 3: SITE-SPECIFIC INCORPORATION OF A FLUORESCENT TERPHENYL UNNATURAL AMINO ACID

Introduction

The use of unnatural amino acids (UAAs) has allowed for expansion of the genetic code by facilitating the production of modified proteins with novel functionalities.¹⁻³ The incorporation of UAAs into proteins provides a means to better study protein function and structure both *in vitro* and *in vivo*. To date, a wide range of chemical functionalities have been introduced into proteins via UAAs including, azides, alkynes, fluorophores, photosensitive moieties, and metal binders.⁴⁻¹¹ Specifically, modifying proteins with fluorescent probes provides the ability to examine the structure and function of proteins as well as the ability to visualize their cellular location via fluorescence spectroscopy.¹² Numerous fluorescent probes have been utilized within a protein context to further advance our understanding of proteins. Different fluorophores possess unique spectral properties for different applications, and thus the generation of multiple fluorophore labels is advantageous as it allows for adaptation to the needs of the experiment (Figure 3.1).¹³⁻¹⁵

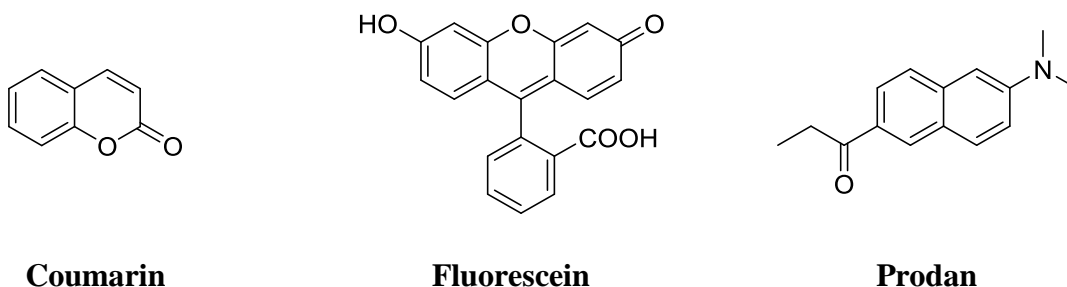


Figure 3.1 Structures of common fluorophores used in biology. Coumarin dyes are often used to provide contrast and depending on the number of charged moieties associated with the general structure, can be either cell permeable or cell impermeable. Fluorescein is a bright green fluorophore that is sensitive to changes in pH. Prodan is a fluorophore used to study membrane surface properties.

Consequently, we aim to investigate the incorporation of a fluorescent terphenyl UAA into *Escherichia coli* utilizing an orthogonal tRNA/aminoacyl-tRNA synthetase (aaRS) methodology.

The introduction of fluorescent probes into proteins can be accomplished through a variety of mechanisms. Perhaps the simplest means involves the chemical modification of a protein with a synthetic fluorophore post-translational. However, this method may be limited due to low availability of reactive surface residues as well as non-specific labeling with limited control over the location of fluorophore modification or the number of residues modified.¹⁶⁻²⁰ Another methodology includes the use of chemically mis-acylated suppressor tRNAs to incorporate UAAs. This methodology, however, affords limited yields of protein and is limited to easily accessible positions on the protein.²¹⁻²³

In order to alleviate these limitations, we aim to utilize an orthogonal tRNA and aminoacyl-tRNA synthetase (aaRS) pair that has previously been developed to incorporate a desired UAA through suppression of the amber codon.¹ This methodology is advantageous in that it affords the site-specific incorporation of UAAs. Due to the high selectivity of this approach, we hypothesized that using an aaRS/tRNA system to successfully incorporate a fluorescent UAA would prove to be more advantageous than other methodologies.² Typically this approach requires a double-sieve selection of an aaRS mutant library to identify a mutant aaRS capable of both recognizing the desired UAA and charging the corresponding orthogonal tRNA.^{3,24} This approach has already been employed to genetically incorporate several fluorescent UAAs, including 1-(7-hydroxycoumarin-4-yl) ethyl glycine (CouA), 2-amino-3(5-dimethylamino)naphthalene-1-(sulfonamide)propanoic acid (DansA), and 6-propionyl-2-(N,N-dimethyl)-aminonaphthalene (Anap) (Figure 3.2).

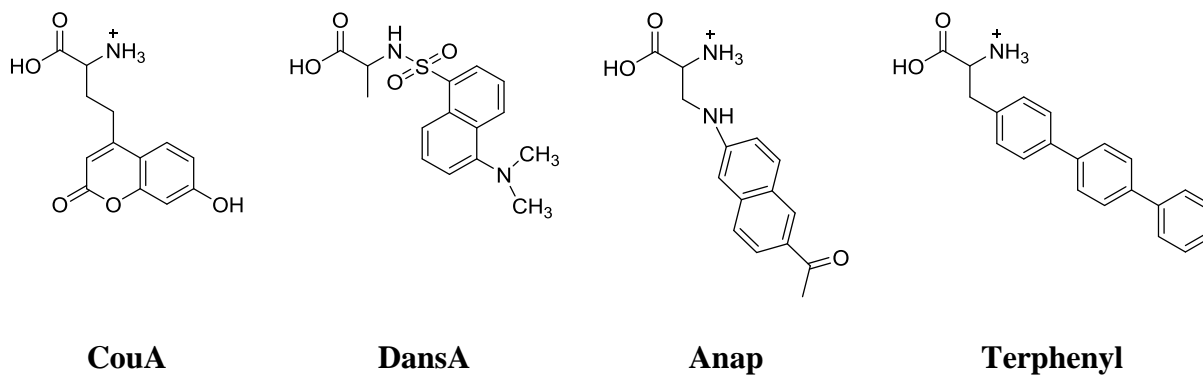


Figure 3.2 Structures of fluorescent unnatural amino acids. From left to right: *l*-(7-hydroxycoumarin-4-yl) ethyl glycine (CouA), 2-amino-3(5-dimethylamino)naphthalene-1-(sulfonamide)propanoic acid (DansA), 6-propionyl-2-(*N,N*-dimethyl)-aminonaphthalene (Anap), as well as 4-biphenyl-*L*-phenylalanine we seek to synthesize (**4**; Terphenyl).

These fluorescent UAAs have been employed in the cellular imaging of several proteins to identify various properties, such as cellular location and protein unfolding. However, expanding the fluorescent genetic code with new UAAs harboring different spectral properties may provide additional advantages. Specifically, we aimed to identify an aaRS capable of incorporating a terphenyl UAA into green fluorescent protein (GFP) in order to further enhance fluorescence activity and probe protein structure.

The terphenyl fluorophore represents an interesting π -conjugated molecule which can be used in biological applications. Characterization studies of terphenyl and other conjugated systems were performed to demonstrate their unique photophysical properties. Terphenyl moieties have high lifetimes ($\Phi_t = 0.49$; $\tau = 4.38$ ns) and novel emission spectra ($\lambda_{\text{ex}}\lambda_{\text{em}} = 280/342$ nm).²⁵ Moreover, these moieties have been found to be sensitive to environmental conditions including solvent.²⁶ Consequently, the terphenyl fluorophore has been utilized in a variety of applications including two-photon laser scanning microscopy,^{27,28} femtosecond fluorescence spectroscopy,²⁹

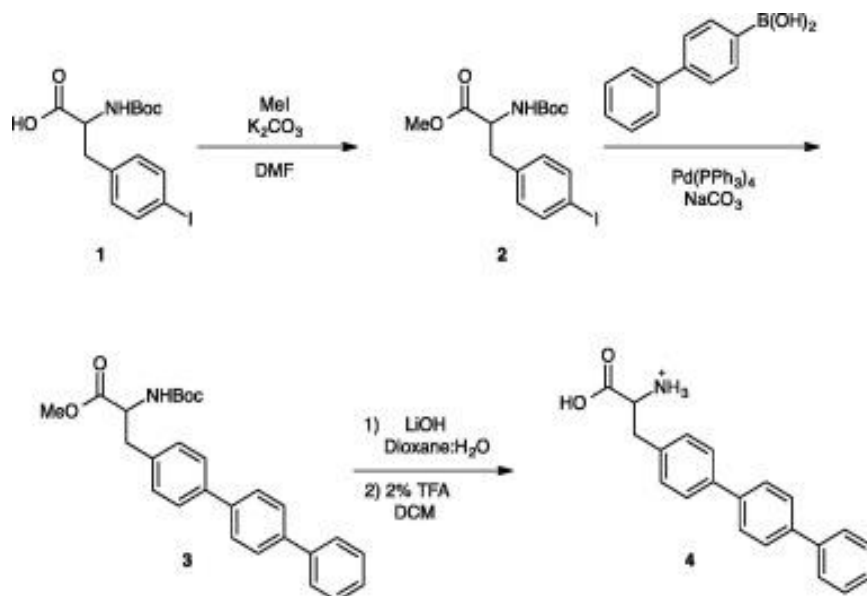
and α -helical secondary structure investigations.³⁰ These studies have facilitated the expanded knowledge of charge transfer, isomerization and protein dynamics within biological systems.

Incorporating a terphenyl UAA as a fluorescent probe into protein is beneficial in that the terphenyl is of relatively small size and allows for conformational mobility within a protein structure. Recently, various terphenyl derivatives have been incorporated into dihydrofolate reductase (DHFR) from *E. coli* for FRET fluorescence studies.^{31,32} These studies utilized a chemically acylated tRNA methodology, requiring extra synthetic manipulations which contribute to lower protein yields. Excitingly, the incorporation of a terphenyl UAA provided a means to measure changes in protein conformations and also provided further knowledge of protein dynamics. When chemically incorporated, these derivatives did not result in any loss of functional catalytic activity of DHFR.³¹ Moreover, they also afforded rotational flexibility within protein folding patterns due to the biphenyl bonding associated with their structures. These studies truly demonstrate the utility of this novel amino acid. Consequently, we aim to facilitate the increased utilization of this UAA via its complete genetic incorporation.

Results and Discussion

In order to assess the feasibility of the approach, the fully deprotected 4-biphenyl-L-phenylalanine (**4**) was synthesized from conditions adapted from the literature (Scheme 3.1).³² The synthesis was initiated with the esterification of N-Boc-4-iodo-L-phenylalanine (**1**) to generate the protected methyl ester (**2**) in good yield (90%). A Suzuki coupling was then employed with 4-biphenylboronic acid to yield the protected terphenyl unnatural amino acid (**3**). Finally, the protection groups were removed in a 2-step process to afford the fully deprotected 4-biphenyl-L-phenylalanine (**4**) in quantitative yield.

Scheme 3.1 Synthesis of 4-biphenyl-L-phenylalanine.



Following the synthesis of **4**, site-specific incorporation into a protein was attempted. Unlike previous approaches involving the chemical aminoacylation of tRNA, we attempted to identify an aminoacyl t-RNA synthetase (aaRS) capable of both recognizing **4** and charging it onto the appropriate tRNA. Based on previous findings that some previously evolved aaRSs demonstrate a degree of polyspecificity, an aaRS screen was undertaken with known polyspecific synthetases to alleviate the potential necessity of an aaRS selection.³³ Several synthetases were selected due to either known polyspecificity or their incorporation of structurally similar UAAs. Specifically, we tested the *p*-cyanophenylalanine (*p*CNF) aaRS, the naphthylalanine (NapA) aaRS, and the *p*-benzoylphenylalanine aaRS. Plasmids encoding the aaRS and tRNA were co-transformed into BL21 (DE3) *E. coli* with a pET-GFP-TAG-151 plasmid, harboring the TAG codon at position 151. Following protein expression, GFP fluorescence was measured using a BioTek multiplate reader and expression cultures grown in the presence and absence of **4** were compared (Figure 3.3). Gratifyingly, a differential was observed for cultures containing either the well documented polyspecific *p*CNF aaRS, or the NapA aaRS (which encodes the fluorescent

naphthylalanine UAA).^{11,34} To confirm the actual incorporation of **4**, expressions were repeated and the GFP mutant was purified using a Ni-NTA resin and then analyzed by gel electrophoresis and mass spectrometry (Figure 3.4). Expressions employing the *p*CNF aaRS occasionally yielded an unknown higher molecular weight band in conjunction with the desired GFP. Consequently, the NapA aaRS was used for further protein expressions to alleviate the need for additional protein purification, despite a slightly decreased protein yield.

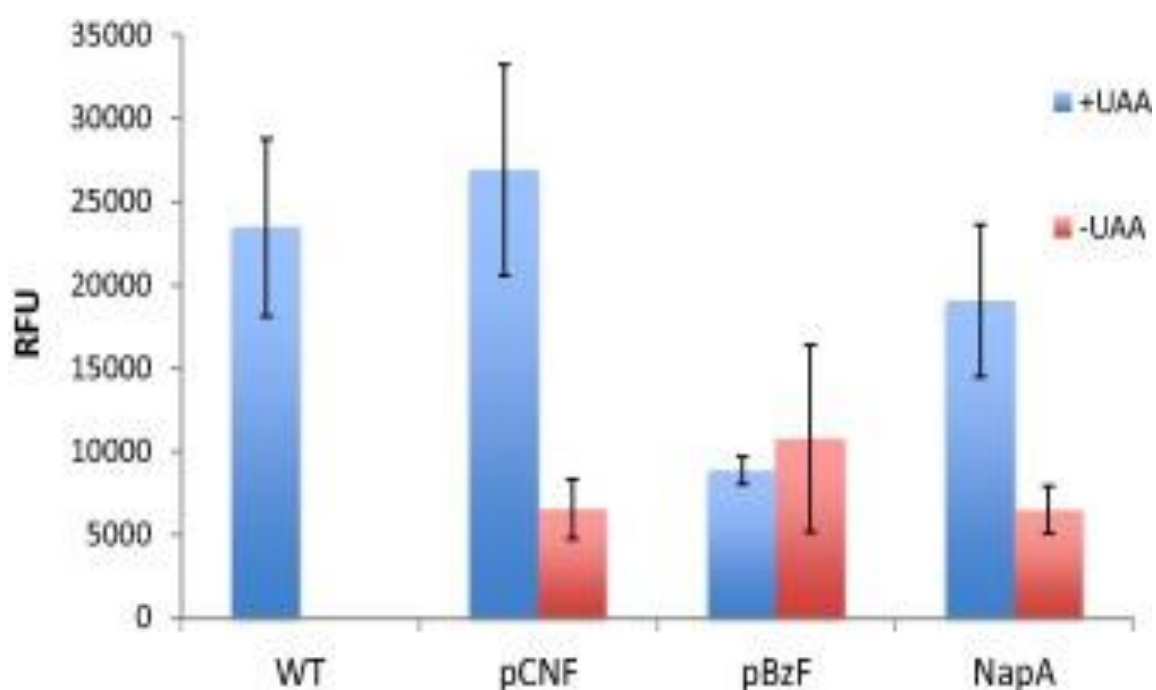


Figure 3.3 Initial aaRS screen to identify previously evolved aminoacyl-tRNA synthetases capable of recognizing **4**. Culture containing different synthetases and a GFP-151TAG were grown in the presence and absence of **4**. Fluorescence indicates functional GFP protein, and thus successful incorporation of **4**.

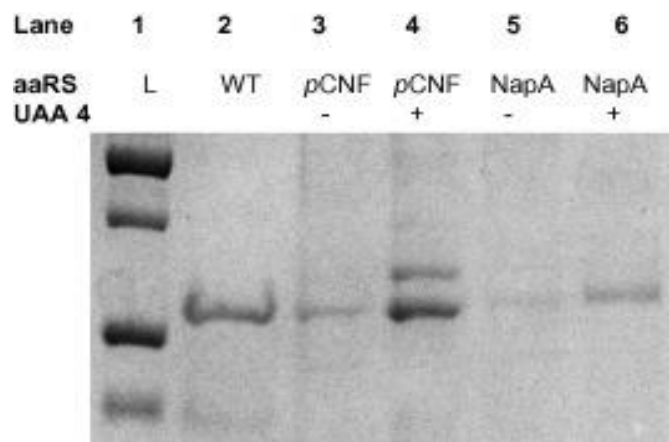


Figure 3.4 SDS-PAGE of GFP expression with cultures containing **4**. Confirmation of the aaRS screen was achieved with the pCNF aaRS and the NapA aaRS displaying differential protein expression in the presence and absence of **4**. Some background activity in the absence of **4** was detected for the pCNF aaRS as previously reported in the literature.

The fluorescent UAA **4** was next incorporated into GFP at multiple residues to probe for environmental alterations in fluorescence and overall effect on the protein. Residues, 3, 66, 133, and 151 were selected in the study due to their varied structural components (Figure 3.5).

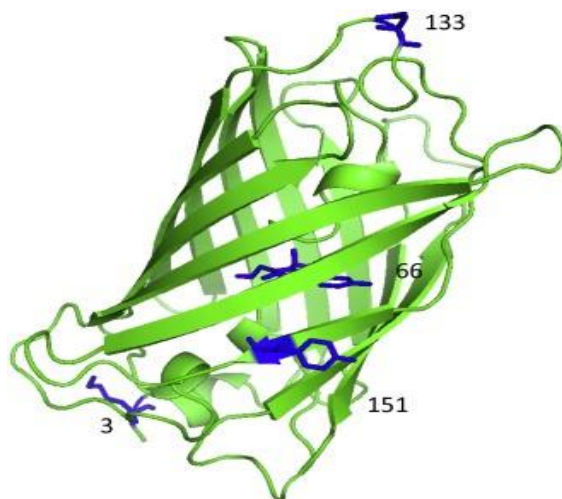


Figure 3.5 Crystal structure of GFP with the sites of **4** indicated in blue (PDB ID: 1EMA).

Residue 3 is at the N-terminus of the protein in a non-structured loop; residue 66 comprises a key member of the normal GFP fluorophore; residue 133 is on a more structured loop opposite

of residue 3; residue 151 is at the terminus of a β -sheet that comprises the β -barrel of the protein and is most rigid. When examining the fluorescent mutants containing **4** by excitation at 395 nm, the UAA has a dramatic effect on the overall spectra based on its position (Figure 3.6). Relative to the wild-type protein containing no UAA, an approximate 3 nm red-shift is observed for all spectra. Moreover, the ~512 nm emission corresponding to the deprotonated tyrosine residue 66 in the core fluorophore is impacted by the presence of **4**, especially in relation to the protonated ~455 nm emission. When located at the rigid 151 position, little change in ratio of the two states is detected relative to the wild type protein. However, at the more flexible positions, the presence of **4** tends to favor the protonated state relative to the deprotonated fluorophore, signifying a structural change in the overall protein that alters the pK_a of tyrosine 66. Moreover, the placement of **4** at that key residue eliminates the ~512 nm emission as an acidic proton is no longer present within the fluorophore.

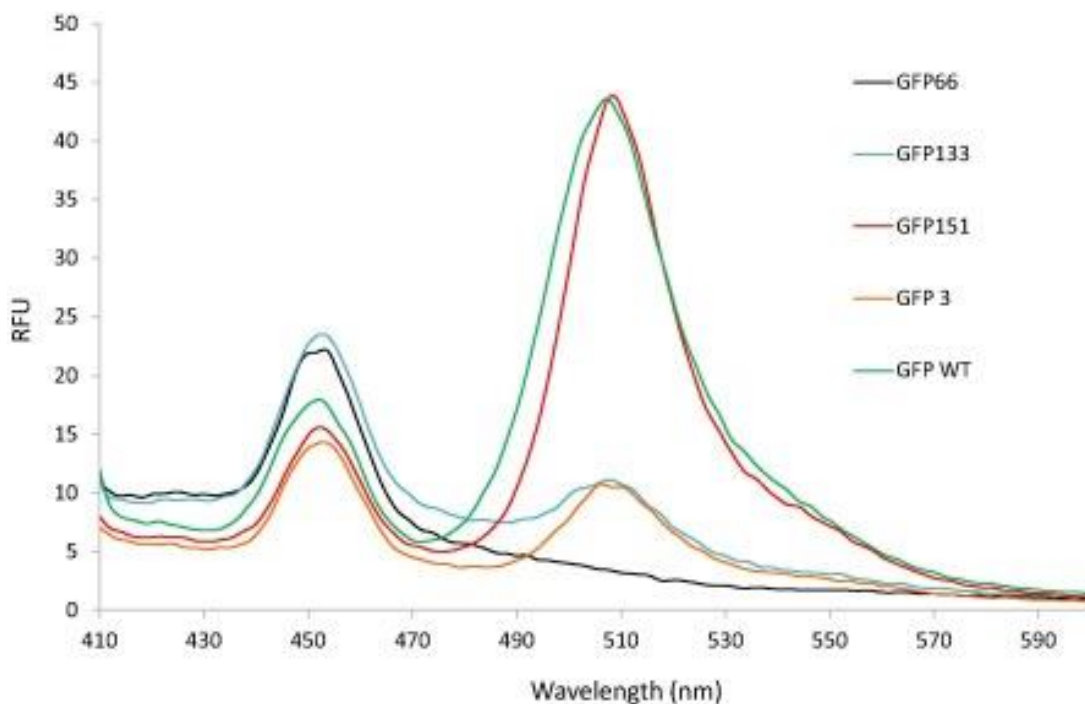


Figure 3.6 Emission spectra of GFP mutants harboring **4** at different residues. Each protein was excited at 395 nm and fluorescence emission was recorded.

In addition to the alterations in the typical GFP fluorescence, the terphenyl fluorophore is also detectable within the protein when exciting at 300 nm (Figure 3.7). While some natural fluorophore emission is present at this wavelength, the terphenyl moiety can be observed with a broadened, blue-shifted, and more intense emission. Moreover, when **4** is incorporated into the fluorophore a more dramatic blue-shift is observed, and the emission intensity doubles. Thus, the incorporation of **4** has the potential to dramatically alter the photo-physical behavior of the GFP protein and provide a mechanism to tune protein fluorescence.

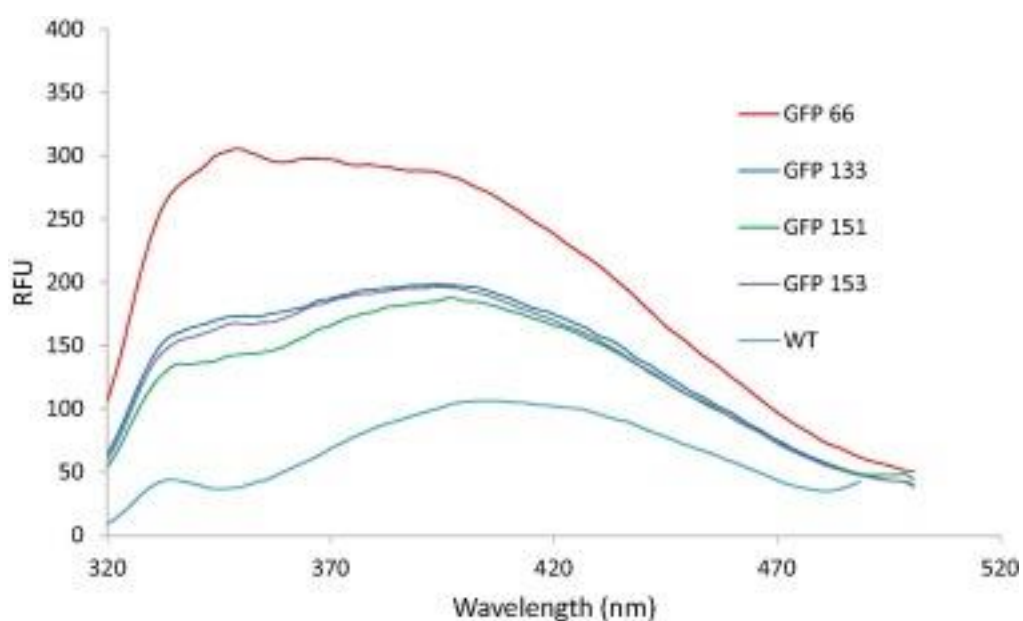


Figure 3.7 Fluorescence emissions spectra of GFP mutants harboring **4** at different residues. Each protein was excited at 300 nm and the fluorescence emission was recorded.

Conclusion

In conclusion, the ability to utilize bacterial translational machinery to incorporate fluorescent UAAs in a site-specific fashion in vivo affords both the production of mutant proteins as well the ability to probe their properties. The incorporation of a 4-biphenyl-L-phenylalanine into GFP has been demonstrated to dramatically alter its spectral properties. Additionally, the location of the UAA has been shown to impact the protonation state of the fluorophore, potentially

expanding the utility of the protein as a biosensor. Future work is underway towards utilizing the *in vivo* site-specific methodology towards the incorporation of the fluorescent UAA into other protein systems to provide a probe for protein function.

Experimental

General. Solvents and reagents were obtained from either Sigma-Aldrich or Fisher Scientific and used without further purification, unless noted. Reactions were conducted under ambient atmosphere with non-distilled solvents. NMR data was acquired on a Varian Gemini 400 MHz. Fluorescence data was measured using a PerkinElmer LS 55 Luminescence Spectrometer. All GFP proteins were purified according to manufacturer's protocols using a Qiagen Ni-NTA Quik Spin Kit. Samples were analyzed on an Agilent 6520 Accurate-Mass Quadrupole-Time-of-Flight (Q-TOF) mass spectrometer equipped with an electrospray (ESI) ionization source and liquid chromatography (LC) (Agilent). Ionization settings were: positive mode; capillary voltage 3500 kV; fragmentor voltage 200 V; drying gas temperature 350 °C. Instrument was set to standard 2 GHz, extended dynamic range and deconvolution was performed by Agilent MassHunter Qualitative Analysis software using the maximum entropy setting. To separate analyte a 2.1x150 mm, C8 reverse phase, wide pore (5 µm, 300 Å, Phenomenex) column was used with a water (A)/acetonitrile (B) (0.1% formic acid) gradient (2% B for 3 min, followed by a 2-95% B gradient over 15 min, and 95% B for 7 min).

Synthesis of N-(tert-butoxycarbonyl)-4-iodo-L-phenylalanine methyl ester (2). To a solution of Boc-Phe(4-I)-OH (500 mg, 1.3 mmol) in 10 mL DMF was slowly added NaHCO₃ (323 mg, 3.8 mmol, 3 eq). Methyl iodide (97 µL, 1.9 mmol, 1.5 eq) was then added to the mixture and the reaction was allowed to stir under argon for 24 hours at 60 °C. The cooled reaction mixture was then extracted and washed with water and EtOAc (3 x 20 mL). The organic layer was dried with MgSO₄ and the solvent was removed *in vacuo* to leave a yellow, oily solid. This product was then purified via silica gel chromatography with an gradient elution hexanes:EtOAc (3:1 → 1:1).

N-(*tert*-butoxycarbonyl)-4-iodo-L-phenylalanine methyl ester was obtained as a white solid (466 mg, 90%).

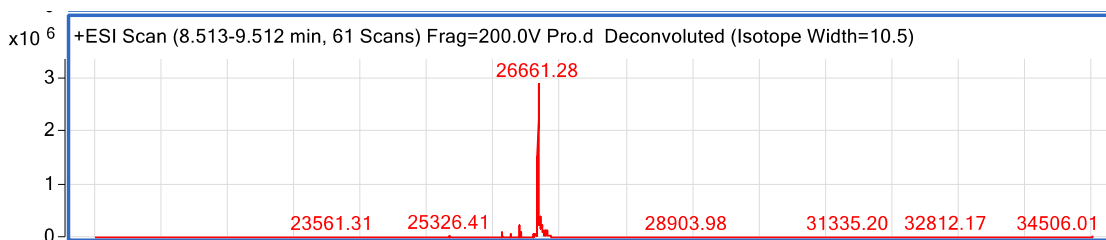
Synthesis of 4-biphenyl-L-phenylalanine (4). To a mixture containing N-(*tert*-butoxycarbonyl)-4-iodo-L-phenylalanine methyl ester (200 mg, 0.24 mmol) and 4-biphenylboronic acid (202 mg, 1.02 mmol) in 1:1 THF:Toluene (24 mL) was added a solution of Na₂CO₃ (108 mg, 1.02 mmol) in water (10 mL). The mixture was degassed with a stream of argon and Pd(PPh₃)₂Cl₂ (15 mg, 0.02 mmol) was added slowly to the reaction. The reaction was then stirred vigorously at 80 °C for 16 hours. The cooled reaction was then extracted using EtOAc and water (3 x 20 mL each) and the organic layer was dried with MgSO₄. Solvent was removed *in vacuo*. The crude product was then purified on a silica gel column using hexanes:EtOAc (5:1 → 1:1). To remove the protecting group, a 1:1 LiOH/Dioxane solution (2 mL) was added to the product on ice and stirred for 2 hours at room temperature. The dioxane was removed *in vacuo*, and the aqueous solution was cooled on ice and 6 M HCl was added to the reaction until a pH of 4 was achieved. The reaction was extracted and washed with water and EtOAc and the organic layer was dried with MgSO₄ and then concentrated *in vacuo*. The yellow oil was resuspended in 50% TFA solution (500 μL TFA/500 μL DCM) on ice and allowed to stir at room temperature for 1 hour. The solvent was then removed *in vacuo* and product was obtained as white solid (208 mg, 99%). ¹H NMR (400 MHz; d-MeOH): δ 7.75-6.83 (m, 18H), 4.20 (t, J=1.5 Hz, 1H), 3.35-3.05 (m, 2H).

General GFP Expression. A pET-GFP-TAG variant plasmid (0.5 μL) was co-transformed with a pEVOL-*p*CNF plasmid (0.5 μL) into *Escherichia coli* BL21 (DE3) cells using an Eppendorf

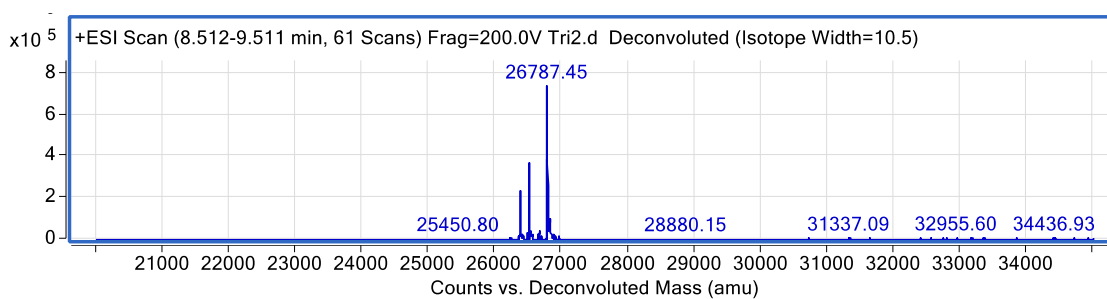
eporator electroporator. The cells were then plated and grown on LB agar in the presence of chloramphenicol (34 mg/mL) and ampicillin (50 mg/mL) at 37 °C overnight. One colony was then used to inoculate LB media (4 mL) containing both ampicillin and chloramphenicol. The culture was incubated at 37 °C overnight and used to inoculate an expression culture (10 mL LB media, 50 mg/mL Amp, 34 mg/mL Chlor) at an OD₆₀₀ 0.1. The cultures were incubated at 37 °C to an OD₆₀₀ between 0.6 and 0.8 at 600 nm, and protein expression was induced by addition of **4** (100 μL, 100 mM) and 20 % arabinose (10 μL) and 0.8 mM isopropyl β-D-1-thiogalactopyranoside (IPTG; 10 μL). The cultures were allowed to shake at 30 °C for 16-20 h then centrifuged at 5,000 rpm for 10 minutes and stored at -80 °C for 3 hours. The cell pellet was re-suspended using 500 μL of Bugbuster (Novagen) containing lysozyme and incubated at 37 °C for 20 minutes. The solution was transferred to an Eppendorf tube and centrifuged at 15,000 rpm for 10 minutes, then the supernatant was poured into an equilibrated His- pur Ni-NTA spin (Qiagen) column with nickel resin (200 μL) and GFP was purified according to manufacturer's protocol. Purified GFP was analyzed by SDS-PAGE (BioRad 10% precast gels, 150V, 1.5h), and employed without further purification.

Mass Spectra of WT GFP vs. Terphenyl GFP

WT GFP



Terphenyl GFP



	Expected	Observed
WT	26657	26661
Terphenyl	26793	26787

References

1. Xie, J.; Schultz, P. G. *Nat Rev Mol Cell Biol* **2006**, *7*, 775.
2. Young, T. S.; Schultz, P. G. *J Biol Chem* **2010**, *285*, 11039.
3. Liu, C.; Schultz, P.; Kornberg, R.; Raetz, C.; Rothman, J.; Thorner, J. *Ann Rev Biochem*, *79* **2010**, *79*, 413.
4. Deiters, A.; Cropp, T. A.; Summerer, D.; Mukherji, M.; Schultz, P. G. *Bioorg Med Chem Lett* **2004**, *14*, 5743.
5. Deiters, A.; Groff, D.; Ryu, Y.; Xie, J.; Schultz, P. *Angew Chem Int Ed* **2006**, *45*, 2728.
6. Bose, M.; Groff, D.; Xie, J.; Brustad, E.; Schultz, P. *J Am Chem Soc* **2006**, *128*, 388.
7. Peters, F. B.; Brock, A.; Wang, J. Y.; Schultz, P. G. *Chemi Biol* **2009**, *16*, 148.
8. Chin, J. W.; Santoro, S. W.; Martin, A. B.; King, D. S.; Wang, L.; Schultz, P. G. *J Am Chem Soc* **2002**, *124*, 9026.
9. Xie, J.; Liu, W.; Schultz, P. *Angew Chem Int Ed* **2007**, *46*, 9239.
10. Wang, J.; Xie, J.; Schultz, P. *J Am Chem Soc* **2006**, *128*, 8738.
11. Lee, H.; Guo, J.; Lemke, E.; Dimla, R.; Schultz, P. *J Am Chem Soc* **2009**, *131*, 12921.
12. Niu, W.; Guo, J. *Mol Biosys* **2013**, *9*, 2961.
13. Fernandez-Suarez, M.; Ting, A. *Nat Rev Mol Cell Biol* **2008**, *9*, 929.
14. Zhang, J.; Campbell, R.; Ting, A.; Tsien, R. *Nat Rev Mol Cell Biol* **2002**, *3*, 906.
15. Cornish, V.; Benson, D.; Altenbach, C.; Hideg, K.; Hubbell, W.; Schultz, P. *Proc Nat Acad Sci* **1994**, *91*, 2910.
16. Giepmans, B.; Martin, B.; Gaietta, G.; Deerinck, T.; Adams, S.; Tsien, R.; Ellisman, M. *Mol Biol Cell* **2004**, *15*, 169A.
17. Martin, B.; Giepmans, B.; Adams, S.; Tsien, R. *Nat Biotechnol* **2005**, *23*, 1308.
18. Keppler, A.; Gendreizig, S.; Gronemeyer, T.; Pick, H.; Vogel, H.; Johnsson, K. *Nat Biotechnol* **2003**, *21*, 86.
19. Gendreizig, S.; Keppler, A.; Juillerat, A.; Gronemeyer, T.; Pick, H.; Vogel, H.; Johnsson, K. *Chimia* **2003**, *57*, 181.

20. Lin, C.; Ting, A. *J Am Chem Soc* **2006**, *128*, 4542.
21. Seyedsayamdost, M. R.; Yee, C. S.; Stubbe, J. *Nat. Protoc.* **2007**, *2*, 1225.
22. Hashimoto, N.; Ninomiya, K.; Endo, T.; Sisido, M. *Chem Comm* **2005**, 4321.
23. Hecht, S.; Alford, B.; Kuroda, Y.; Kitano, S. *J Biol Chem* **1978**, *253*, 4517.
24. Mendel, D.; Cornish, V.; Schultz, P. *Ann Rev Biophys Biomol Struct* **1995**, *24*, 435.
25. Yamaguchi, Y.; Matsubara, Y.; Ochi, T.; Wakamiya, T.; Yoshida, Z. *J Am Chem Soc* **2008**, *130*, 13867.
26. Liu, K.; Chen, Y.; Lin, H.; Hsu, C.; Chang, H.; Chen, I. *J Phys Chem C* **2011**, *115*, 22578.
27. Quentmeier, S.; Denicke, S.; Ehlers, J.; Niesner, R.; Gericke, K. *J Phys Chem B* **2008**, *112*, 5768.
28. Denicke, S.; Gericke, K.; Smolin, A.; Shternin, P.; Vasyutinskii, O. *J Phys Chem A* **2010**, *114*, 9681.
29. Braem, O.; Penfold, T.; Cannizzo, A.; Chergui, M. *Phys Chem Chem Phys* **2012**, *14*, 3513.
30. Hutt, K.; Hernandez, R.; Heagy, M. *Bioorg Med Chem Lett* **2006**, *16*, 5436.
31. Chen, S.; Fahmi, N.; Bhattacharya, C.; Wang, L.; Jin, Y.; Benkovic, S.; Hecht, S. *Biochem* **2013**, *52*, 8580.
32. Chen, S.; Fahmi, N.; Wang, L.; Bhattacharya, C.; Benkovic, S.; Hecht, S. *J Am Chem Soc* **2013**, *135*, 12924.
33. Young, D.; Young, T.; Jahnz, M.; Ahmad, I.; Spraggon, G.; Schultz, P. *Biochem* **2011**, *50*, 1894.
34. Schultz, K.; Supekova, L.; Ryu, Y.; Xie, J.; Perera, R.; Schultz, P. *J Am Chem Soc* **2006**, *128*, 13984.
35. Ormö, M.; Cubitt, A. B.; Kallio, K.; Gross, L. A.; Tsien, R. Y.; Remington, S. J. *Science* **1996**, *273*, 1392.

CHAPTER 4: PHOTOREGULATION OF PROTEIN ARGININE

METHYLTRANSFERASE 1

Introduction

The importance of protein arginine methyltransferases (PRMTs) is seen in the diverse range of effects this enzyme has both on cellular and systems level processes. PRMTs catalyze the methylation of arginine residues in proteins, often histones, by transferring methyl groups from S-adenosyl-L-methionine (SAM or AdoMet) to histones.¹ Though different types of PRMTs catalyze the transfer of different numbers of methyl groups, the methyl groups transferred via PRMT are always attached to the guanidinium group of the arginine residue (Figure 4.1). Histone methylation impacts gene expression by regulating transcription. Depending on the location and number of PRMT catalyzed methyl tags, other binding proteins are recruited. These binding proteins can either activate or represses transcription. Methyl transfer does not change the formal charge on the nitrogen to which the methyl is transferred, but it does change the number of hydrogen bond donor sites on the guanidinium group.² Unmethylated, the guanidino group of arginine contains five hydrogen bond donor sites. The addition of each methyl group results in the loss of one of these hydrogen bond donor sites, thereby altering and weakening the electrostatic interactions of arginine's R-group. The nitrogen-containing guanidinium group confers the basicity associated with arginine and can be either mono- or dimethylated to form three different products: monomethylated arginine (MMA), symmetrically dimethylated arginine (SDMA), and assymmetrically dimethylated arginine (ADMA) (Figure 4.1).^{1,2}

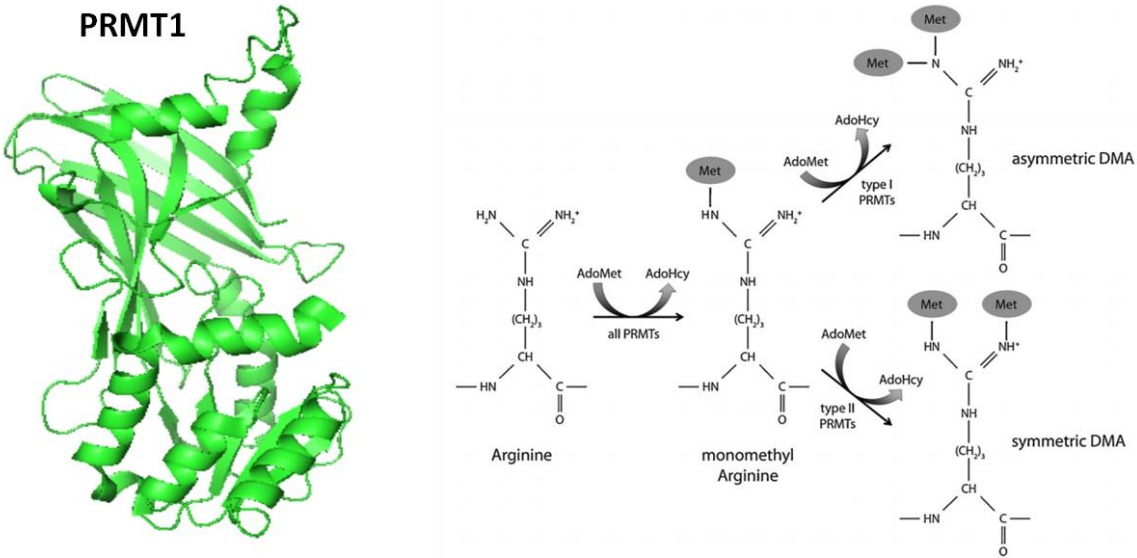


Figure 4.1 Left: Structure of PRMT1 (created using PyMol; PDB 1OR8) Right: Depicts the sites of methylation of the guanidinium group of arginine and the possible products of PRMT methylation based on the type of PRMT. Note that type III PRMTs catalyze a single methylation of arginine while both type I and II proceed to transferring another methyl to the guanidino group of arginine. Adapted from *Pharmacological research*, **2009**, 60(6), 466-474.³

Methylation is a prominent form of transcriptional regulation and thus an important factor in determining gene expression.² Though PRMTs may act on arginines within a wide range of protein types, histone methylation by PRMTs is of greater interest due to its potential role in epigenetic control.² Methylation, specifically histone methylation, can either repress or activate gene expression.⁴ The covalent methyl modification can either activate or inhibit a substrate by affecting its conformation in relation to other marks, such as methylated or acetylated lysine, or by affecting its interaction with other binding partners. For example, methylation of arginine 3 on histone 4 (H4) by PRMT1 can serve as a transcriptional activator. The methyl tag employed by PRMT enables the acetylation of H4 via p300 (a co-activator with histone acetyltransferase capability) and thereby acts as an activator for transcription. The interaction between p300 and the methylated histone could be stabilized by increased Van der Waals interactions due to the

additional nonpolar, methyl groups. Additionally, methylation by PRMT1 on H4 is involved in the activation of the target genes of p53, a key protein involved in tumor suppression.⁵ Like p300, the methyl groups added by PRMT1 aid in transcription of p53 target genes and therefore help to regulate tumor suppression. Conversely, methylation by PRMT could be repressive, as is the case with histone methylation by PRMT5. By methylating the guanidinium group of arginine, the number of potential hydrogen bonds it can form are limited and its electrostatic interactions are weakened. This modification could inhibit interactions with a binding partner whose active site requires stabilization through the hydrogen bonds donated by the guanidinium group when unmethylated.

Overall, the effect of methylation by PRMT varies and is determined by the context of the substrate protein and its binding partners. PRMTs, especially PRMT1s, are involved in many aspects of cellular function. Therefore, misregulation of PRMTs is often a downstream indication of many diseases. This varies from up-regulation of PRMT1 in mixed lineage leukemia to down-regulation of PRMT1 in breast cancer, as well as to increases PRMT metabolites like ADMA in non-cancerous diseases like coronary disease and renal failure.^{2,3} Due to the diverse effects of methylation by PRMTs, understanding the physiological role of PRMTs in disease formation is crucial to the development of new biomedical tools ranging from diagnostic tests to therapeutic treatments.

Given the role of PMRTs in gene regulation, Rust et al. (2014) aimed to better characterize the regulation of PRMT1 and sought to determine the effect phosphorylation has on PRMT1 activity.⁶ To do so, the UAA *p*-carboxymethyl-L-phenylalanine (*p*CmF), was site specifically incorporated into PRMT1. *p*CmF serves as a phosphotyrosine mimic. Therefore, changes in activity due to the presence of *p*CmF can be attributed to the altered phosphorylation of the protein. It was

hypothesized that introducing a negatively charged phosphate group on the tyrosine at position 291 would effectively inhibit the activity of the enzyme by destabilizing interactions between negatively charged AAs and the conserved threonine-histidine-tryptophan (THW) loop in the enzyme's catalytic core (Figure 4.2).

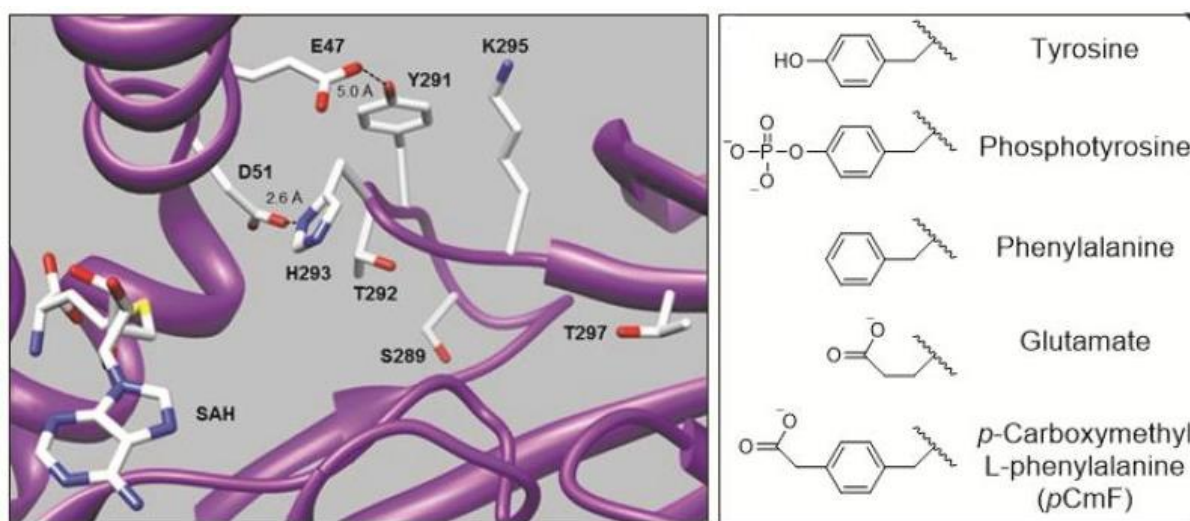


Figure 4.2 Left: Structure of the area surrounding the THW loop (AAs 292, 293, and 294) present in PRMT1. The loop is stabilized by interactions with negatively charged AAs (D51 and E47). The presence of a phosphate group on tyrosine 291 would repel glutamate 47 and electrically alter interactions that stabilize the THW loop. Right: Allows for comparison of the R groups of varying AAs as well as the utilized UAA (pCMF.) Adapted from ACS Chem. Biol. **2014**, 9, 649-655.

The catalytic core of each PRMT dimer is highly conserved and consists of 310 amino acids with five characteristic regions, each of which play an important role in protein function.² The first region, motif I, forms the base of the SAM-binding site. The site contains a group of three glycines and is structurally homologous to the glycine triad found in the binding sites of nucleotide-binding proteins.⁷ In nucleotide kinases, the presence of a glycine-rich loop functions to minimize water in the active sites as well as to stabilize and position the nucleotide in the binding pocket. Adenine, a principle nitrogenous base of some nucleotides, is also present as a residue

within SAM. Therefore, the homology in structure of motif I to that of nucleotide-binding proteins is not surprising. The second characteristic region, post I, stabilizes the ribose component of SAM via amino acid residues which form hydrogen bonds between the hydroxyl groups of the sugar.² This includes acidic amino acids such as glutamic acid, that contain a carboxylate group capable of forming bonds with the hydrogens of hydroxyl groups. The third and fourth regions, motif II and III, are parallel β -sheets which serve to stabilize motifs I and II respectively. The last characteristic region of the catalytic core is the threonine-histidine-tryptophan (THW) loop. This region stabilizes the portion of the enzyme at the N-terminal, which is involved in substrate recognition. This active site structure is present in all PRMTs and thus is key to PRMT's enzymatic activity. Therefore, altering key sites involved in catalytic function, as was done by Rust et al. to the THW loop, should inhibit the activity of the enzyme.

Gratifyingly, introduction of *p*CMF into position 291 did indeed alter PRMT1's substrate specificity as well as its protein-protein interactions. Therefore, position 291 is crucial to PRMT1's functioning. With the identification of this crucial regulatory position within PRMT1, we hypothesized that introduction of a photocaged UAA could temporarily inhibit enzymatic activity which could be subsequently restored following photocleavage via UV irradiation.

The incorporation of photocaged UAAs into protein allows for greater spatiotemporal control of protein activity.⁸ Photoregulation employs a caging moiety which inhibits the reactivity of the substrate to which it is bound. UV irradiation removes the caging group, restoring the activity of the decaged compound (Figure 4.3). This is especially advantageous because the light serves as a non-cytotoxic external modulation source.

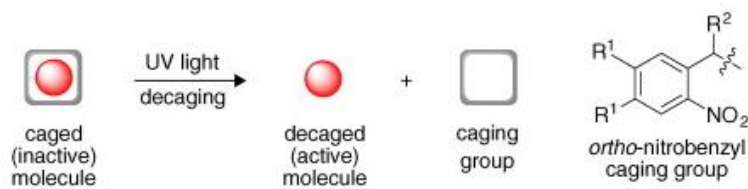


Figure 4.3 Presence of a caging group inactivates a molecule. UV light removes the caging moiety, thus restoring the activity of the molecule that was previously caged. Adapted from Deiters 2009.

Nitrobenzyl groups are a commonly used class of caging groups and were first identified for their use as photo-protecting groups by Baltrop et al. in 1966. The incorporation of a photocaged UAA can be used to regulate and selectively turn on a protein. Photocaging PRMT1 could allow for greater temporal and spatial control of methylation and can be achieved through the site specific incorporation of a photocaged UAA such as ortho-nitrobenzyl tyrosine (ONBY) (Figure 4.4).

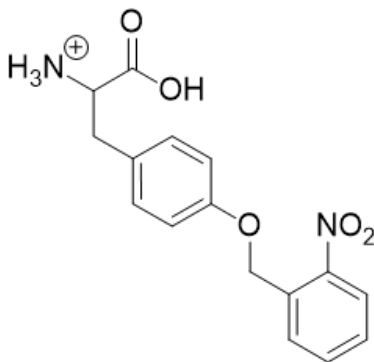


Figure 4.4 Structure of ortho-nitrobenzyl tyrosine (ONBY), which is a photocaged UAA.

The presence of a photo-caged tyrosine (ONBY) at position 291 within PRMT1 should inhibit substrate binding, thereby altering the function of the enzyme. Enzymatic activity can be restored to the inactive protein by irradiating briefly with UV light, which decages the tyrosine at position 291, restoring functionality (Figure 4.5). Given that the post-translational modification of methylation is an important regulatory feature in the function of a number of physiological

pathways, the ability to both spatially and temporally control methyl transfer is of extreme use. In this context, photocaging PRMT1 in particular could be advantageous in selectively controlling gene expression through the epigenetic modification of histones.

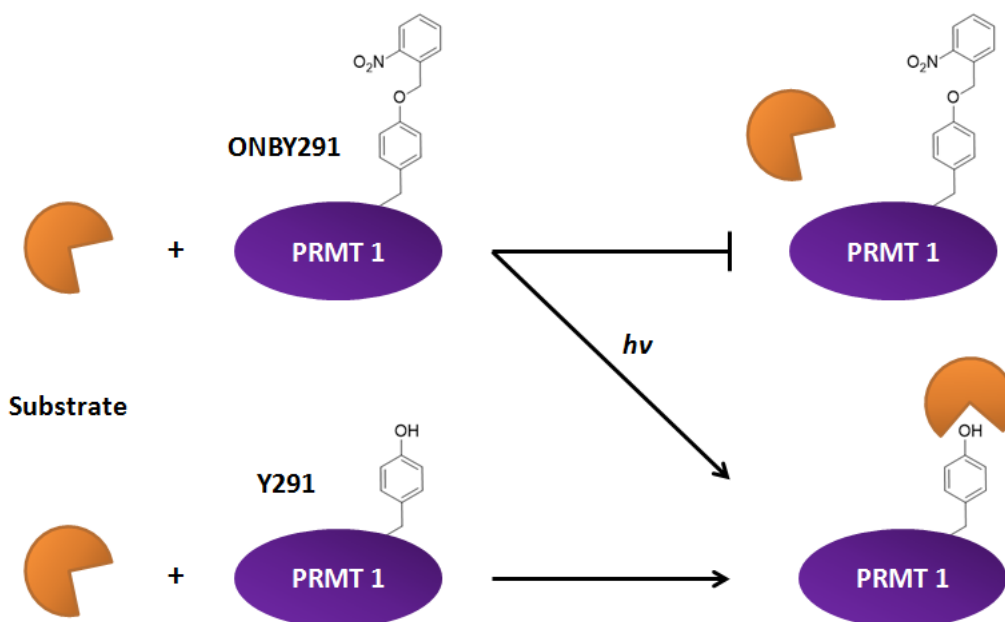
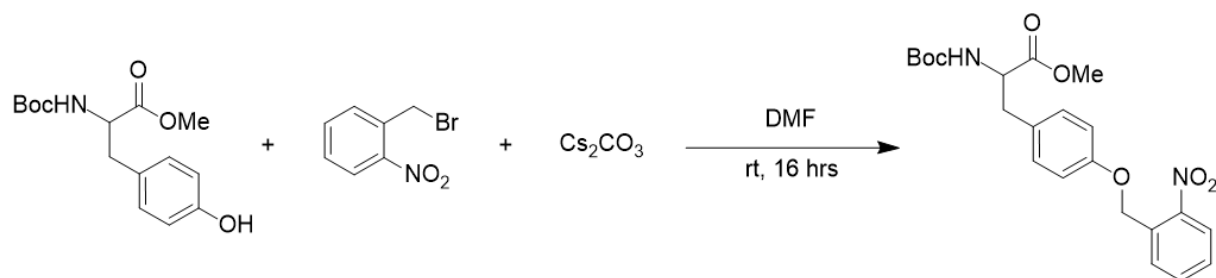


Figure 4.5 Photoregulation of PRMT1. Adapted from *ACS Chem. Biol.* **2014**, *9*, 649-655.

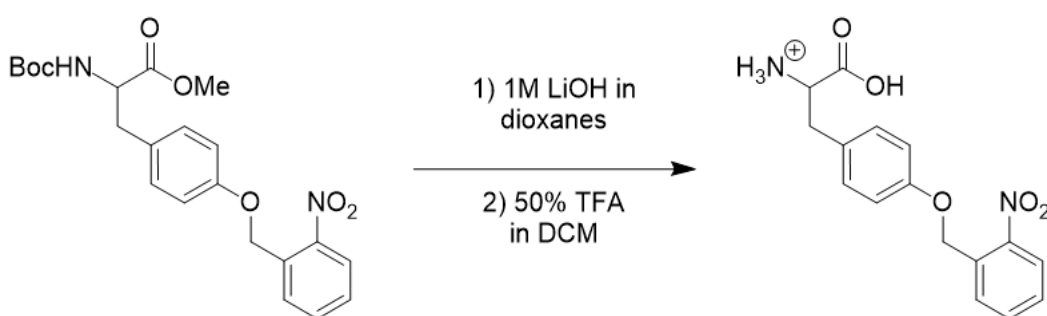
Results and Discussion

In order to prepare the caged PRMT1 protein, the ONB-tyrosine first needed to be synthesized under light-free conditions to prevent undesired decaging. Following the one-step synthesis of the protected UAA (Scheme 4.1) in a 90% yield, both the C- and the N- terminus were deprotected in order to obtain a UAA that could be readily incorporated (Scheme 4.2).

Scheme 4.1 Synthesis of Protected ONBY.



Scheme 4.2 Deprotection of ONBY.



Following the synthesis of ONBY, site-specific incorporation of the UAA was attempted using a previously evolved aaRS capable of recognizing and charging ONBY to the appropriate tRNA. Plasmids encoding the aaRS and tRNA were co-transformed into BL21 (DE3) *E. coli* with a pET-PRMT1-TAG-291 plasmid, harboring the TAG codon at position 291.

Due to the potential toxicity of nitrobenzyl groups, optimization studies indicated that the protein expression level as was greatest when 40% of the normally administered volume of the 100mM UAA solution was added when protein expression was induced. To confirm that ONBY was successfully incorporated into the PRMT1 mutant, the elution was analyzed by gel electrophoresis following protein purification using Ni-NTA resin (Figure 4.6). Additionally, a control expression of wild type PRMT1 was performed to be used as a comparison for protein expression, as well as later kinetic studies of protein activity.

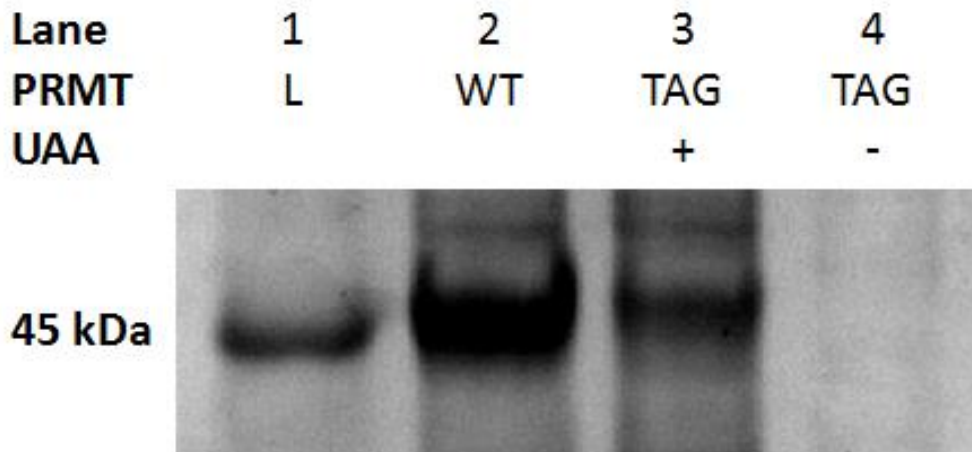


Figure 4.6 Successful incorporation of *ONBY* into *PRMT1* is indicated by the presence of the protein band at 42 kDa when the UAA is present and absence of the protein band in absence of the UAA.

Following successful incorporation of the UAA into the protein, the kinetic activity of the mutant could be analyzed using a GBiosciences SAM510: Methyltransferase Assay (Figure 4.7). The assay was used to analyze and compare the methylation activity of *PRMT1* WT, irradiated *PRMT1* TAG + *ONBY* and non-irradiated *PRMT1* TAG + *ONBY*. As methyl groups are transferred to Histone H4, SAM is converted to S-adenosyl-L-homocysteine (SAH), resulting in a color change in the reaction mixture. The color change is quantitatively monitored via absorbance readings taken every 15 seconds at 510 nm. Using the assay, six different conditions were examined to identify the potential photoactivation of *PRMT1* (Table 4.1).

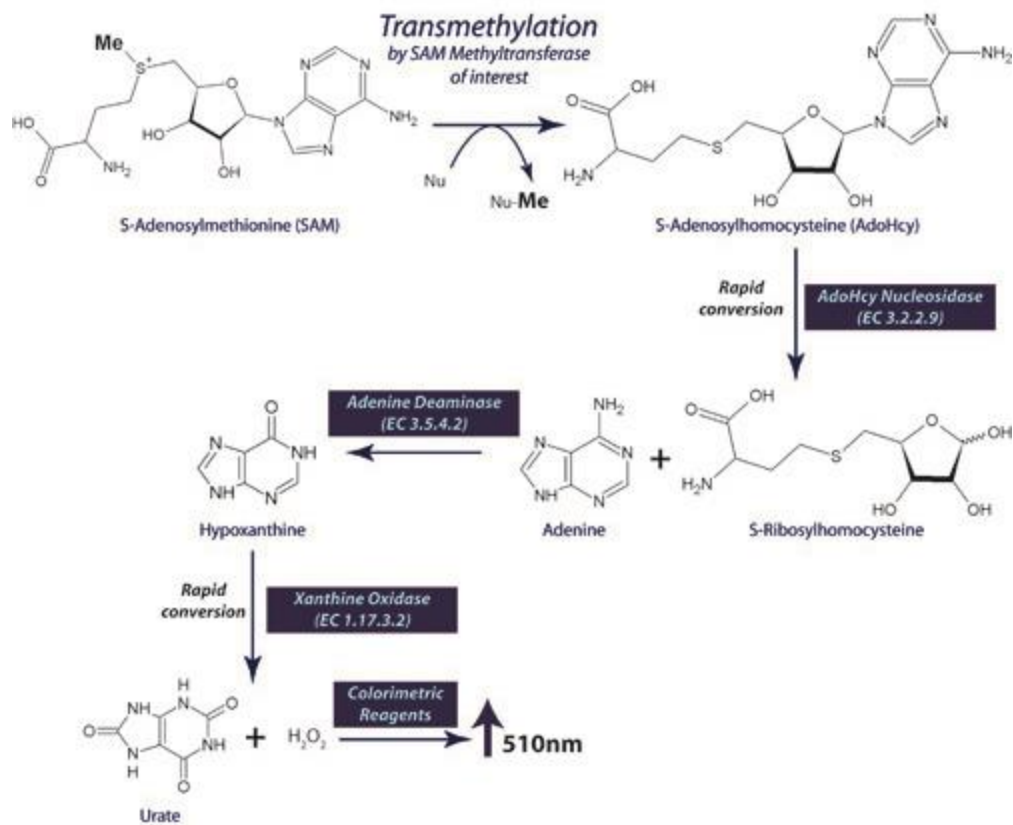


Figure 4.7 The general schematic of the G-Biosciences SAM 510 nm Methyltransferase Assay. Nu represents arginine 3 on histone 4. PRMT1 activity is measured by the change in absorbance at 510 nm resulting from the activation of the colorimetric indicator by hydrogen peroxide formation.

Following PRMT1 catalyzed methyl transfer from the methyl donor, SAM, to the methyl acceptor, H4, S-Adenosylhomocysteine (AdoHcy) is produced. The assay measures changes in absorbance at 510 nm, the absorbance wavelength of the colorimetric reagent which is activated by hydrogen peroxide. Hydrogen peroxide is formed in the last of a series of reactions which converts the immediate product of PRMT1 methyl transfer, AdoHcy, to urate and hydrogen peroxide. The rapid conversion of AdoHcy prevents feedback inhibition of AdoHcy on PRMT1 and provides an indirect measure of PRMT1 activity.

Table 4.1 List of Testing Conditions Employed During SAM510: Methyltransferase Assay

	Conditions Tested					
	1	2	3	4	5	6
Histone H4	1 μ L	1 μ L	1 μ L	1 μ L	---	1 μ L
PRMT 1 WT	14 μ L	14 μ L	---	---	---	---
PRMT 1 TAG + ONBY	---	---	14 μ L	14 μ L	---	---
Positive Control	---	---	---	---	5 μ L	---
Buffer	---	---	---	---	10 μ L	14 μ L
Irradiation	Yes	No	Yes	No	No	No

Differences in activity between WT conditions in the presence and absence of irradiation, 1 and 2, were compared to differences in activity between the irradiated and non-irradiated UAA-incorporated protein conditions 3 and 4. This allowed for significant differences only seen between conditions 3 and 4 to be attributed to successful decaging of the UAA via irradiation. This ensured that irradiation does not alter WT activity. Condition 5 served as a positive control (1 mM AdoHyc) for enzyme activity, and condition 6 allowed for measurement of background activity. Each condition was plated in triplicate and 100 μ L of SAM Master Mix was added to each well.

Immediately following the addition of the SAM Master Mix, absorbance measurements were taken every minute for one hour.

Preliminary data indicated that the activity of ONBY-incorporated PRMT1 is indeed subject to photo-regulation (Figure 4.8). The activity of irradiated PRMT1 + ONBY displays levels of activity similar to that of non-irradiated WT protein. Additionally, the activity of non-irradiated PRMT1 + ONBY mirrors the activity of the background control, indicating that the activity of PRMT1 is inhibited by the presence of the photo-caged UAA.

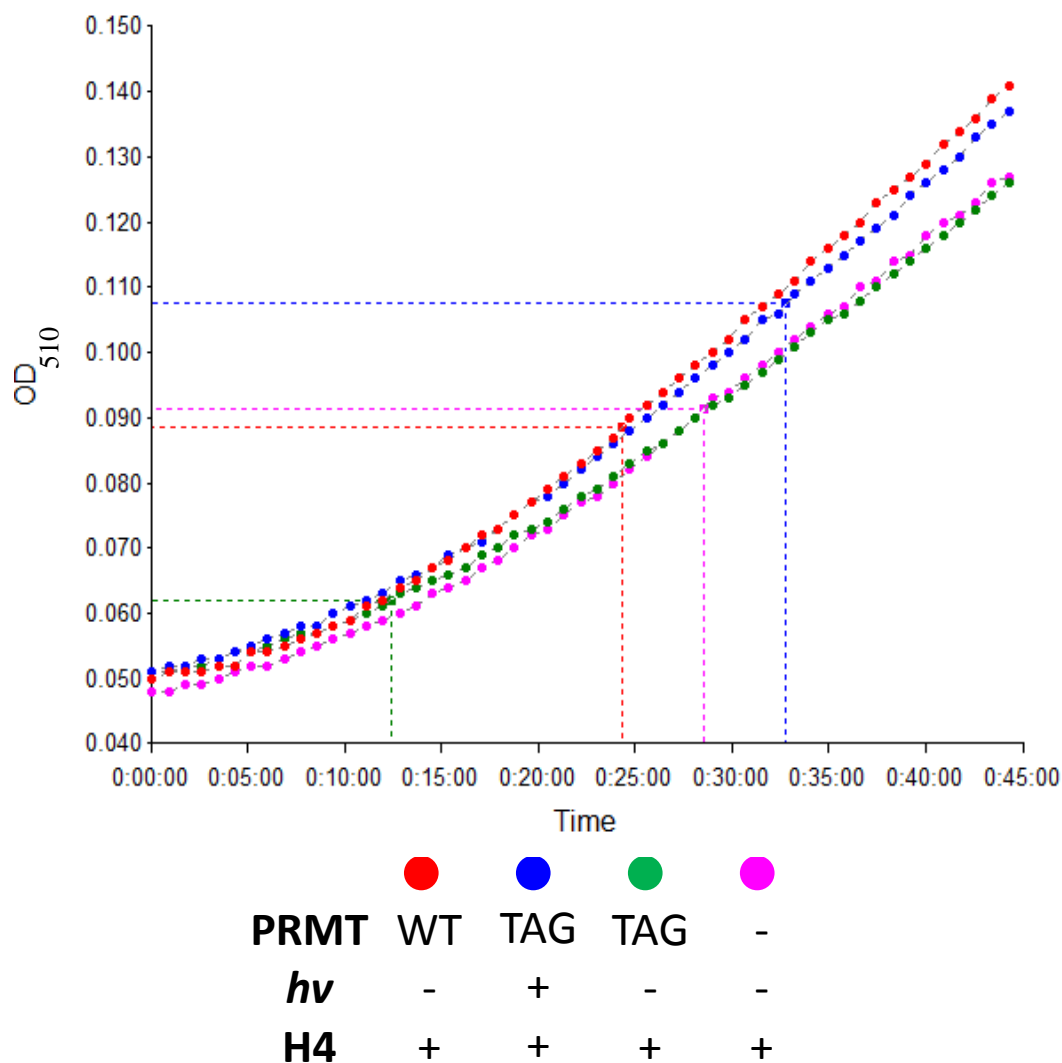


Figure 4.8 Preliminary absorbance data comparing the activity of WT PRMT1 and ONBY-incorporated PRMT1. Each data point represents the average of absorbance readings for the particular tested condition. The activity of the irradiated PRMT1 + ONBY follows a pattern of activity similar to the WT protein while the non-irradiated PRMT1 + ONBY shows a level of activity consistent with the background control. This indicated that the changes in activity between irradiated and non-irradiated PRMT1 + ONBY could be attributed to photo-cleavage of the caging group from the UAA.

Following expression of both the WT and TAG mutant protein in high yields, the assay was conducted again. Gratifyingly, analysis of the overall change in absorbance indicated that though irradiation did not significantly alter the activity of WT PRMT1, irradiating the ONBY-

incorporated TAG mutant resulted in a change in absorbance similar to that of the WT. Additionally, significantly different changes in absorbance between the irradiated and non-irradiated ONBY-incorporated PRMT1 indicated that irradiation induced successful decaging of the ONBY. Further, the similar changes in absorbance between the protein with the decaged UAA and the WT protein indicated that following irradiation, activity of the mutant protein was restored (Figure 4.9).

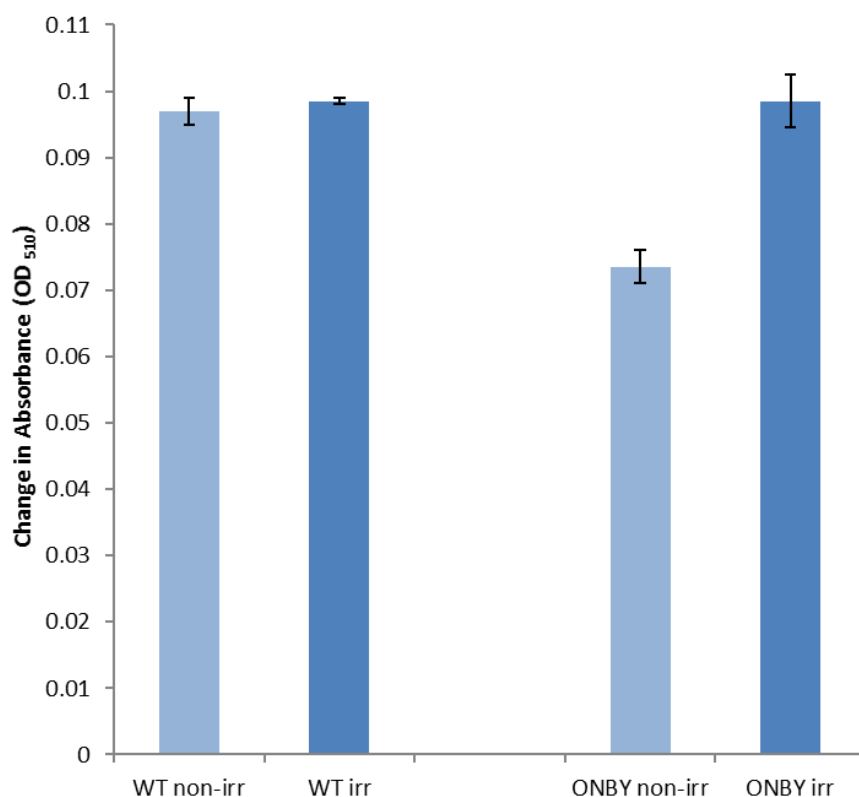


Figure 4.9 Comparison of change between irradiated and non-irradiated wild type and ONBY-incorporated PRMT1. For each condition, the change in absorbance was calculated as the difference between the averaged final and initial absorbance readings.

Conclusion

The use of UAAs allows for site-specific incorporation, which adds a sophisticated level of control in dictating protein function. Specifically, caging proteins provides both spatial and

temporal control over protein activity. PRMTs can act on arginines within a wide range of protein types, indicating their critical function in homeostatic maintenance. Additionally, the range of disease phenotypes that can result from PRMT misregulation also demonstrates the critical role of PRMTs. However, the precise regulation of PRMT1 has not been fully characterized.

In this study, it is demonstrated that the activity of PRMT1 can be altered and controlled via the site-specific incorporation of ONBY at position 291. In a methyltransferase assay, caged PRMT1 displayed limited activity. However, when ONBY was decaged, the activity of the protein was restored. Thus, ONBY caging regulates PRMT1 through the irreversible process of providing inactivation followed by activation after photocleavage. In order to expand knowledge of PRMT1, future research could explore a reversible caging group and its ability to regulate the protein.

Experimental

General: Solvents and reagents were obtained from Sigma Aldrich or Acros Organics and used without further purification. The Boc-OMe-Tyr was purchased from Matrix Scientific. Plasmids were provided by the laboratory of Dr. Peter Schultz at The Scripps Research Institute. Reactions were conducted under ambient atmosphere with solvents directly from the manufacturer without further purification. All proteins were purified according to manufacturer's protocols using a Qiagen Ni-NTA Quik Spin Kit. All NMRs were acquired on an Agilent Technologies 400 MHz NMR. Compound purities were assessed by NMR and found to be 90% or greater for all compounds. Enzyme activity was measured with a 510 nm SAM methyltransferase assay by GBiosciences. Absorbance was measured at 510 nm using a BioTek Synergy HT microplate reader and Greiner BioOne UV 96-well plates. Human recombinant Histone H4 was obtained from New England Biolabs.

Synthesis of O-(2-Nitrobenzyl)-L-tyrosine: A solution of Boc-Tyrosine-OMe (1.00 g, 1 eq, 3.35 mmol) in DMF (10 mL) was prepared in a flame-dried vial. To this solution, cesium carbonate (3.27 g, 3 eq, 10.0 mmol) was added, followed by the addition of 2-nitrobenzylbromide (0.60 g, 1.5 eq, 5.04 mmol). The reaction stirred overnight at room temperature and was filtered into a round-bottom flask. The reaction was then extracted using DCM and water (3 x 20 mL each) and the organic layer was dried with MgSO₄. Solvent was removed *in vacuo*. The crude product was then purified on a silica gel column using hexanes:EtOAc (3:1). To remove the methyl protecting group a 1:1 LiOH/Dioxane solution (2 mL) was added to the product on ice and stirred for 2 hours at room temperature. The dioxane was then removed *in vacuo* and the aqueous solution was cooled on ice and 6 M HCl was added to the reaction until a pH of 4 was achieved. The reaction was

extracted and washed with water and EtOAc, and the organic layer was dried with MgSO₄, and then concentrated *in vacuo*. To remove the tert-butyloxy protecting group, the yellow oil was resuspended in 50% TFA solution (500 μL TFA/500 μL DCM) on ice and allowed to stir at room temperature for 1 hour. The solvent was then removed *in vacuo*, and the product was obtained as white solid (408 mg, 90%). ¹H NMR (400 MHz; d-MeOH): δ 8.062 (d, J=3325, 1H), 7.775 (d, J=3110, 1H), 7.675 (t, J=3070, 1H), 7.518 (t, 3009, 1H), 7.210 (d, J=2885, 2H), 6.934 (d, J=1775, 2H), 5.287 (s, J=2116, 2H), 4.174 (m, J=1670, 1H), 3.644 (s, J=1458, 1H), 3.204 (m, J=1282, 1H), 1.988 (s, J=785, 1H), 1.153 (m, J=454, 1H).

Protein Expression: A pET-PRMT1-TAG-291 plasmid (0.5 μL) was co-transformed with a pEVOL-ONBY plasmid (0.5 μL) into *Escherichia coli* BL21 (DE3) cells using an Eppendorf eporator. The cells were then plated and grown on LB agar in the presence of chloramphenicol (34 mg/mL) and kanamycin (10 mg/mL) at 37 °C overnight. One colony was then used to inoculate LB media (10 mL) containing both kanamycin and chloramphenicol. The culture was incubated at 37 °C overnight and used to inoculate an expression culture (50 mL LB media, 10 mg/mL Kan, 34 mg/mL Chlor) at an OD₆₀₀ 0.1. The cultures were incubated at 37 °C to an OD₆₀₀ of 0.8, and protein expression was induced by addition of UAA (200 μL, 100 mM) and 20 % arabinose (50 μL) and 0.8 mM isopropyl β-D-1-thiogalactopyranoside (IPTG; 50 μL). The cultures were incubated at room temperature for 24 h then centrifuged at 5,000 rpm for 10 minutes and stored at -80 °C for 3 hours. The cell pellet was resuspended using 1 ml of Bugbuster (Novagen) containing lysozyme, and incubated at 37 °C for 20 minutes. The solution was transferred to an Eppendorf tube and centrifuged at 15,000 rpm for 10 minutes, then the supernatant was added to an equilibrated His-pur Ni-NTA spin (Qiagen) column and PRMT1 was purified according to manufacturer's protocol.

Purified PRMT 1 was analyzed by SDS-PAGE (BioRad 10% precast gels, 150V, 1.5h) and employed without further purification.

PRMT1 Kinetics Assay: SAM510: Methyltransferase Assay was used according to the manufacturer's protocol and 6 different conditions were tested (see Table 1). Irradiation conditions consisted of subjecting samples to UV light (365 nm) for 25 minutes. Following irradiation, samples were returned to ice for 10 minutes and plated for the assay. Differences in activity between wild type PRMT1 with and without irradiation (conditions 1 and 2) were compared to differences in activity between ONBY incorporated PRMT1 both with and without irradiation (conditions 3 and 4). This allowed for significant differences only seen between conditions 3 and 4 to be attributed to successful decaging of the UAA via irradiation. Condition 5 served as a positive control for enzyme activity, and condition 6 allowed for measurement of background activity. Each condition was repeated in triplicate and 100 μ L of SAM Master Mix was added to each well. Immediately following the addition of the SAM Master Mix, absorbance measurements were taken at an OD₅₁₀ every minute for one hour. The data was plotted as a function of absorbance vs. time for each condition. The slope of the best-fit line was used as a rough measure to compare enzymatic activity between the tested conditions. Additionally, for each condition, the change in absorbance between the initial and final absorbance readings was compared in order to compare absorbance changes between conditions.

References

1. Zhang, X.; Xiaodong, C. *Structure* 11.5 (2003): 509-520.
2. Fuhrmann, J., Clancy, K. W., & Thompson, P. R. (2015). *Chem. Rev*, 115(11), 5413-5461.
3. Nicholson, T. B., Chen, T., & Richard, S. (2009). *Pharmacological research*, 60(6), 466-474.
4. Zhang, Y., & Reinberg, D. (2001). *Genes & development*, 15(18), 2343-2360.
5. Scoumanne, A., & Chen, X. (2008). *Histology and histopathology*, 23(9), 1143.
6. Rust, H.; Subramanian, V.; West, G.; Young, D.D.; Schultz, P.G.; Thompson, P. *ACS Chem. Biol.* 2014. 9, 649-655.
7. Hemmer, W., McGlone, M., Tsigelny, I., & Taylor, S. S. (1997). *Journal of Biological Chemistry*, 272(27), 16946-16954.
8. Deiters A. *Curr Opin Chem Biol* 2009; 13(5):678-686.

CHAPTER 5: INTRODUCTION TO THE SYNTHESIS AND BIOLOGICAL SIGNIFICANCE OF ASYMMETRIC POLYYNES

Antibacterial resistance is one of the most immediate and deadly threats to society.¹ These resistant infectious agents alone are responsible for illness in two million people each year, as well as the deaths of more than 23,000. The development of resistance is inevitable — it is a known and accepted risk that comes with the use of antibiotics; however, the rate at which pathogens are becoming resistant is alarming and unacceptable.

In 2012, only five major pharmaceutical companies had active antibacterial discovery programs.² Given our highly competitive economic market, it can be understood why antibiotic production has come to a standstill.³ Antibiotics afford a poor return on investment when compared to drugs that treat chronic illnesses and thus are less lucrative pharmaceutical targets. In addition to the financial obstacles associated with antibiotic production, the molecular libraries from which antibiotics are built are lacking in variety.^{4,5} Many of the antibiotics utilized today have been produced using a similar set of molecular scaffolds.⁶ Therefore, production of antibiotics can be increased by expanding the library of viable building blocks.

Polyynes, molecules that contain multiple conjugated triple bonds, are a class of compounds that are readily found in nature and often possess unique biological properties. Various natural products contain a polyyne core structures with multiple conjugated acetylenic units and have been isolated from organisms like plants, fungi, and coral.⁷⁻⁹ These structures exhibit numerous biological activities including antibacterial, antifungal, anti-HIV, and anticancer properties.⁹⁻¹³ Therefore, synthetic routes to the preparation of these structures are necessary to further study their benefits and develop novel therapeutic analogs. However, a key characteristic of naturally occurring polyynes is a degree of asymmetry which is challenging to synthetically

produce (Figure 5.1). Common synthetic approaches yield a mixture of compounds due to the typical lack of chemoselectivity.

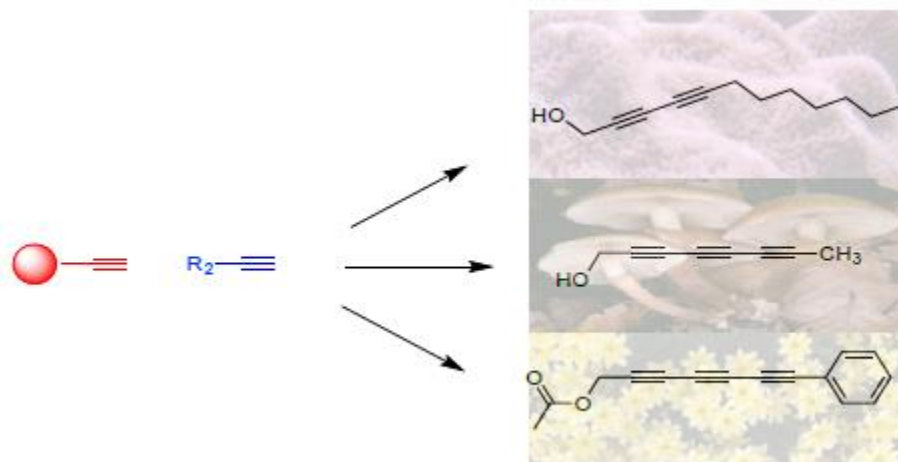
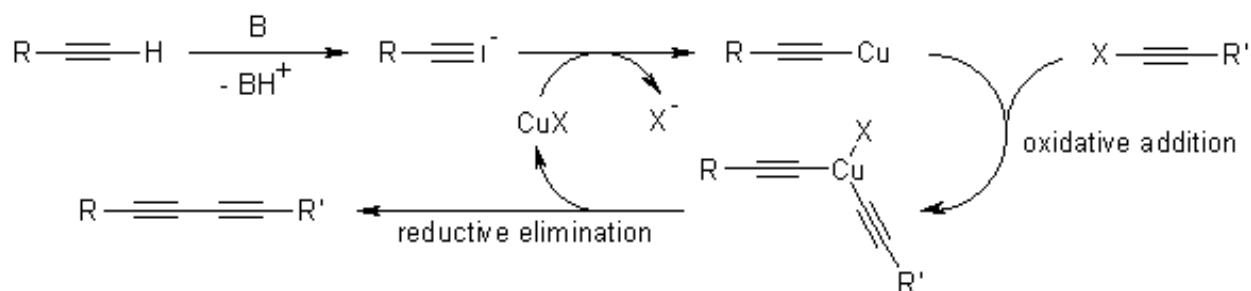


Figure 5.1 Natural products possessing conjugated acetylenic units with asymmetrical terminal groups. Top: Montiporic acid A derived from the stony coral *Montipora digitata*. Middle: Octatriyn-1-ol. Originally isolated from the fungus *Kuehneromyces mutabilis*. Bottom: Phenylhepta-2,4,6-trinyl acetate. Originally isolated from several species of *Bidens* in the Aster family of plants.

One such approach to access these conjugated alkyne cores is the Glaser–Hay reaction. This reaction was developed in the 1800s and involves the coupling of two terminal alkynes.¹³ The reaction was later optimized to lower the temperature and increase the rate of the reaction; however, the lack of chemoselectivity precluded its use, as a mixture of three coupling products could be obtained when using two unique terminal alkyne reagents (Figure 1).^{15,16} The products that result are the symmetric products of each terminal alkyne and the desired asymmetric product from the reaction of the two alkynes. This lack of chemoselectivity has been synthetically addressed via the transition to the Cadiot–Chodkiewicz reaction between a halo-alkyne and a terminal alkyne to differentiate the reaction partners (Scheme 5.1).^{17,18}

Scheme 5.1 Cadiot– Chodkiewicz reaction.



While this approach does offer a degree of chemoselectivity, homocoupling is still observed and additional synthetic effort must be employed to prepare the halo-alkynes.¹⁹⁻²¹ Based on the asymmetrical nature of many of these natural product derivatives, a more efficient mechanism to address chemoselectivity issues is required. Recently, we reported the solid supported Glaser–Hay reaction as a mechanism to address several key pitfalls associated with the Glaser–Hay reaction (Figure 5.2).²²⁻²⁴

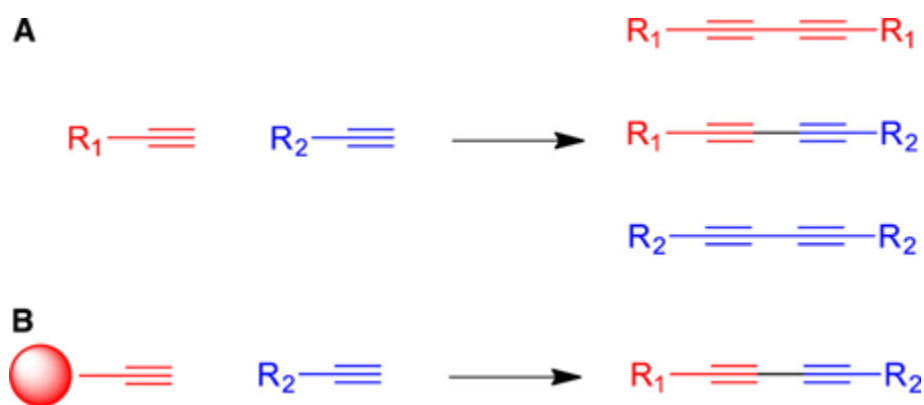


Figure 5.2 Glaser–Hay coupling of terminal alkynes. (A) Traditional Glaser–Hay reactions result in three diynes. (B) Solid-supported Glaser–Hay reaction yields only the heterodimeric product after resin cleavage.

This project utilizes this solid-supported Glaser-Hay methodology to synthesize and add to the library of biologically active polyynes. These asymmetrical synthetic products can then be tested against naturally occurring polyynes for anti-biological properties.^{21,23}

To quickly assess the biological activity of the synthetic products, the products were added to cell solutions and optical density measurements were taken over a time course. Changes in absorbance of the cell culture relative to the control were attributed to the addition of the polyynes product. In these quick assessments, continual decreases in absorbance of the cell solution following the addition of the polyynes was taken to indicate cell death. Additionally, maintained absorbance of a cell solution following the addition of the polyynes solution (relative to increased absorbance of a control) was taken to indicate growth inhibition.

Though this methodology may be useful in generating a preliminary assessment of biological activity, the characterization of biological activity can be improved through the use of different techniques that enable more specific distinctions between live and dead cells. For example, the use of a cell viability kit could address whether membrane integrity is compromised by the addition of the polyynes product. Such a kit would utilize two-color fluorescence staining to differentially stain cells on the basis of whether their membrane was intact (live cells) or damaged (dead cells). Though one fluorescent dye would bind cellular membranes and therefore bind to both damaged and intact cells with no specificity, the other fluorescent dye could be specific to nucleic acids and therefore could only stain cells in which a damaged cell membrane allowed for the nuclear material to be readily accessed. The fluorescent reading of dead cells (which can be stained by both fluorescent dyes), thus would be different from the fluorescent reading emitted by the live cells (only stained by one fluorescent dye) allowing the researcher to distinguish between dead and live cells when examined under a microscope. Additionally, using flow cytometry in conjunction with the two color fluorescence cell viability kit would enable quantification and comparison of the number of live and dead cells that result from the addition of a specific polyynes. Overall, the methodology we used to quickly assess the biological activity of our synthesized

compounds is a necessary preliminary test that can be used to better inform the use of more sophisticated methodologies.

References

1. US Dept. of Health and Human Services. **2013**, *CDC. Atlanta, GA* .
2. Spellberg, Brad. *Bull World Health Organ.* **2011**, *89*, 88-89.
3. Spellberg, Brad. *Rising plague*. Prometheus Books, **2009**.
4. Singh, Sheo B. *Bioorg. Med. Chem. Lett.* **2014**, *24.16*, 3683-3689.
5. Silver, Lynn L. *Clin. Microbiol. Rev.* **2011**, *24.1*, 71–109.
6. Fischbach, M. A., and C. T. Walsh. *Science.* **2009**, *325*, 1089-1093.
7. Wong, W. J. *Inorg. Organomet. Polym. Mater.* **2005**, *15*, 197– 219.
8. Shi Shun, A. L.; Tykwinski, R. R. *Angew. Chem., Int. Ed.* **2006**, *45*, 1034– 57.
9. Lu, W.; Zheng, G.; Aisa, H.; Cai, J. *Tetrahedron Lett.* **1998**, *39*, 9521– 9522.
10. Nakayama, S.; Uto, Y.; Tanimoto, K.; Okuno, Y.; Sasaki, Y.; Nagasawa, H.; Nakata, E.; Arai, K.; Momose, K.; Fujita, T.; Hashimoto, T.; Okamoto, Y.; Asakawa, Y.; Goto, S.; Hori, H. *Bioorg. Med. Chem.* **2008**, *16*, 7705– 14.
11. Pan, Y.; Lowary, T.; Tykwinski, R. *Can. J. Chem.* **2009**, *87*, 1565– 1582.
12. Lee, Y.; Lim, C.; Lee, H.; Shin, Y.; Shin, K.; Kim, S. *Bioconjugate Chem.* **2013**, *24*, 1324– 1331.
13. Bae, B. H.; Im, K. S.; Choi, W. C.; Hong, J.; Lee, C. O.; Choi, J. S.; Son, B. W.; Song, J. I.; Jung, J. H. *J. Nat. Prod.* **2000**, *63*, 1511– 4.
14. Glaser, C. *Ber. Dtsch. Chem. Ges.* **1869**, *2*, 422– 424.
15. Hay, A. *J. Org. Chem.* 1962, *27*, 3320. Vilhelmsen, M.; Jensen, J.; Tortzen, C.; Nielsen, M. *Eur. J. Org. Chem.* **2013**, *2013*, 701– 711.
16. Chodkiewicz, W.; Cadiot, P.; Willemart, A. *Comp Rendus Hebds Des Seances* **1957**, *245*, 2061-2062.
17. Montierth, J.; DeMario, D.; Kurth, M.; Schore, N. *Tetrahedron* **1998**, *54*, 11741– 11748. Berná, J.; Goldup, S. M.; Lee, A. L.; Leigh, D. A.; Symes, M. D.; Teobaldi, G.; Zerbetto, F. *Angew. Chem., Int. Ed.* **2008**, *47*, 4392– 6.
18. Nie, X.; Wang, G. *J. Org. Chem.* **2006**, *71*, 4734– 41.

19. Marino, J. P.; Nguyen, H. N. *J. Org. Chem.* **2002**, *67*, 6841–4.
20. Lampkowski, J. S.; Durham, C. E.; Padilla, M. S.; Young, D. D. *Org. Biomol. Chem.* **2015**, *13*, 424–7.
21. Tripp, V. T.; Lampkowski, J. S.; Tyler, R.; Young, D. D. *ACS Comb. Sci.* **2014**, *16*, 164–7.
22. Lampkowski, J.; Maza, J.; Verma, S.; Young, D. *Molecules* **2015**, *20*, 5276–5285.
23. Fusetani, N.; Toyoda, T.; Asai, N.; Matsunaga, S.; Maruyama, T. *J. Nat. Prod.* **1996**, *59*, 796–797.

CHAPTER 6: APPLICATION OF THE SOLID-SUPPORTED GLASER–HAY REACTION TO NATURAL PRODUCT SYNTHESIS

Introduction

Polyynes core structures are prevalent in various natural products and consist of a series of conjugated acetylenic units.^{1–3} Over 1,000 of these naturally occurring molecules have been isolated from organisms such as plants, fungi, and coral.² These structures exhibit numerous biological activities including antibacterial, antifungal, anti-HIV, and anticancer properties.^{3–7} Therefore, synthetic routes to the preparation of these structures are necessary to further study their benefits and develop novel therapeutic analogs. Herein, we report the application of the solid-supported Glaser-Hay reaction to the preparation of four natural products and their subsequent screening for antibacterial activity.

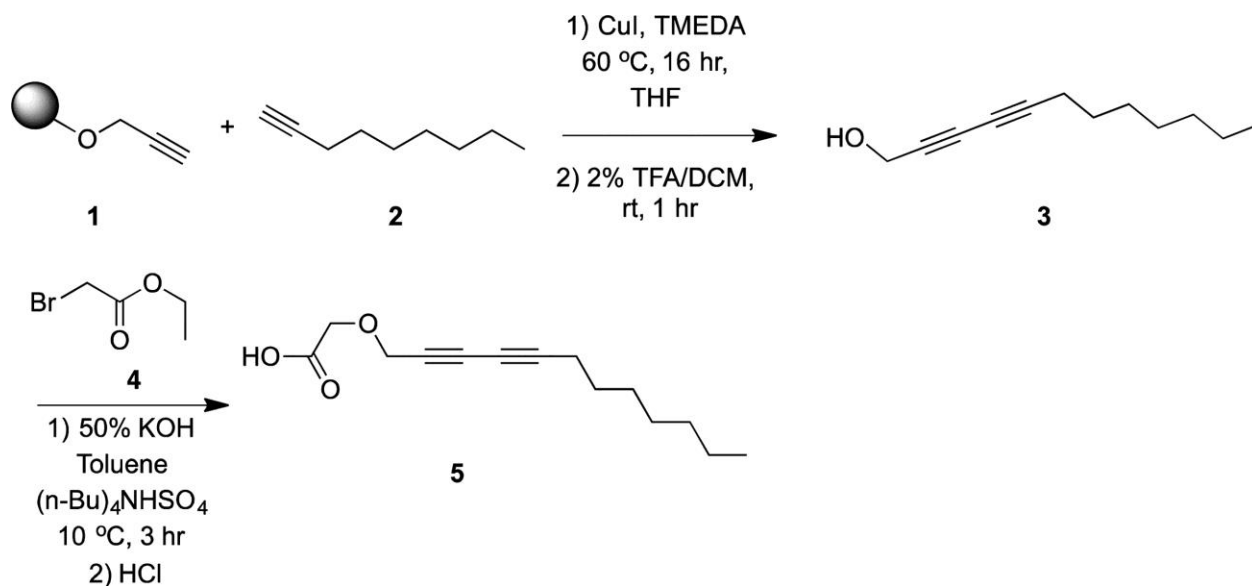
Results and Discussion

Many corals have been found to be rich in natural products that contain antibacterial, antifungal, and cytotoxic properties. Specifically, numerous acetylenic polyynes have been isolated from the genus *Montipora*, a velvet coral.⁸ The most directly accessible natural product that lends itself to this technology is 2,4-dodecadiynyl alcohol (**3**), an asymmetrical diyne shown to exhibit cytotoxicity against human tumor lines.² Numerous research groups have described the synthesis of this natural product.^{9–13} For example, Stefani et al. (1999) report this synthesis via a Cadiot–Chodkiewicz coupling at a yield of 76%.¹³ However, this reported synthesis requires hazardous reagents and requires a preliminary synthetic step to synthesize a halogenated alkyne. Another synthesis reported by Fiandanese et al. (2005) requires numerous and sometimes harsh reagents in a total of six synthetic steps and has just a 42% yield.¹² Both syntheses also required tedious purification steps postreaction. We hypothesized that the solid-supported Glaser–Hay

reaction would be optimal to obtain this product in fewer steps using milder conditions, while also affording higher yields.

Immobilization of propargyl alcohol on a trityl chloride polystyrene resin (**1**) at ~0.7 mmol/g, as previously describe, facilitated the subsequent Glaser–Hay reaction with 1-nonyne (**2**) in the presence of a CuI/TMEDA catalyst system (Scheme 6.1).¹⁴ Following successive DCM/MeOH washes of the resin, **3** was cleaved from the resin using 2% TFA in DCM in 1 h. After a silica plug, **3** was obtained in a 75% yield in high purity after essentially a single synthetic step. Analysis via ¹H NMR, ¹³C NMR, and GC/MS confirmed its identity and was in accordance with previously reported literature values. Overall, utilizing the solid-supported Glaser–Hay methodology to synthesize this product eliminated harsh reagents, halogenated precursor compounds, and synthetic steps required in previously reported syntheses and produced the product in better or comparable yield.

Scheme 6.1



A derivative of **3**, Montiporic Acid A (**5**) is another common polyynol isolated from this velvet coral species.² **5** has been isolated from the eggs of this coral and was shown to possess

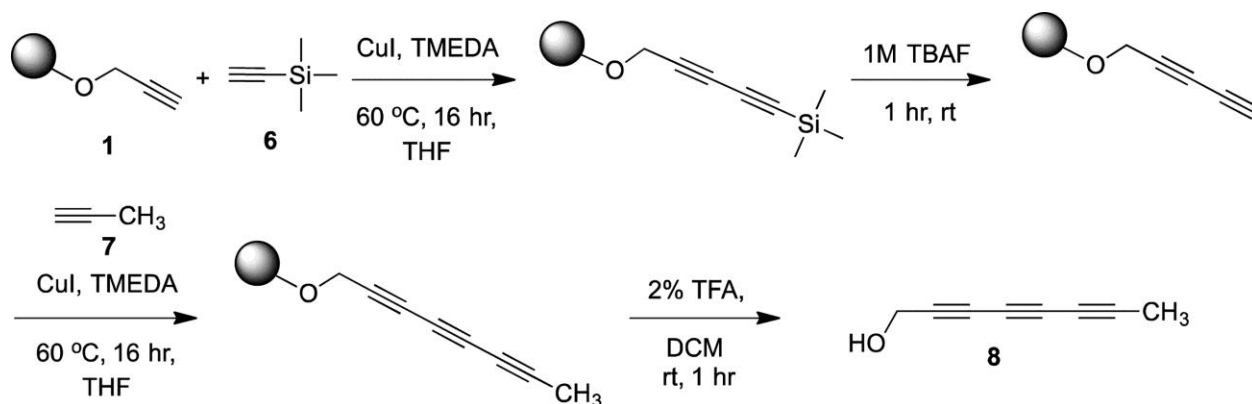
significant cytotoxicity against P-338 murine leukemia cells. It has also been proven to be an efficient antibacterial agent against *E. coli*.¹² Conveniently, **5** can be accessed directly from **3** via an SN2 reaction with 2-bromoacetate (**4**), followed by an ester hydrolysis as previously reported (Scheme 6.1). Synthesis of **5** was achieved in good yield (49%) and analyzed via ¹H NMR, ¹³C NMR, and GC/MS to confirm its purity and identity. Thus, our methodology allowed us to prepare **5** in three synthetic steps and in comparable yield to the previously reported synthesis that required six steps.

This methodology can also readily be employed toward triyne natural products. Toward this end, we initially targeted the preparation of octatriyn-1-ol (**8**), originally isolated from the fungus, *Kuehneromyces mutabilis*, in 1973.¹⁵ This compound and similar derivatives were shown to possess antibacterial activities. Previous syntheses have utilized a Fritsch–Buttenberg–Wiechell rearrangement to prepare the triyne core.¹⁶ Overall, this synthesis requires eight synthetic steps to generate **8**. This reported methodology also requires numerous reagents, including some that are hazardous, and careful reaction temperature control leading to an overall yield of only 3%.¹⁶

Building on our previously reported methodology for extending the acetylenic scaffold, we developed a synthetic route toward octatriyn-1-ol (Scheme 6.2), decreasing the number of synthetic steps as well as the number of reagents used in previous reports, as well as increasing yield.¹⁷ Beginning with the previously described propargyl alcohol polystyrene resin (**1**), TMS-acetylene (**6**) was coupled using the Glaser–Hay conditions. The TMS group was then removed using a TBAF/DCM solution, regenerating the terminal alkyne. Propyne (**7**) was then coupled to the resin using the Glaser–Hay reaction and the product was cleaved with a 2% TFA solution, affording the desired asymmetrical triyne natural product, **8**. Following a silica plug purification,

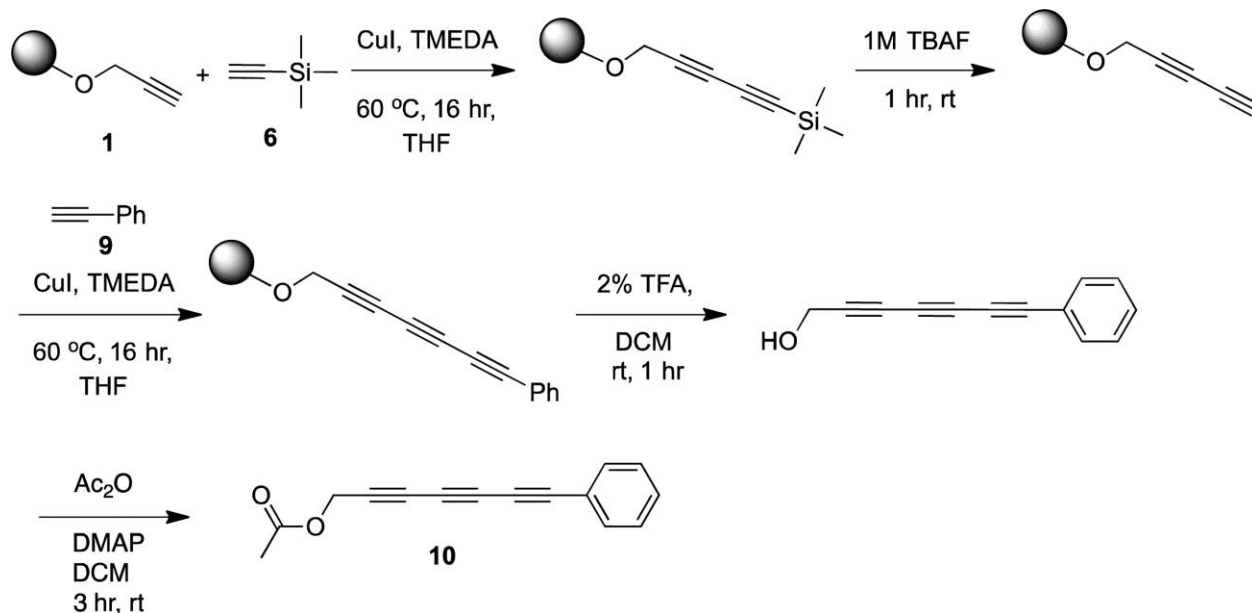
8 was obtained in a 68% yield and analyzed by NMR and MS, which corresponded to previously reported values. This is a dramatic increase over the current literature synthesis, which was performed with only a 3% overall yield and in an additional four steps.¹⁶

Scheme 6.2



Finally, another triyne natural product is readily accessible using a similar methodology to the preparation of octariyn-1-ol. Phenylhepta-2,4,6-trinyl acetate (**10**) was originally isolated from several species of *Bidens* in the Aster family of plants and has shown antibacterial properties.² A previously reported synthesis started from 1,4-butyne diol, and following the addition of a TBDPS protecting group, was reacted with a lithiated phenylacetylene and underwent a Fritch–Butenberg–Wiechell rearrangement to produce the triyne core.¹⁶ This synthetic strategy requires eight total steps and the use of harsh chemical conditions, affording **10** in a 14% yield. Utilizing our previously described solid-supported strategy, the triyne core is readily accessible in minimal steps and can be further elaborated to generate the acetate (Scheme 6.3).

Scheme 6.3



The previously described Glaser–Hay coupling with TMS followed by TBAF-induced TMS deprotection was employed to prepare the immobilized polyne core, followed by the capping of the polyne with phenylacetylene (**9**). The solid support was then cleaved to afford the triynol product. The alcohol was acetylated with acetic anhydride in the presence of DMAP to afford the desired product. Upon acetylation, the reaction was extracted and washed with $\text{DCM}/\text{H}_2\text{O}$ and the organic layer dried with MgSO_4 . The triyne **10** was then purified on a silica column, affording the desired natural product in a 46% yield, a marked improvement. The product was then analyzed via NMR and MS and matched to previously reported spectra. Utilizing the solid supported Glaser–Hay methodology we were able to eliminate synthetic steps, as well as harsh and excessive reagents, and drastically improve the yield of this natural product.

With the natural products in hand, we wanted to quickly assess their antibacterial properties. Some have already been classified as antibacterial, while others exhibited other biological relevance, but all harbor a similar alkynyl core. Each of the products was dissolved in DMSO to generate stock solutions at concentrations of 50 mg/mL. The compounds were then

introduced in triplicate at various concentrations to *E. coli* cultures at different cellular densities to assess if the compounds either prevented bacterial growth (assay at low density) or simply induced cell death (assay at high density). The cellular density of the bacteria was then observed over a 48h period. When added to dense cultures ($OD_{600} \approx 0.5$), no decrease in cell density was observed with any of the natural products, even at 5 mM concentrations (Figure 6.1). Chloramphenicol, a well-documented antibiotic, was used as a positive control, and a significant decrease in bacterial density was observed at much lower concentrations of 0.05 mM. However, when the natural products were introduced to newly inoculated *E. coli* cultures, **5** and **8** prevented bacterial growth at 2 μ M concentrations, and **10** prevented bacterial growth at 3 mM concentrations. No growth inhibition was observed for **3** at even high concentrations (Figure 6.2; Figure 6.3).

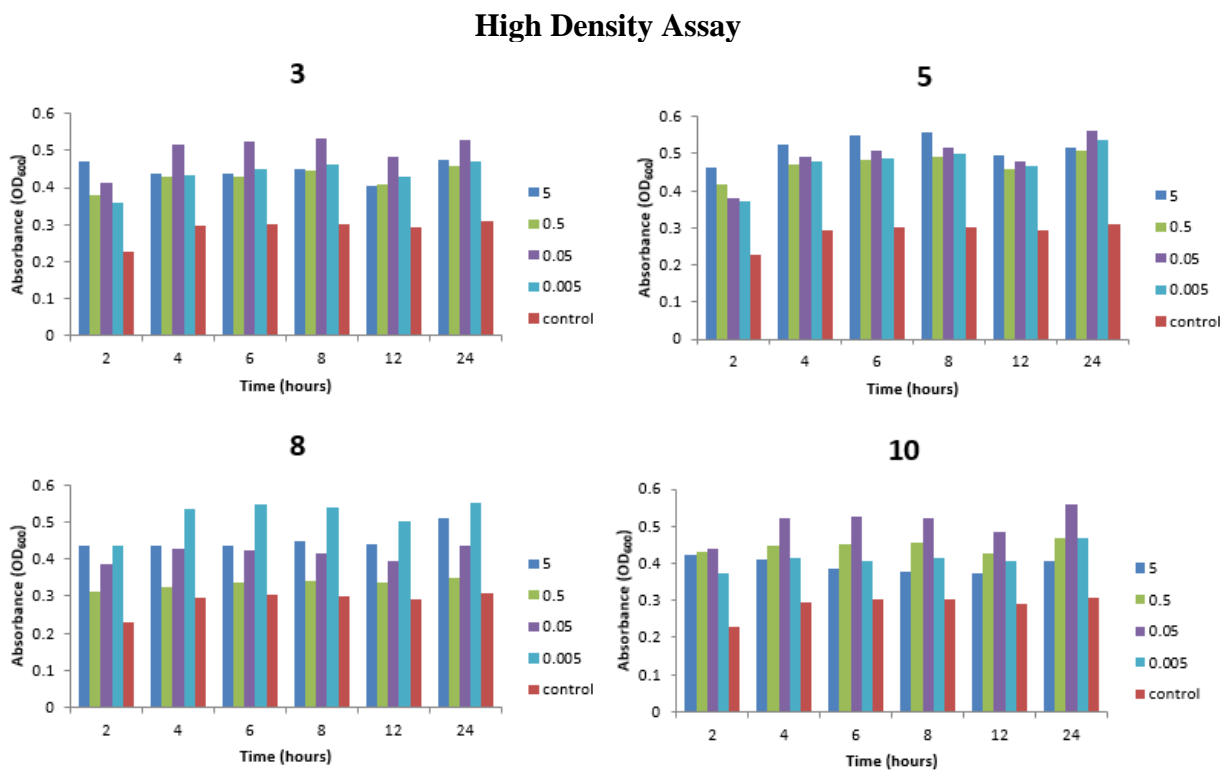


Figure 6.1 High density *E. coli* viability assay for each natural product at varying working concentrations over a 24 hour time course. No decrease in absorbance was seen in any of the cell cultures regardless of the concentration of natural product added. A DMSO control was used.

Low Density Assay

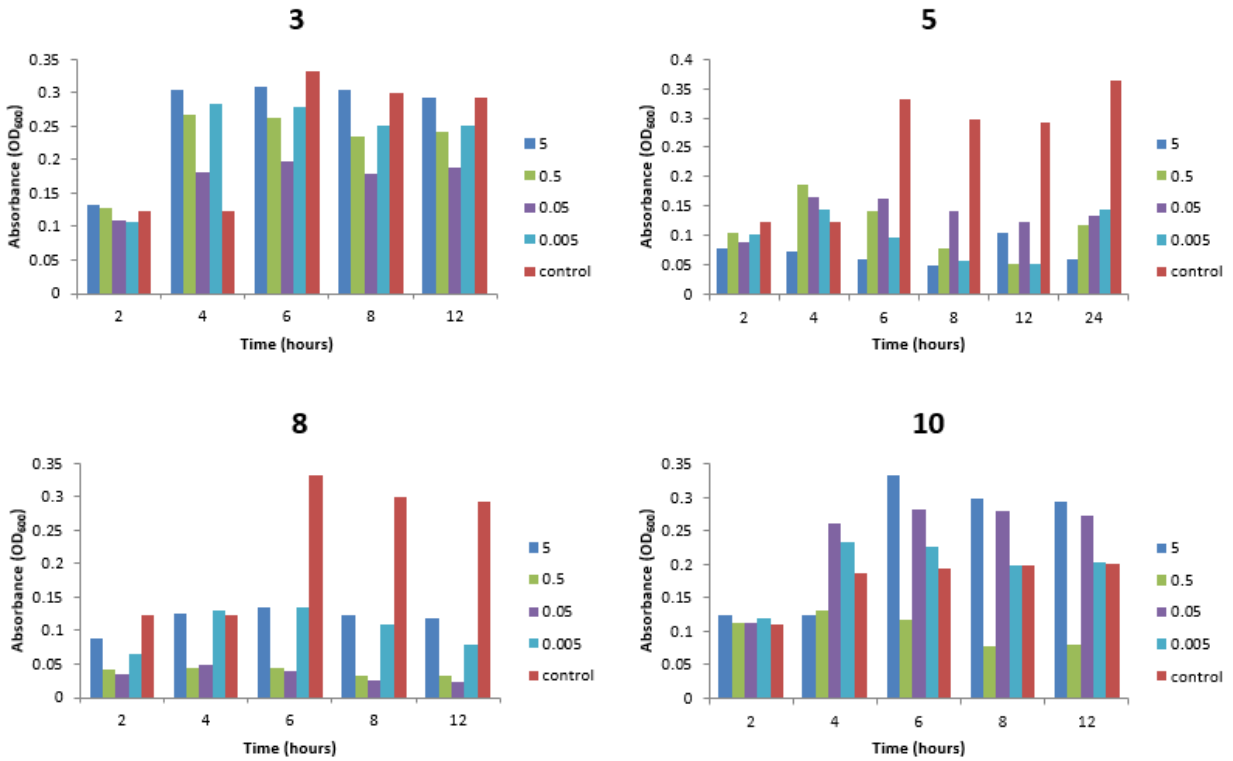


Figure 6.2 Low density *E. coli* viability assay for each natural product at varying working concentrations over a 24 hour time course. At a working concentration of 0.50 mg/mL (final concentration of 2 μ M), **5** and **8** resulted in a decreased absorbance over time. **10** resulted in a decreased absorbance over time when used at the highest concentration tested (a working concentration of 5mg/mL; final concentration 3 mM). Though addition of **3** to cell cultures did not result in decreased absorbance over time, absorbance remained relatively constant in comparison to the DMSO control.

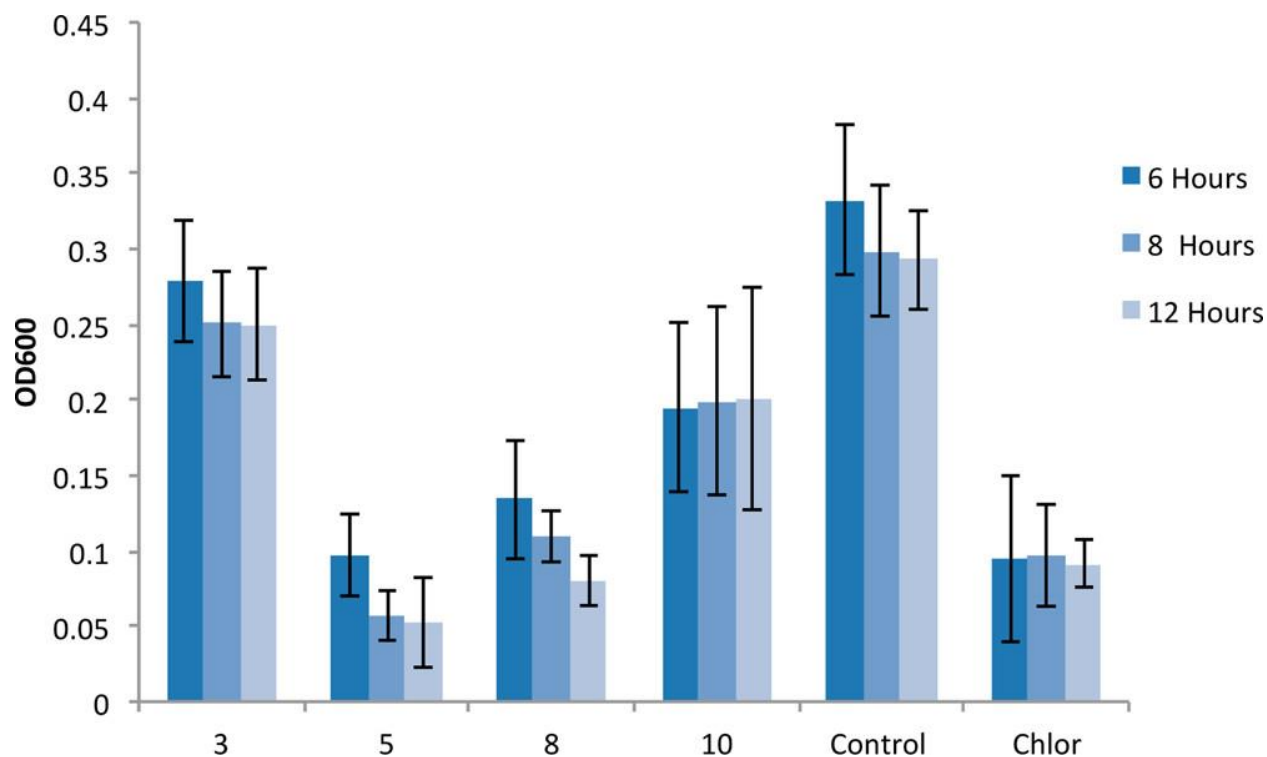


Figure 6.3 Summary of *E. coli* screens with natural products prepared via the solid-supported Glaser–Hay methodology. Cultures were inoculated at an OD₆₀₀ of 0.1 and grown in the presence of the compounds at approximately 2 μ M in a 96-well plate. The bacterial growth was monitored at 6, 8, and 12 h. A DMSO control exhibited significant culture growth, while a positive control of chloramphenicol at 0.05 mM exhibited no growth. All cultures were grown in triplicate to establish experimental error.

Conclusion

This suggests that these synthesized natural products do indeed possess antibacterial properties and can be easily prepared with the solid-supported Glaser–Hay methodology. Future work includes the use of more sophisticated bacterial assays to determine their mechanism of action and their investigation for other biological activity. Moreover, due to the modular synthesis, various analogs can be rapidly generated to conduct an extensive SAR study to further optimize their antibacterial properties. The application of the solid support also facilitates a wide range of

combinatorial strategies to be employed toward the facile generation of large and varied polyynes libraries.

Overall, we have demonstrated that the solid-supported Glaser–Hay reaction is a useful methodology in the synthesis of natural products. The methodology has been employed to access four key natural products in fewer synthetic steps, at higher yields, and with less purification. These natural products have been assessed for their antibacterial properties and found to be comparable in efficacy to traditional antibacterials such as chloramphenicol.

Experimental

General. Solvents and reagents were obtained from either Sigma-Aldrich or Fisher Scientific and used without further purification, unless noted. Tritylchloride resin, 100-200 mesh, 1% DVB crosslinking, was purchased from Advanced Chemtech. Reactions were conducted under ambient atmosphere with non-distilled solvents. NMR data was acquired on a Varian Gemini 400 MHz. GC/MS analysis was conducted on an Agilent Technologies 6890N GC system interfaced with a 5973N mass selective detector. An Agilent J&W GC capillary column (30 m length, 0.32 mm diameter, 0.25 nm film) was employed with a splitless injection (250 °C inlet, 8.8 psi) with an initial 70 °C hold (2 min) and ramped for 15 min to 230 °C. BL21 (DE3) *E. coli* were obtained from Novagen and cell growth was monitored using a BioTek Synergy HT microplate reader.

Immobilization of Alcohol onto Trityl Chloride Resin in Low Loading Conditions. Trityl chloride resin (200 mg, 0.36 mmol, 1 eq) was added to a flame dried vial charged with dichloromethane (5 mL). The resin was swelled at room temperature with gentle stirring for 15 min. Alcohol (25.0 μ L, ~1.2 eq) was added to reaction, followed by triethylamine (10.0 μ L, 0.072 mmol, 0.2 eq). The mixture was stirred at room temperature for 16 h. The resin was transferred to a syringe filter and washed with DCM and MeOH (five alternating rinses with 5 mL each). The resin was swelled in CH_2Cl_2 and dried under vacuum for 45 min before further use.

Polyne Extension Protocol. Trimethylsilylacetylene (160 μ L, 1.05 mmol, 15 eq) was added to a flame dried vial containing the alcohol derivatized trityl resin (100 mg, 0.07 mmol, 1 eq), and tetrahydrofuran (2.0 mL). The CuI (20 mg, 1.06 mmol) and tetramethylethylenediamine (20 μ L, 0.132 mmol) were added to a separate flame-dried vial then dissolved in tetrahydrofuran (2.0 mL).

The catalyst mixture was then added to the resin in one portion and stirred at 60 °C for 16 h. The resin was transferred to a syringe filter and washed with DCM and MeOH (five alternating rinses with 5 mL each). The TMS group was then cleaved by incubation in 1 M tetra-*n*-butylammonium fluoride trihydrate in DCM (TBAF, 1 mL, 1 h). Then the reaction was again transferred to a syringe filter, washed with DCM and MeOH (five alternating rinses with 5 mL each), and dried under vacuum for 45 minutes. Product was weighed and transferred to flame dried vial for future use.

Dodeca-2,4-diyne-1-ol (3). 1-Nonyne (115 μ L, 0.70 mmol, 10 eq) was added to a flame dried vial containing the propargyl alcohol derivatized trityl resin (100 mg, 0.070 mmol, 1 eq), and tetrahydrofuran (2 mL). CuI (10 mg, 0.053 mmol, ~0.7 eq) and tetramethylethylenediamine (30 μ L) were added to a separate flame-dried vial then dissolved in tetrahydrofuran (2 mL). The catalyst mixture was then added to the resin in one portion and stirred at 60 °C for 16 h. The resin was transferred to a syringe filter and washed with DCM and MeOH (five alternating rinses with 5 mL each). The product was then cleaved from the resin by treatment with 1 mL 2% TFA (DCM, 1 h), and filtered into a vial. A short silica plug was utilized to remove unreacted starting material (1:1 EtOAc/Hex) and pure product was obtained (0.010 g, 0.052 mmol, 75%). ^1H NMR (CDCl_3 , 400 MHz): δ 4.27 (s, 2H), 2.24 (t, $J = 7.2$ Hz, 2H), 1.55 (quint, $J = 7.2$ Hz, 2H), 1.39–1.31 (m, 2H), 1.30–1.19 (m, 6H), 0.90 (t, $J = 6.9$ Hz, 3H) (Figure 6.4). ^{13}C NMR (CDCl_3 , 400 MHz): $\delta = 51.7, 31.8, 29.5, 28.7, 28.1, 22.4, 19.2, 14.0$. GC: $t_{\text{R}} = 10.43$ min; MS: m/z calcd for $\text{C}_{12}\text{H}_{18}\text{O}$ [M^+]: 178.136; found: 178.092 (Figure 6.5).

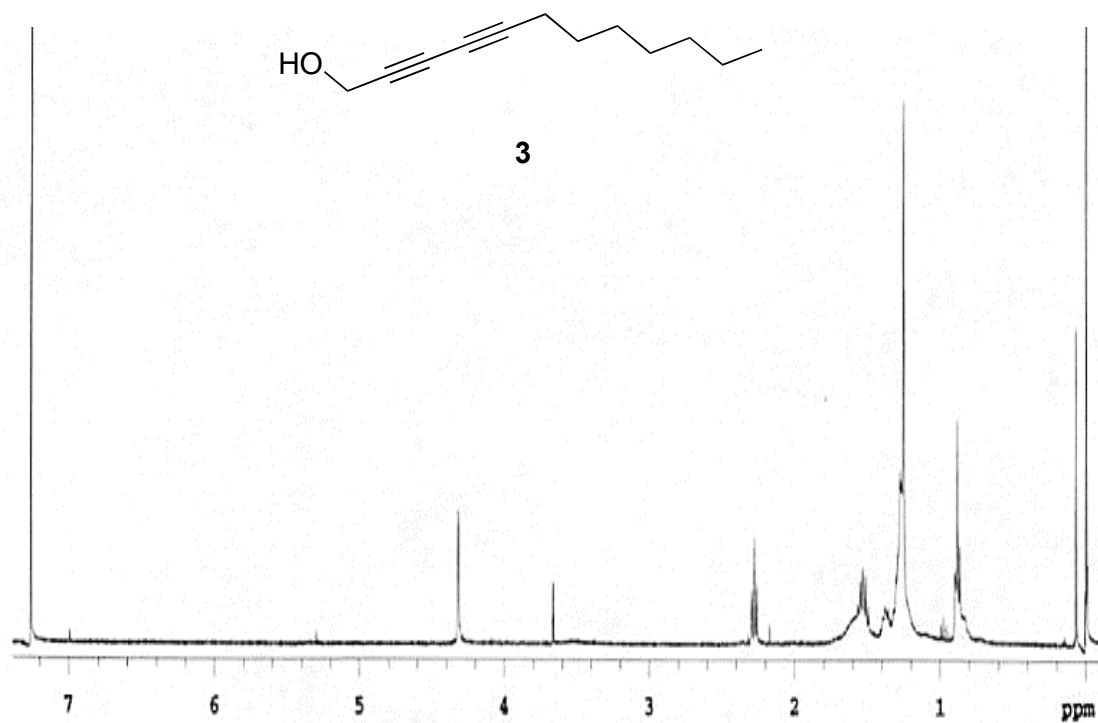


Figure 6.4 ^1H NMR of **3** in CDCl_3

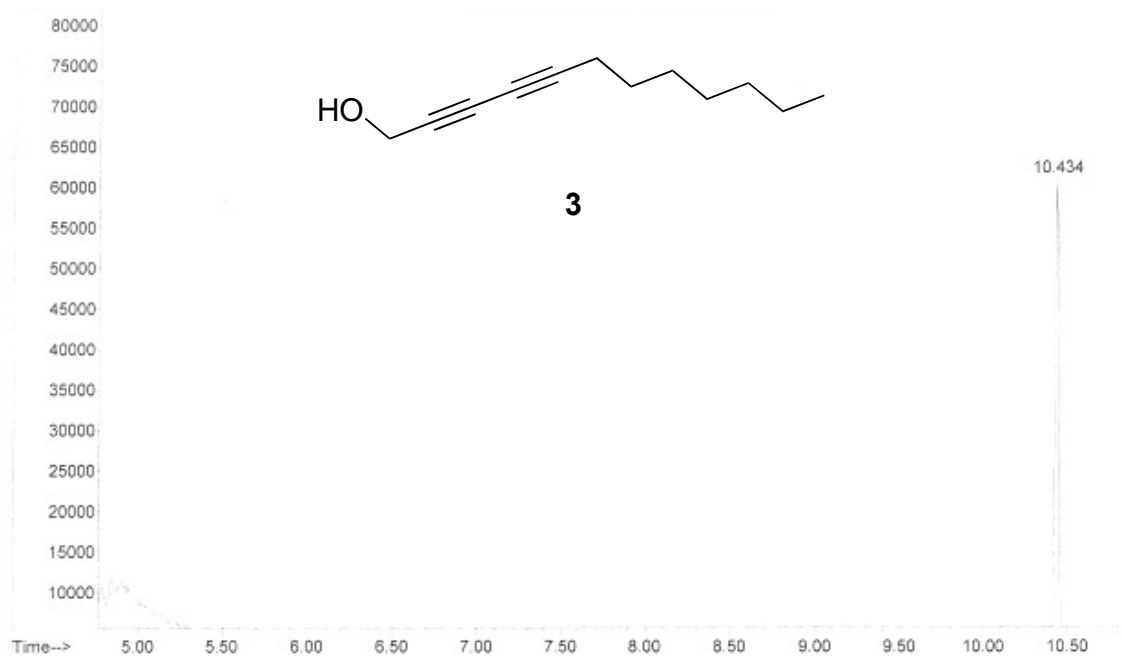


Figure 6.5 GC trace of **3**.

Montiporic Acid A (5). Ethyl bromoacetate (10 μ L, 0.1 mmol, 2 eq) was added at 10 $^{\circ}$ C to a vial containing **3** (0.010 g, 0.052 mmol, 1 eq) dissolved in toluene (1 mL), 50% KOH (200 μ L), and tetra-butyl ammonium sulfate (10 mg, 0.03 mmol, \sim 0.5 eq). The reaction was then vigorously stirred at 10 $^{\circ}$ C for 3h. Upon completion, the reaction was quenched with dilute HCl (5 mL), extracted with EtOAc, and washed with H₂O. (3x5 mL) The product was then dried over anhydrous MgSO₄ and solvent removed *in vacuo*. Purification was performed via column chromatography (hexanes:EtOAc 10:1 \rightarrow 1:3) to yield the desired product (8 mg, 0.039 mmol, 49%). ¹H NMR (CDCl₃: δ 4.38 (s, 2H), 4.21 (s, 2H), 2.24 (t, J = 7.2 Hz, 2H), 1.49 (quint, J = 7.2 Hz, 2H), 1.34–1.31 (m, 2H), 1.29–1.19 (m, 6H), 0.84 (t, J = 6.9 Hz, 3H) (Figure 6.6); ¹³C NMR (CDCl₃, 400 MHz): δ 74.5, 71.1, 64.8, 64.6, 58.0, 51.5, 4.8; GC: t_R = 11.02 min; MS: m/z calcd for C₁₄H₂₀O₃ [M⁺]: 236.141; found: 236.172 (Figure 6.7)

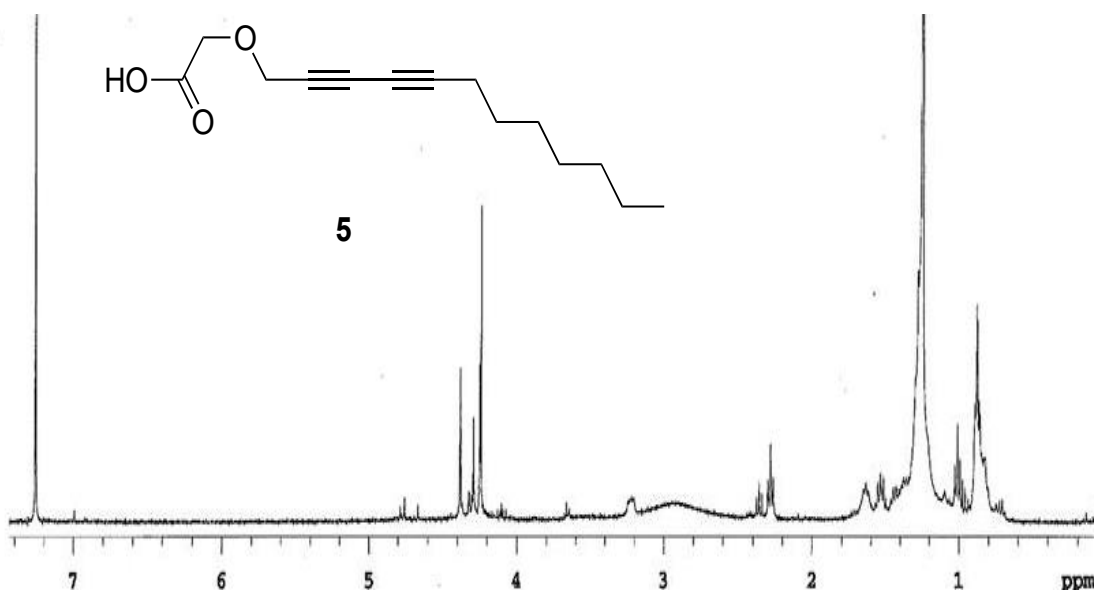


Figure 6.6 ¹H NMR of **5** in CDCl₃

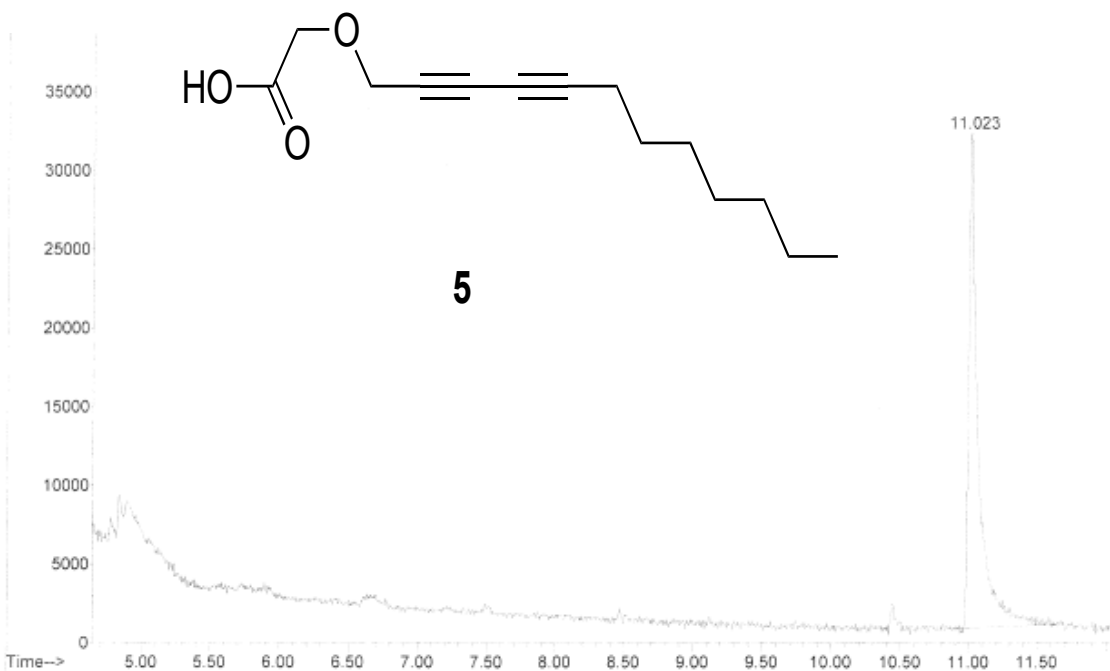


Figure 6.7 GC trace of **5**.

Octatriyn-1-ol (**8**). The previously described polyene extension protocol was used to obtain the immobilized terminal alkyne diyne. 1-Propyne (53 μ L, 0.70 mmol, 10 eq) was added to a flame dried vial containing the immobilized resin (100 mg, 0.07 mmol, 1 eq) and tetrahydrofuran (2 mL). The copper catalyst (10 mg, 0.053 mmol, \sim 0.7 eq) and tetramethylethylenediamine (30 μ L) were added to a separate flame-dried vial then dissolved in tetrahydrofuran (2 mL). The catalyst mixture was then added to the resin reaction in one portion and stirred at 60 $^{\circ}$ C for 16 h. The resin was transferred to a syringe filter and washed with DCM and MeOH (five alternating rinses with 3 mL each). The product was then cleaved from the resin by treatment with 1 mL 2% TFA (DCM, 1 h) and filtered into a vial. A short silica plug was performed to remove unreacted starting material (5:1 EtOAc/Hex), affording product **8**. (4 mg, 0.040 mmol, 68%) ^1H NMR (CDCl_3 , 400 MHz) δ 4.70 (s, br, 1H), δ = 4.34 (s, 2H), 1.96 (s, 3H) (Figure 6.8); ^{13}C NMR (CDCl_3 , 400 MHz): δ 74.2, 71.1, 65.0, 64.8, 58.4, 51.7, 4.5; GC: t_{R} = 10.99 min; MS: m/z calcd for $\text{C}_8\text{H}_6\text{O}$ [M^+]: 118.042; found: 118.051 (Figure 6.9).

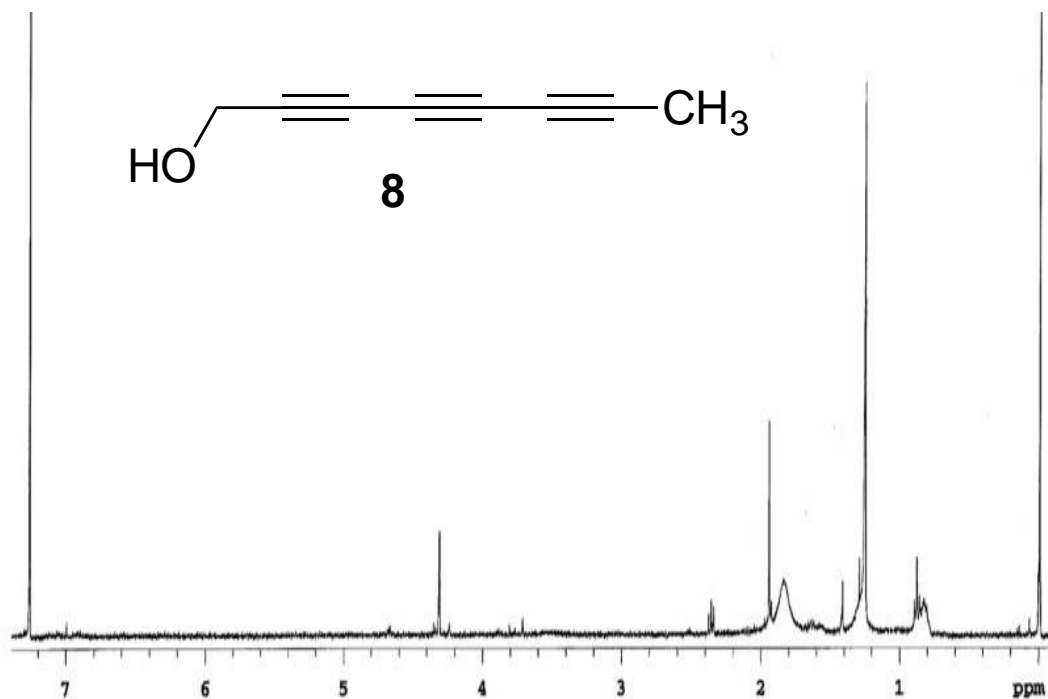


Figure 6.8 $^1\text{H NMR}$ of **8** in CDCl_3

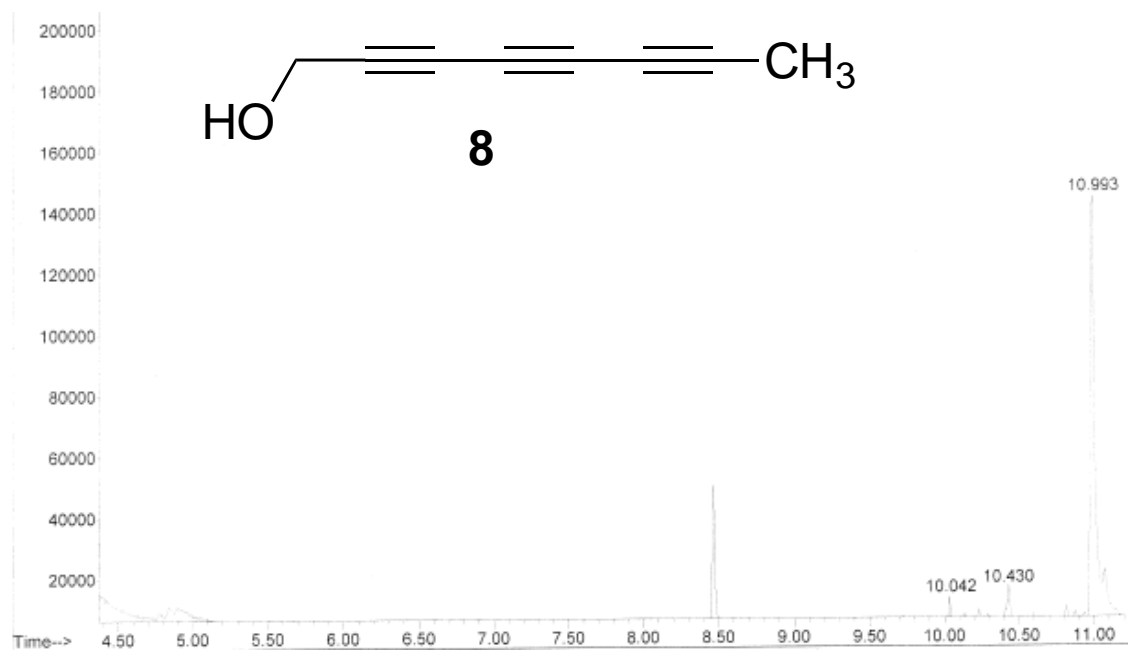


Figure 6.9 GC trace of **8**.

Phenylhepta-2,4,6-triynyl acetate (10). The previously described polyynes extension protocol was used to obtain the immobilized terminal alkyne diyne. Phenylacetylene (0.70 mmol, 10 eq) was added to a flame dried vial containing the starting material (100 mg, 0.070 mmol, 1 eq) and tetrahydrofuran (2 mL). The CuI (10 mg, 0.053 mmol) and tetramethylethylenediamine (30 μ L) were added to a separate flame-dried vial then dissolved in tetrahydrofuran (2 mL). The catalyst mixture was then added to the resin reaction in one portion and stirred at 60 °C for 16 h. The resin was transferred to a syringe filter and washed with DCM and MeOH (five alternating rinses with 5 mL each). The product was then cleaved from the resin by treatment with 1 mL 2% TFA (DCM, 1 h), and filtered into a vial. Solvent was removed *in vacuo* to afford the free alcohol (10 mg, 0.056 mmol, 80%). Acetic anhydride (1 mL) and a catalytic amount of DMAP were added and dissolved in 1 mL DCM. The reaction was allowed to stir at room temperature for 3h, followed by an extraction using DCM/H₂O (3x5 mL) and drying with MgSO₄. The product was then purified on a silica gel column using 5:1 hex:EtOAc yielding **10** (9 mg, 0.041 mmol, 46%), which was then analyzed via ¹H NMR (CDCl₃, 400 MHz): δ 7.70-7.61 (m, 2H), 7.56-7.32 (m, 3H), 4.85 (s, 2H), 2.16 (s, 3H) (Figure 6.10); ¹³C NMR (CDCl₃, 400 MHz): δ 171.0, 134.5, 131.5, 129.9, 121.2, 78.5, 76.3, 74.3, 70.8, 66.2, 63.8, 53.1, 20.9; GC: t_R = 10.89 min; MS: m/z calcd for C₁₅H₁₁O₂ [M⁺]: 222.068; found: 222.079 (Figure 6.11).

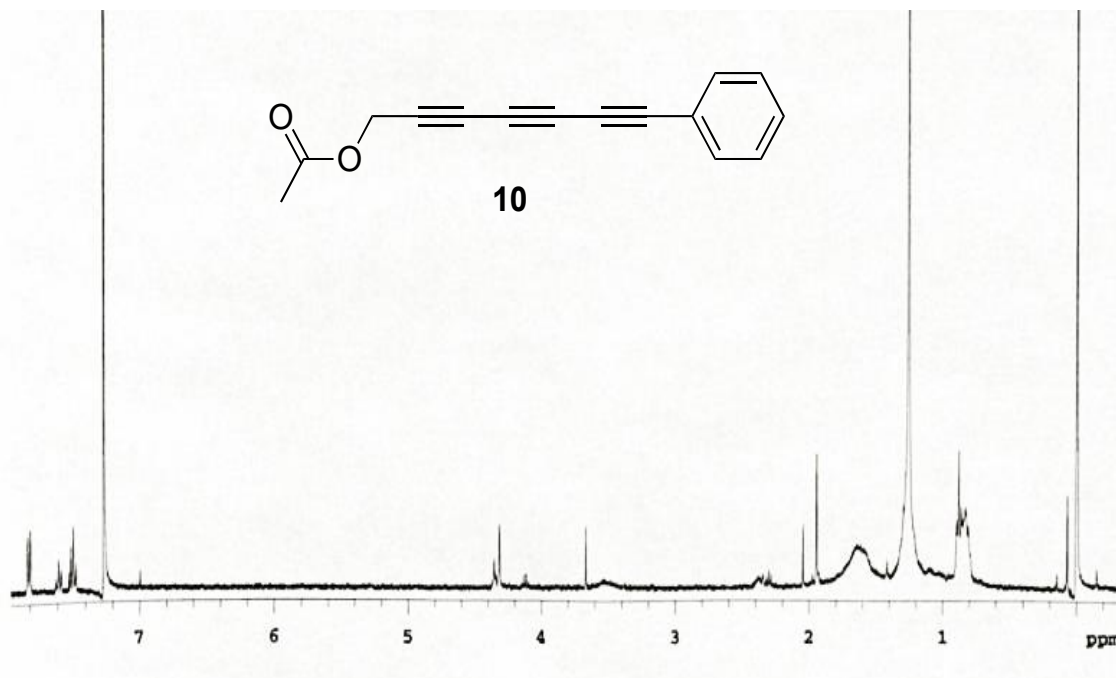


Figure 6.10 ^1H NMR of **10** in CDCl_3

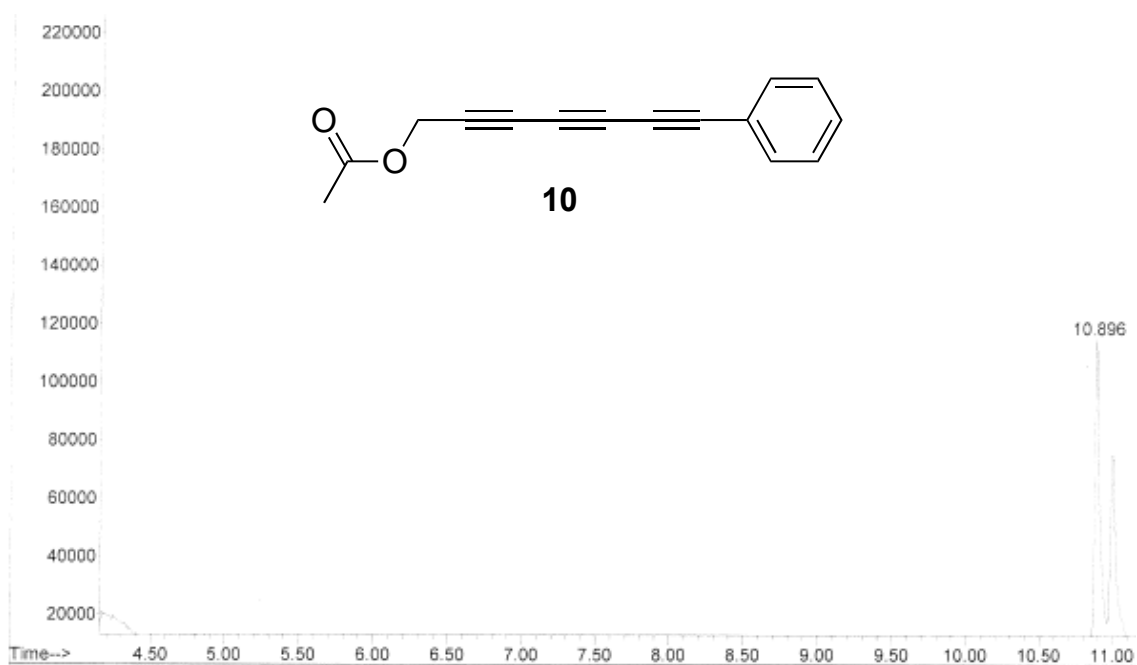


Figure 6.11 GC trace of **10**.

Preparation of Stock Solutions. Following synthesis, each natural product analog was transferred to a pre-weighed, flame dried vial. The mass of each product was noted and dimethyl sulfoxide

(DMSO) was added (between 40 to 180 μL) to create 50 mg/mL stock solutions of each product. Each solution was then transferred to eppendorf tubes and stored at $-26\text{ }^{\circ}\text{C}$.

Preparation of Working Plate. A serial dilution of the stock solution for each product was performed in order to produce working solutions with concentrations of 5, 0.5, 0.05, and 0.005 mg/mL. For each product, 15 μL of the stock solution was transferred into the well of a 96-well microplate (Greiner Bio-One). DMSO (135 μL) was subsequently added to the well to create a 5 mg/mL solution of the product. The 5 mg/mL solution (15 μL) was then pipetted into a neighboring well and DMSO (135 μL) was added to create a 0.5 mg/mL solution. This process was repeated to form the 0.05 mg/mL and 0.005 mg/mL solutions, respectively. Similarly, a serial dilution of chloramphenicol (34 mg/mL) as well as DMSO controls. The completed plate was stored at $-26\text{ }^{\circ}\text{C}$.

Low Cell Density Absorbance Assay. Luria-Bertani (LB) media (10 ml) was inoculated with *Escherichia coli* Novagen BL21 (DE3) strain of cells and then incubated for 16 h at $37\text{ }^{\circ}\text{C}$. Optical density measurements on a spectrophotometer at 600 nm (OD_{600}) were used to assess the density of the starter culture. The culture was diluted to an OD_{600} of 0.1 (low density) by addition of fresh LB media. In a new 96-well microplate (Greiner Bio-One), the solutions of varying concentration for each product from the working plate were plated including chloramphenicol and DMSO (20 μL). Subsequently, the low density cell solution was added to each well in which solution had been previously added. An initial absorbance was read using a Synergy HT Microplate Reader set to shake the plate for 10 seconds prior to reading the OD_{600} . Absorbance readings were taken again at 2, 4, 6, 8, 12, and 24 h. Between OD_{600} readings the microplate was allowed to shake at $37\text{ }^{\circ}\text{C}$.

High Cell Density Absorbance Assay. Luria-Bertani (LB) media (10 ml) was inoculated with *Escherichia coli* Novagen BL21 (DE3) strain of cells and then incubated for 16 h at 37 °C. Optical density measurements on a spectrophotometer at 600 nm (OD₆₀₀) were used to assess the density of the starter culture. The culture was diluted to an OD₆₀₀ of 1.0 (high density) by addition of fresh LB media. In a new 96-well microplate (Greiner Bio-One), the solutions of varying concentration for each product from the working plate were plated including chloramphenicol and DMSO (20 µL). Subsequently, the low density cell solution was added to each well in which solution had been previously added. An initial absorbance was read using a Synergy HT Microplate Reader set to shake the plate for 10 seconds prior to reading the OD₆₀₀. Absorbance readings were taken again at 2, 4, 6, 8, 12, and 24 h. Between OD₆₀₀ readings the microplate was allowed to shake at 37 °C.

References

1. Wong, W. J. *Inorg. Organomet. Polym. Mater.* **2005**, *15*, 197– 219.
2. Shi Shun, A. L.; Tykwinski, R. R. *Angew. Chem., Int. Ed.* **2006**, *45*, 1034– 57.
3. Lu, W.; Zheng, G.; Aisa, H.; Cai, J. *Tetrahedron Lett.* **1998**, *39*, 9521– 9522.
4. Nakayama, S.; Uto, Y.; Tanimoto, K.; Okuno, Y.; Sasaki, Y.; Nagasawa, H.; Nakata, E.; Arai, K.; Momose, K.; Fujita, T.; Hashimoto, T.; Okamoto, Y.; Asakawa, Y.; Goto, S.; Hori, H. *Bioorg. Med. Chem.* **2008**, *16*, 7705– 14.
5. Pan, Y.; Lowary, T.; Tykwinski, R. *Can. J. Chem.* **2009**, *87*, 1565– 1582.
6. Lee, Y.; Lim, C.; Lee, H.; Shin, Y.; Shin, K.; Kim, S. *Bioconjugate Chem.* **2013**, *24*, 1324– 1331.
7. Bae, B. H.; Im, K. S.; Choi, W. C.; Hong, J.; Lee, C. O.; Choi, J. S.; Son, B. W.; Song, J. I.; Jung, J. H. *J. Nat. Prod.* **2000**, *63*, 1511– 4.
8. Fusetani, N.; Toyoda, T.; Asai, N.; Matsunaga, S.; Maruyama, T. *J. Nat. Prod.* **1996**, *59*, 796– 797.
9. Coll, J.; Bowden, B.; Meehan, G.; Konig, G.; Carroll, A.; Tapiolas, D.; Alino, P.; Heaton, A.; Denys, R.; Leone, P.; Maida, M.; Aceret, T.; Willis, R.; Babcock, R.; Willis, B.; Florian, Z.; Clayton, M.; Miller, R. *Mar. Biol.* **1994**, *118*, 177– 182.
10. Doolittle, R. *Synthesis* **1984**, *1984*, 730– 732.
11. Wityak, J.; Chan, J. *Synth. Commun.* **1991**, *21*, 977– 979.
12. Fiandanese, V.; Bottalico, D.; Marchese, G.; Punzi, A. *J. Organomet. Chem.* **2005**, *690*, 3004– 3008.
13. Stefani, H.; Costa, I.; Zeni, G. *Tetrahedron Lett.* **1999**, *40*, 9215– 9217.
14. Tripp, V. T.; Lampkowski, J. S.; Tyler, R.; Young, D. D. *ACS Comb. Sci.* **2014**, *16*, 164– 7.
15. Hearn, M.; Jones, E.; Pellatt, M.; Thaller, V.; Turner, J. *J. Chem. Soc., Perkin Trans. I* **1973**, 2785– 2788.
16. Luu, T.; Shi, W.; Lowary, T.; Tykwinski, R. *Synthesis* **2005**, *2005*, 3167– 3178.

17. Lampkowski, J.; Maza, J.; Verma, S.; Young, D. *Molecules* **2015**, *20*, 5276– 5285.

CHAPTER 7: EXPLORING PROPERTIES OF POLYYNES

Introduction

Following our finding that natural products synthesized using a solid-supported Glaser-Hay methodology do indeed possess antibacterial properties, we next sought to test and expand the existing library of polyynes to elucidate novel antibacterial compounds with more potent properties.¹ In these screenings, we aimed to determine the relationship between the molecular structure of a compound and its corresponding biological activity. As in the previous chapter biological activity was quickly assessed through the use of optical density measurements to deduce cell viability at discrete time intervals. For this measurement, either the formation of clearer cell solutions over time resulting in a subsequent decrease in absorbance were taken to represent decreased cell viability, while maintained absorbance relative to an increased absorbance in the DMSO control was taken to represent cell growth inhibition. Through initial screenings, we were able to identify those compounds that were most active. Following analysis of the structure of these compounds we expanded the current library of polyynes accordingly to increase the prevalence of those moieties which were present in the most active compounds. The analysis of a structure-activity relationship enables researchers to begin to determine the chemical group responsible for a particular observed function, which in this case is anti-biological activity. By knowing what part of the molecule is useful for activity, you can then begin to identify how these compounds are achieving their antibiological properties.

Since the core conjugated acetylenic units found within the synthesized natural products may be partially responsible for biological activities found in the molecules, we aimed to diversify our library around this core structure.²⁻⁶ Using the solid-supported methodology we previously reported, a library of polyynes differing in number of conjugated acetylenic units, symmetry, and

terminal functionalities was prepared.⁷ To further explore the biological properties of the library of polyynes, the compounds were tested for antibacterial, antifungal, and anti-biofilm properties.

Similar to the sharp rise in antibiotic resistance, resistance to antifungal medications is a growing problem as some fungal infections are no longer responsive to the normal course of treatment. Of particular concern is the rise in antifungal resistance within the genus *Candida*, which can cause invasive infections which affect the blood, brain, and heart.⁸ Considering that a common infection in hospitalized patients is candidemia, a bloodstream *Candida* infection, inability to treat the infection due to increased antifungal resistance is extremely concerning. In addition to the threat of antibacterial and antifungal resistance, biofilm formation on medical equipment is a leading contributor to the occurrence of nosocomial infections.^{9,10} Biofilms have an extracellular matrix that make them particularly challenging to kill. This, coupled with increasing antibacterial resistance in biofilms, makes the removal of biofilms extremely difficult. Overall, the identification of molecules with anti-biological activity is critical in order to facilitate the creation of novel therapeutic compounds.

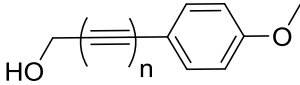
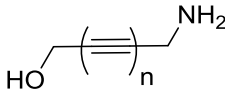
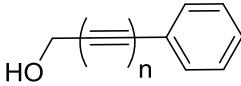
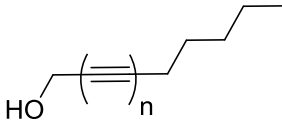
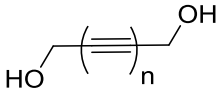
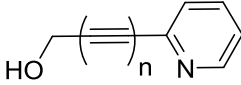
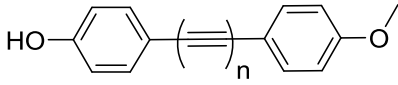
Results and Discussion

Antibacterial Screenings

I. Initial Screening

The existing library of polyynes synthesized using the solid-supported Glaser-Hay methodology was screened under low and high cell density plates in a similar fashion as described in Chapter 6 (Table 7.1).

Table 7.1 Tested Polyynes

Structure	n	Compound Number
	3	1
	4	2
	5	3
	3	4
	4	5
	5	6
	3	7
	4	8
	5	9
	3	10
	4	11
	5	12
	3	13
	4	14
	5	15
	3	16
	4	17
	5	18
	3	19
	4	20
	5	21

A 50 mg/mL stock solution was made in order for each product to be screened. A working plate was then made and each compound was diluted to 5 mg/mL. The working solution for each compound was plated in triplicate and then incubated with cell culture at either high ($OD_{600} = 4.8$) or low density ($OD_{600} = 1.0$). Absorbance readings were taken initially as well as after 2, 4, 6, 8, 12 and 24 h. After the final measurement was taken, it was compared to the initial absorbance reading to identify the most active compounds (Figure 7.1).

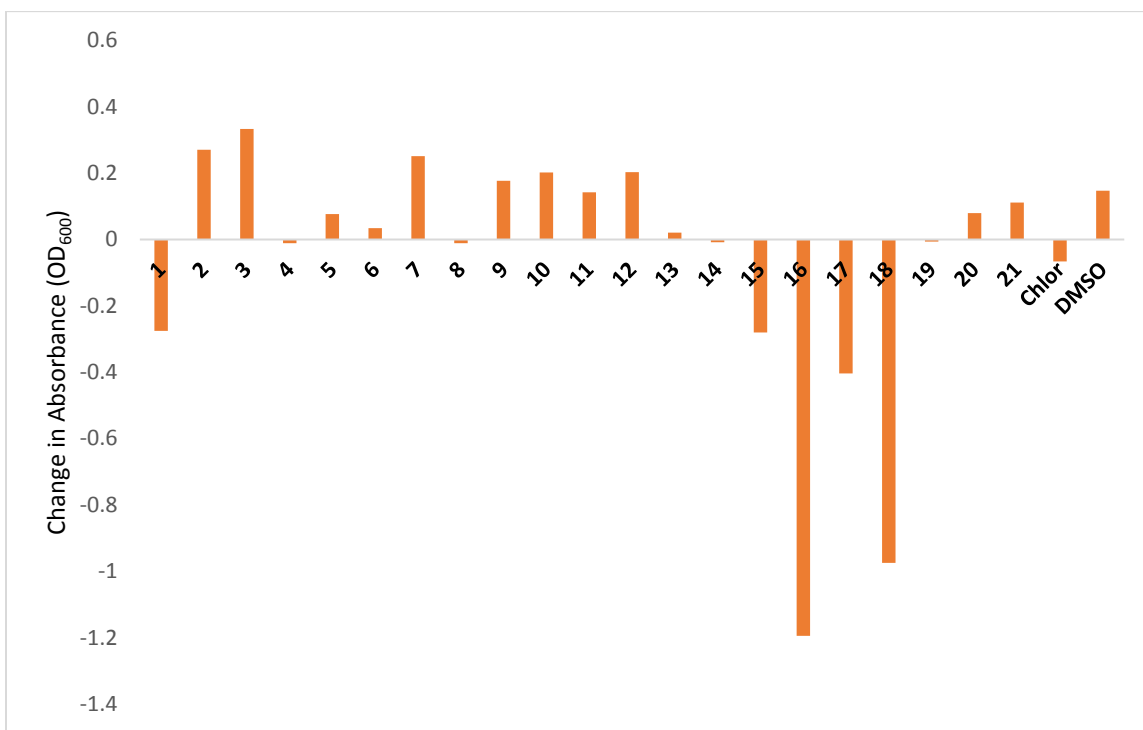


Figure 7.1 Absolute change in density relative to initial absorbance for compounds tested using a cell culture of $OD_{600} = 1$. Following a 24 h incubation period, the final absorbance for each compound was compared relative to the initial absorbance taken at time T_0 . Chloramphenicol, a well-documented antibacterial agent was used as positive control and subsequently resulted in decreased absorbance over the 24 h period, while DMSO was used as a negative control and overall cell growth was observed under this condition. Cells grown in the presence of compounds **1**, **15**, **16**, **17**, and **18** exhibited an observable decrease in absorbance.

Additionally, given the large change in absorbance seen in compounds **1**, **15**, **17**, and **18**, the activity of each compound was examined relative to the initial absorbance reading for each of the measured time points (Figure 7.2).

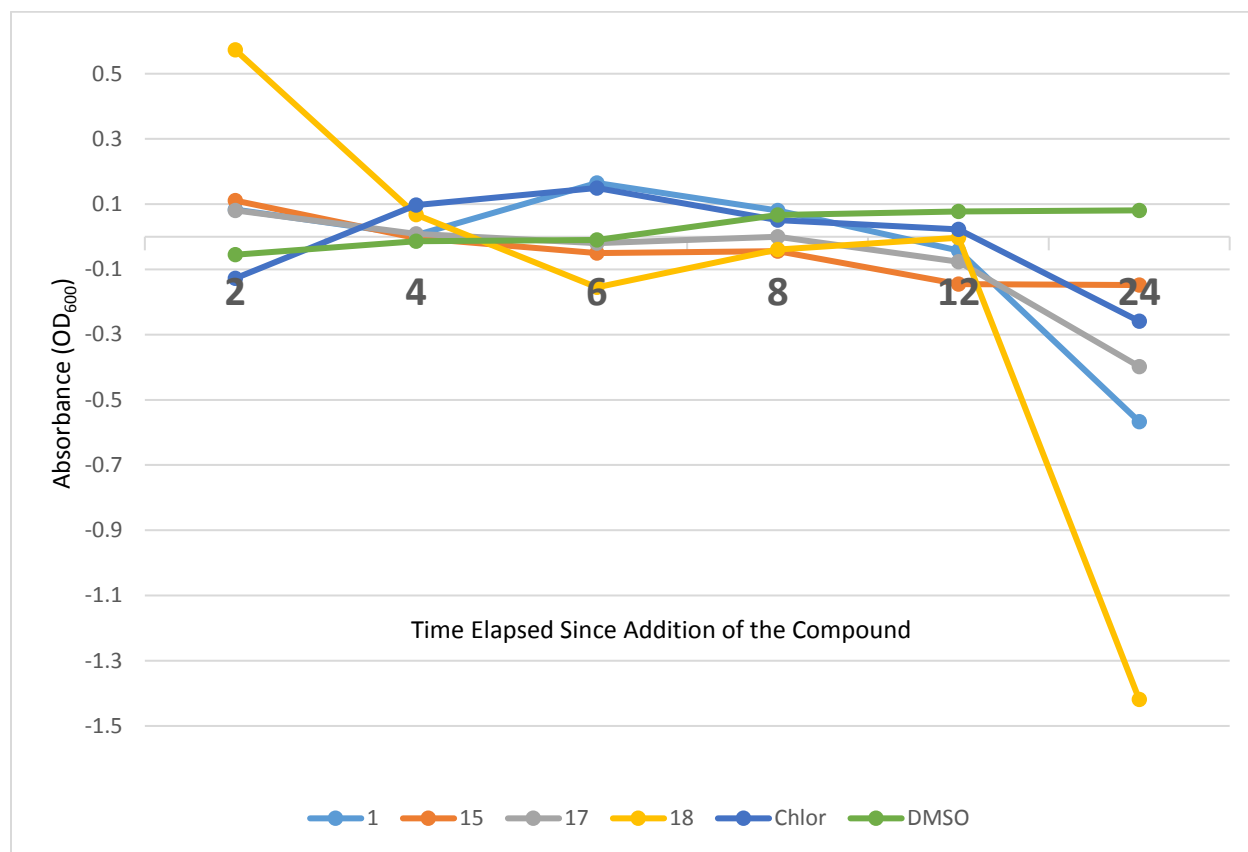


Figure 7.2 Time course that tracks the absorbance of cell treated with a 5 mg/mL solution of either compounds **1**, **15**, **17**, or **18** relative to the initial absorbance reading taken over the course of the 24 h experiment.

II. Specified Polyynes Screening

The top hit compounds identified from the initial screening were then re-screened at 5, 0.5, 0.05, and 0.005 mg/mL concentrations in both high and low cell density solutions. Absorbance readings were taken initially and after 2, 4, 6, 8, 12 and 24 h. After each reading, the absorbance was compared to the initial reading (Figure 7.3).

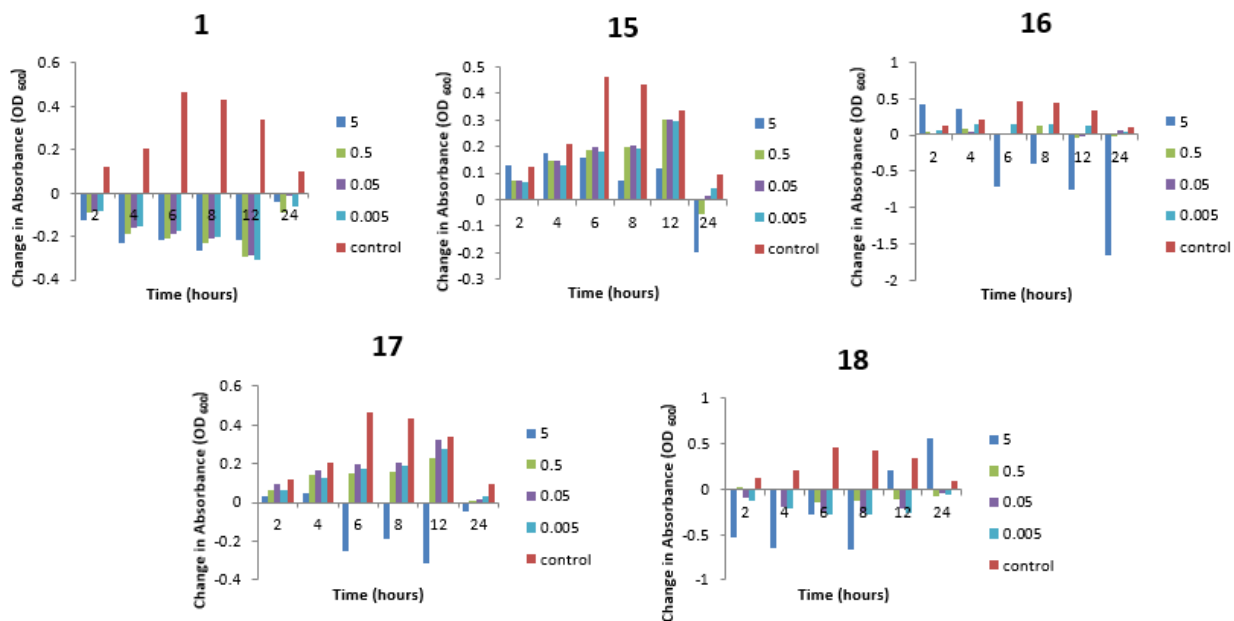
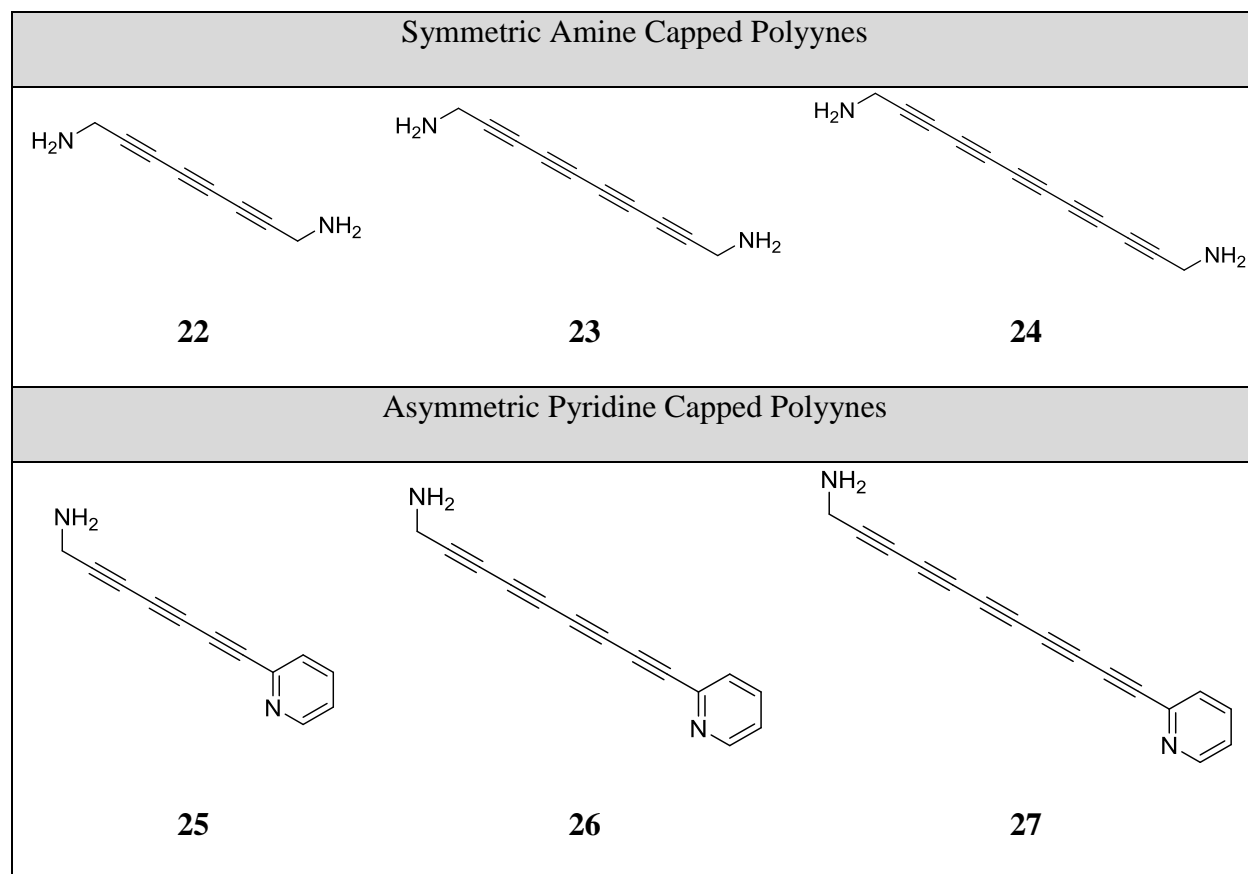


Figure 7.3 Each of the top hit compounds were tested at a range of concentrations. Each absorbance reading taken was compared to the initial absorbance reading. A decrease in absorbance over time is seen in compounds **16**, **17**, and **18** when tested at a concentration of 5 mg/mL, while a decrease in absorbance over time from all concentrations of compound **1**.

Analysis of the structures of the top hit polyynes revealed that three of the five top hit compounds possessed a terminal pyridine, which is a nitrogen-containing moiety. This prompted a second examination of the initial screenings for polyynes that possessed a nitrogen-containing terminal group. Interestingly, compounds **4**, **5**, and **6**, each of which is capped with a terminal amine group, displayed diminished growth in comparison to the other compounds tested. Given these results, we proceeded to prepare and assay a series of polyynes using an amine-derivatized resin to synthesize polyynes containing three to five conjugated triple bonds and capped with either an amine group (a symmetric polyynes) or a pyridine (an asymmetric polyynes) (Table 7.2).

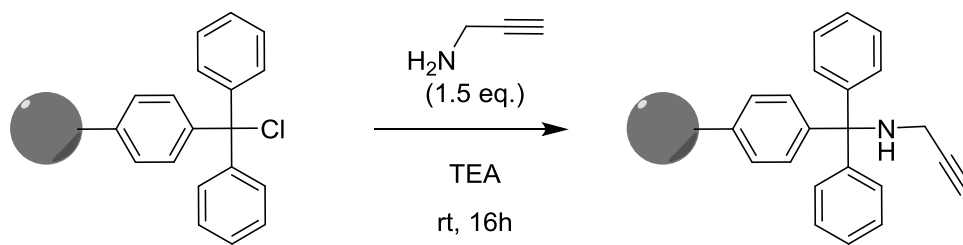
Table 7.2 Series Containing Nitrogenous Terminal Functionality to Be Synthesized



III. Synthesis of Polyynes with Nitrogenous Terminal Functionalities

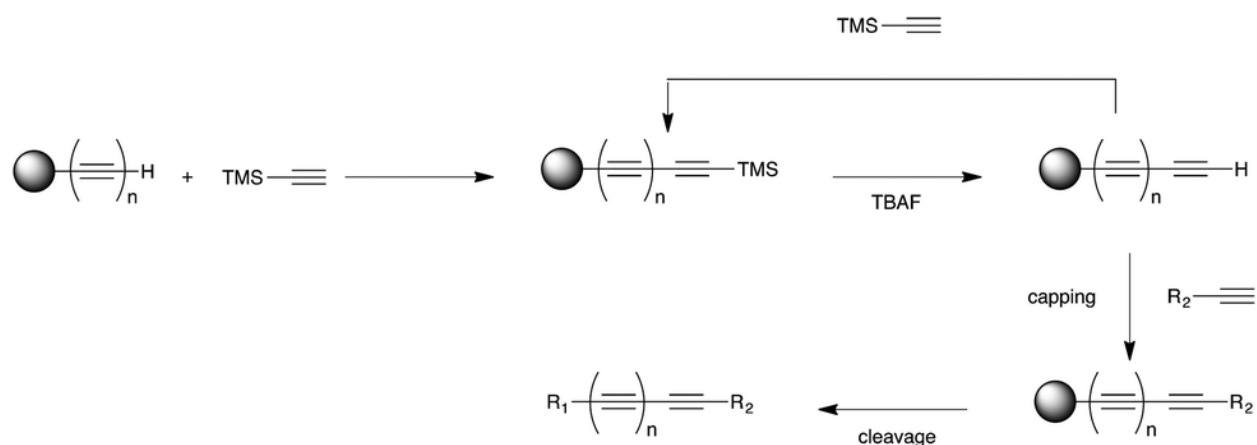
Synthesis began with derivatization of trityl chloride resin, the solid support. The resin was swelled in dichloromethane, and then propargyl amine (~1.5 eq) and triethylamine (0.2 eq) was added and stirred at room temperature for 16 h (Scheme 7.1).

Scheme 7.1 Immobilization of Propargyl Amine onto Trityl Chloride Resin



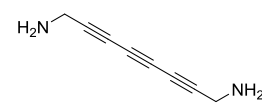
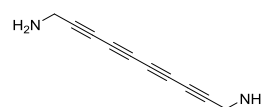
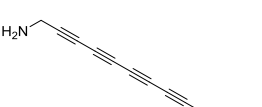
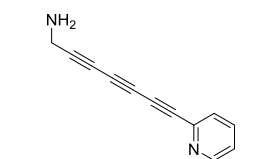
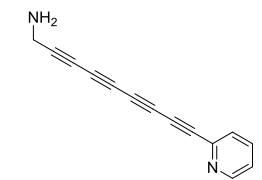
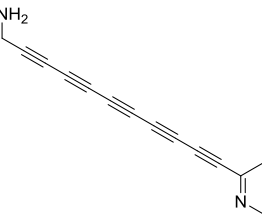
The resin was then washed with repeated DCM-MeOH cycles. Following derivitization of the resin, the acetylenic scaffold was elongated through the Glaser-Hay coupling of the immobilized resin with trimethylsilylacetylene (TMS acetylene). Following elongation, the cleavage of the TMS group can be accomplished through the addition of tetra-*n*-butylammonium fluoride (TBAF), thus restoring the terminal alkyne functionality. Either elongation can be continued through a subsequent Glaser-Hay reaction with another TMS acetylene followed by cleavage of the TMS with the addition of TBAF, or the terminal alkyne moiety can be capped through Glaser-Hay coupling with another terminal alkyne (Scheme 7.2).

Scheme 7.2 Synthetic Route to Elongation of the Acetylenic Scaffold



To synthesize the series of polyynes with nitrogenous terminal functionalities, elongation was performed on the immobilized resin 1-3 cycles, and following the cleavage of the bound terminal TMS group, the elongated structures were capped with either propargyl amine or ethynyl pyridine. A 2% TFA solution was used to cleave the molecule from the resin to obtain the desired polyynic compounds (Table 7.3).

Table 7.3 Percent Yield Following Synthesis of Polyynes with Nitrogenous Terminal Functionalities

Product	% Yield
 <p>22</p>	45%
 <p>23</p>	41%
 <p>24</p>	39%
 <p>25</p>	40%
 <p>26</p>	34%
 <p>27</p>	27%

IV. Screening Polyynes with Nitrogenous Terminal Functionalities

A 50 mg/mL stock solution of each product was made and tested at concentrations of 5, 0.5, 0.05, and 0.005 mg/mL in dense ($OD_{600} = 1.0$) and less dense ($OD_{600} = 0.01$) *E. coli* cell solutions.

Absorbance readings were taken initially and at 2, 4, 6, 8, 12 and 24 h after the addition of the polyynes. Unfortunately, screening the compounds in the series did not result in a decrease in absorbance of the cell solutions relative to the DMSO control (Figure 7.4). However, these same polyynes products could also be screened with yeast or biofilms and may exhibit other biological activity.

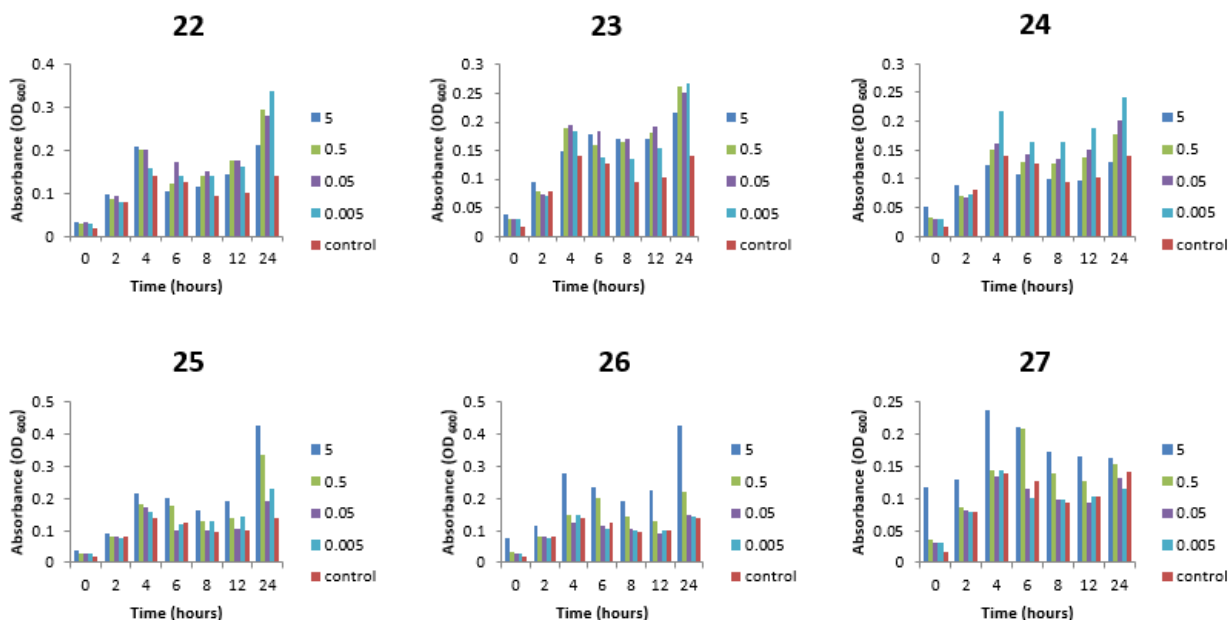


Figure 7.4 Screening of polyynes with nitrogenous terminal functionalities in *E. coli* at low cell density ($OD_{600} = 0.1$). Relative to the DMSO control, bacterial growth inhibition is not seen for any of the tested compounds.

Antifungal Screenings

We sought to expand the scope of our study to examine the antifungal properties of the previously and newly synthesized polyynes products. To do so, we performed the assay of various yeast strains at either high density (plated and allowed to grow overnight before adding the polyynes solution) or low density (polyynes solution added immediately following plating). Additionally, we also tested to see if addition of the polyynes affected the ability of the cells to re-grow following 24 h

exposure to the polyynes compound (cells from the dense plates were re-plated and allowed to inoculate new media). In these studies, fluconazole, a known antifungal agent, was used as a positive control and DMSO was used as a negative control.

I. Optimization of Assay Conditions

Initial screenings revealed that, compared to the *E. coli* cell solutions, the yeast cell solutions could not withstand as substantial an amount of DMSO (20 μ L) as the bacteria, leading to significant cytotoxicity. Therefore, optimization studies were conducted to reveal that yeast cells (200 μ L) could retain normal growth with the addition of 5 μ L or less of DMSO (2.5% DMSO by volume). To cut the amount of DMSO to one-quarter of the amount used in the *E. coli*, the working concentrations were quadrupled to 20, 2, 0.2, and 0.02 mg/mL to maintain a consistent dosage of each polyne between the bacterial and fungal trial.

II. Screens with Non-Clinical Yeast Strains

Initial screens were conducted with non-clinical yeast strains to optimize assay conditions. For these screenings, yeast strains HMY 215 and HMY 223 were used and changes in cell growth were monitored through absorbance measurements taken once an hour for 24 h.

For each of the yeast strains, polyne products were added to dense cell plates (allowed to grow overnight before addition of the polyne) and low density cells (plate immediately before addition of the polyne). The following day, 20 μ L of the dense cell culture with the added polyne solution from each well was added a well containing only fresh media. The growth of these 'regrowth' plates was then monitored for the next 24 hours via absorbance readings. Interestingly, in the less dense cell conditions differential growth was seen between both of the tested strains for each of the newly synthesized polyne (**23**, **24**, **26**, **27**) with nitrogen-containing terminal

functionalities well as **19** (Figure 7.5). This indicates that the polyynes may inhibit yeast growth and proliferation and are toxic at these concentrations.

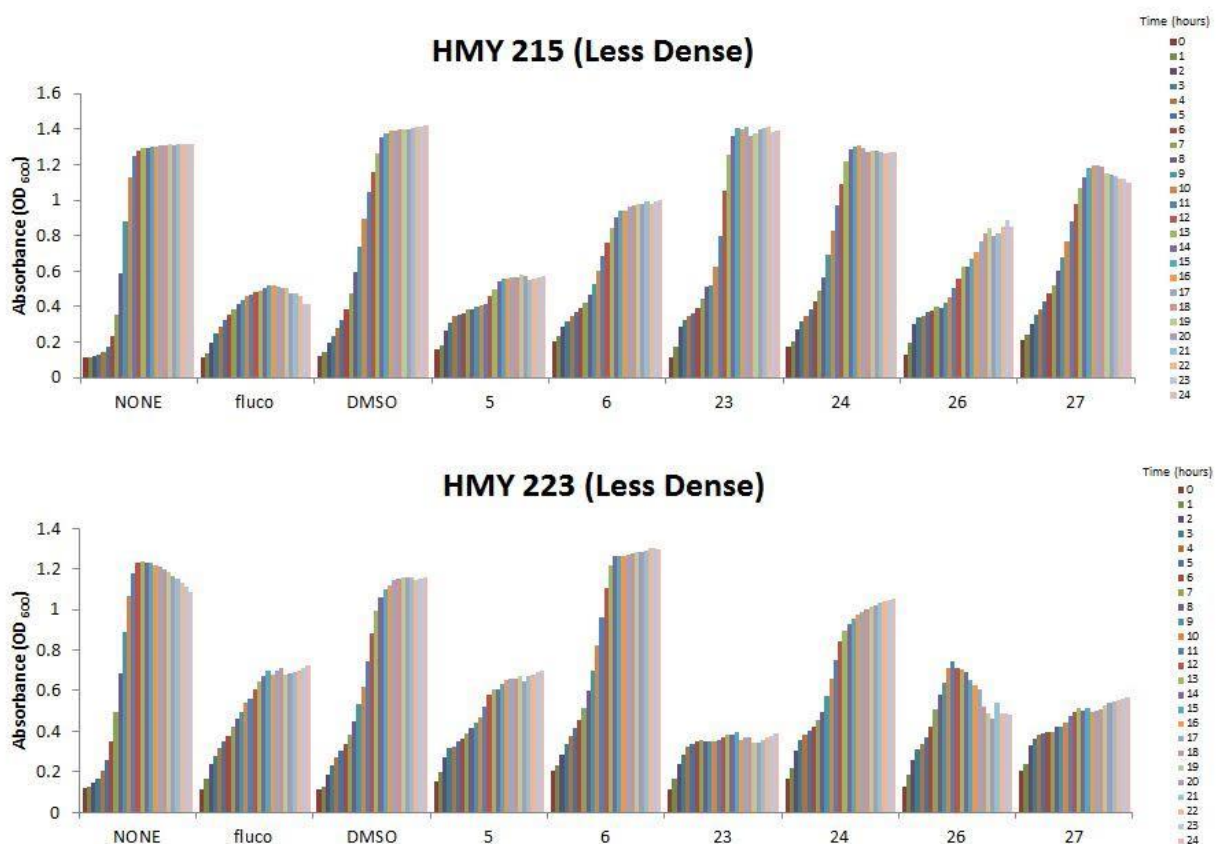


Figure 7.5 Growth curve comparisons for HMY 215 and HMY 223 in low density plates tested with various polyne products at 20 mg/mL concentration.

Additionally, differential growth was seen again in the regrowth conditions between both tested strains for each of the newly synthesized polyynes (**23**, **24**, **26**, **27**) as well as **6** (Figure 7.6). This indicates that, in the dense cultures, the cells were killed, but not lysed, and the yeast are no longer viable to inoculate new cultures. A stark difference is seen in the regrowth curves between HMY 215 and HMY 223 in response to the addition of **6**. This growth differential is of extreme interest because it indicates that the same polyne can have differing effects within yeast strains.

Through SAR studies, this result can help to inform the synthesis of yeast strain-specific compounds to selectively target a specific strain.

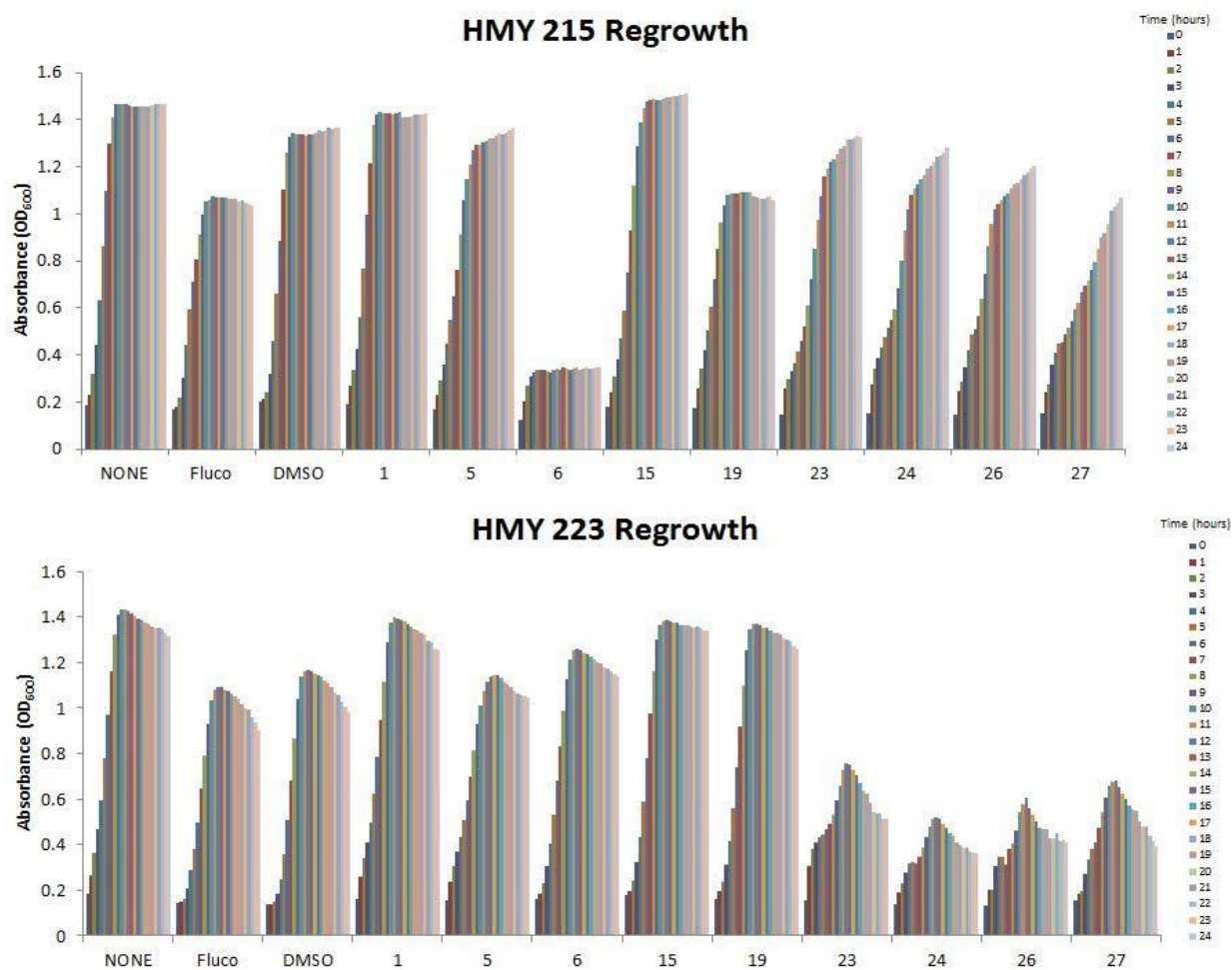


Figure 7.6 Growth curve comparisons for HMY 215 and HMY 223 tested for regrowth from dense plates to which various polyne products at 20 mg/mL concentration were administered.

Given these promising results in these non-clinical yeast strains, we proceeded to test the effectiveness of the antifungal properties of our polyne products on clinical yeast strains.

III. Screens with Clinical Yeast Strains

Following the promising screenings of the non-clinical yeast strains, we transitioned to screening HMY 127 and HMY 234, both of which are clinical yeast strains. Interestingly, when tested at a low cell density, differential growth was also seen between these two strains for various polyynes

tested, especially those with nitrogen-containing terminal functionalities (23, 24, 26, 27) (Figure 7.7).

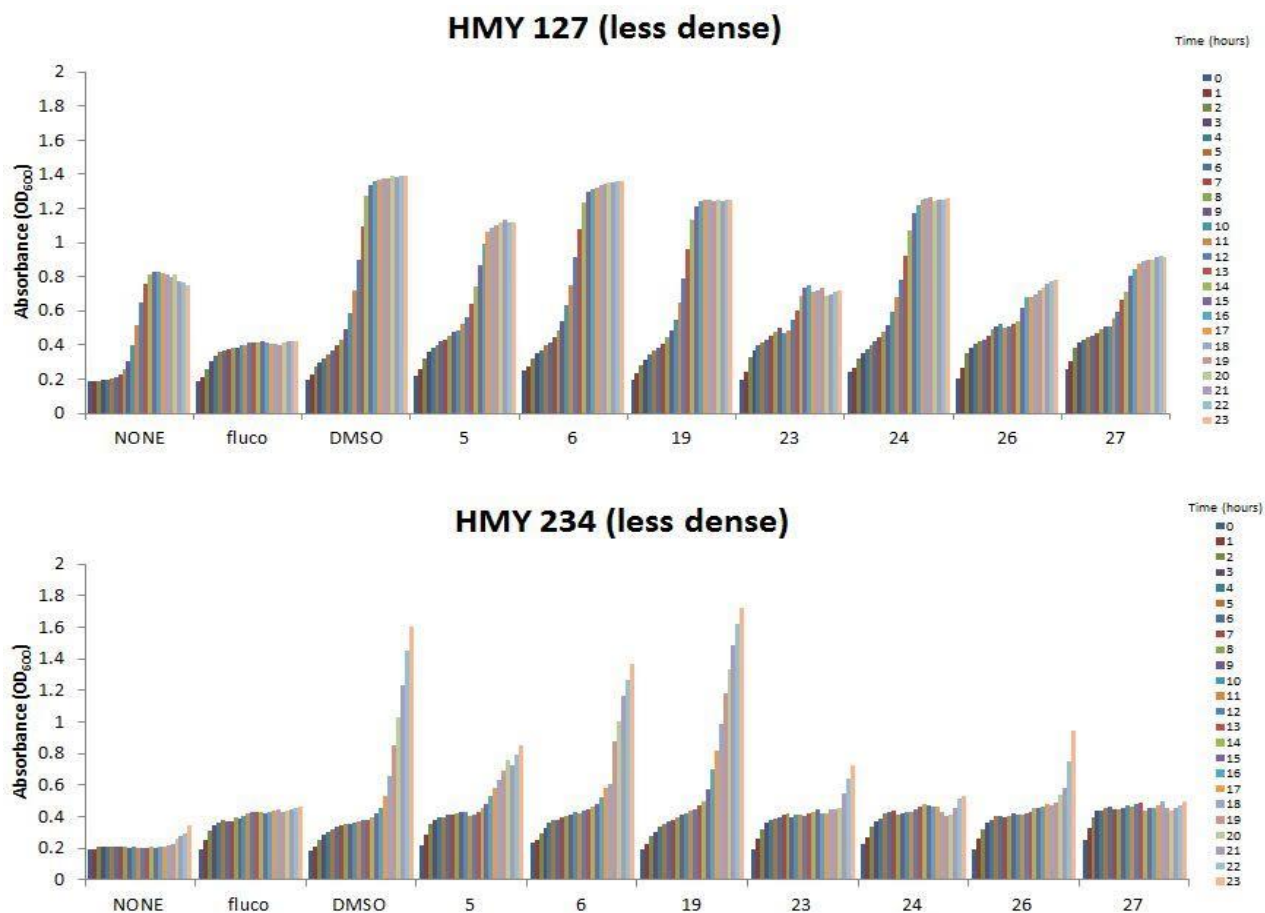


Figure 7.7 Growth curve comparisons for HMY 127 and HMY 234 in low density plates tested with various polyne products at 20 mg/mL concentration. Though the two strains exhibit different growth patterns (comparison of the DMSO condition in both), in which HMY 234 exhibits an overall slower rate of growth than HMY 127, the differential growth between the two strains is evident for 23, 24, 26, and 27. Though it appears that the presence of the those compounds alter growth in both strains relative to the DMSO control, it appears that, in HMY 234, the compounds act to inhibit further cell growth while in HMY 127 the compounds appear to slow but not inhibit growth.

IV. Future Directions

Future research should focus on re-screening the clinical strains, using the top hit compounds identified in the initial antibacterial screens. Unfortunately, depletion of the top hit compounds limited their use in the antifungal screens. However, each of the top hit polyynes have been re-synthesized. Next steps should include screening of both HMY 127 and HMY 234 at low and high cell density conditions as well as the regrowth of each yeast strain following overnight exposure to the polyynes compounds. Growth differentials between the two strains should be noted as these indicate the differing effects of the same polyynes and could be used as a building block for or inform the synthesis of a compound that could specifically target either of the yeast strains.

Anti-Biofilm Assays

Lastly, we turned to examining the effects of synthetic polyynes on the viability of biofilms. Characteristically, the bacterial macro colonies of biofilms are surrounded by an extracellular matrix (ECM).⁹ The rigid ECM not only provides support but also protects the colonies from antibacterial agents. Therefore, elucidating any effects the synthetic polyynes may have on biofilm viability is of extreme interest. The disruption of biofilms has substantial therapeutic importance as these films tend to form on medical instruments, which leads to patient infections.

A biofilm viability assay utilizes changes in absorbance to quantitatively compare biofilm growth in the presence of various synthetic polyynes. Biofilms can be inhibited by either preventing their formation or by disrupting them when they are formed. In this assay, we aim to study the former to determine whether the addition of a polyynes can alter biofilm formation. Solutions of bacterial culture and individual polyynes were grown in the wells of microtiter plates forming biofilms along the walls and sides of each well. Following overnight incubation,

unattached cells and media were removed from the wells by submerging each plate in water and staining with crystal violet solution. The wells were dried and later dissolved with a solution of acetic acid, thus permitting absorbance readings of each well to be taken and compared.

The assay was conducted using *Pseudomonas fluorescens*, a bacterium known for the formation of biofilms. *P. fluorescens* is a biosafety level 1, Gram-negative bacterium. It was employed here given its safety rating and ability to readily form biofilms.

I. Optimization of Testing Conditions

As indicated from the initial antifungal screenings, tests were needed to optimize the amount of DMSO tolerated by the organism. Cell growth and biofilm formation were best maintained when 5 μ L of DMSO was added to 100 μ L of cell solution (5% DMSO by volume). To maintain a consistent dosage of each polyynes (as was used in antibacterial and antifungal trials), working concentrations of 20, 2, 0.2, and 0.02 mg/mL were used.

II. Future Directions

Following the optimization of testing conditions, next steps should include an initial screen of our current polyynes library at a working concentration of 20 mg/mL (including the newly synthesized polyynes with nitrogen-containing terminal moieties), followed by screening of the most potent compounds diluted to different concentrations (20, 2, 0.2, and 0.02 mg/mL). SAR studies must then be completed to inform the synthesis of additional polyynes. In addition to testing the effects of polyynes on the synthesis of biofilms, regrowth studies could be conducted in which cells, following the addition of a polyynes, are incubated overnight and then re-plated to determine if the presence of the polyynes alters biofilm formation.

Conclusion

Overall, this study broadly surveyed the anti-biological properties of polyynes, specifically discussing screenings performed to assess antibacterial, antifungal, and anti-biofilm properties. Following an initial screen of the then-current library of polyynes created using a solid-supported Glaser-Hay methodology, SAR analysis was done to inform the synthesis of new polyynes structures. Like in the initial screenings, these structures were tested in *E. coli* cultures to assess antibacterial properties. Though these newly synthesized compounds have limited effects on bacterial cultures, they observably inhibited normal cell growth when tested in both the non-clinical and clinical yeast strains. Following the optimization of testing conditions in the biofilm formation assay, these new compounds can be tested to examine the effects of the polyynes on biofilm formation.

Though this screening methodology crudely attributes changes in cell viability to changes in absorbance reading, this methodology offers a preliminary analysis of the anti-biological properties of polyynes which could be more clearly elucidated through the use of Live/Dead assay kits as well as the use of cell flow cytometry

Experimental

General. Solvents and reagents were obtained from either Sigma-Aldrich or Fisher Scientific and used without further purification, unless noted. Tritylchloride resin, 100-200 mesh, 1% DVB crosslinking, was purchased from Advanced Chemtech. Reactions were conducted under ambient atmosphere with non-distilled solvents. NMR data was acquired on a Varian Gemini 400 MHz. Nonclinical *Saccharomyces cerevisiae* yeast strains HMY 215 and HMY 223 and clinical *Saccharomyces cerevisiae* strains HMY 127 and HMY 234 were prepared. *Psuedomonas fluorescens* plates were also prepared.

Immobilization of Propargyl Amine onto Trityl Chloride Resin in Low Loading Conditions. Trityl chloride resin (200 mg, 0.36 mmol, 1 eq) was added to a flame dried vial charged with dichloromethane (5 mL). The resin was swelled at room temperature with gentle stirring for 15 min. Propargyl amine (34.6 μ L, ~1.5 eq) was added to reaction, followed by triethylamine (10.0 μ L, 0.072 mmol, 0.2 eq). The mixture was stirred at room temperature for 16 h. The resin was transferred to a syringe filter and washed with DCM and MeOH (five alternating rinses with 5 mL each). The resin was swelled in DCM and dried under vacuum for 45 min before further use.

Polyyne Extension Protocol. Trimethylsilylacetylene (160 μ L, 1.05 mmol, 15 eq) was added to a flame dried vial containing the amine derivatized trityl resin (140 mg, 0.07 mmol, 1 eq) and tetrahydrofuran (2.0 mL). CuI (20 mg, 1.06 mmol) and tetramethylethylenediamine (20 μ L, 0.132 mmol) were added to a separate flame-dried vial then dissolved in tetrahydrofuran (2.0 mL). The catalyst mixture was then added to the resin in one portion and stirred at 60 °C for 16 h. The resin was transferred to a syringe filter and washed with DCM and MeOH (5 alternating rinses with 5

mL each). The TMS group was then cleaved by incubation in 1M tetra-n-butylammonium fluoride trihydrate in DCM (TBAF, 1 mL, 1 h). Then the reaction was again transferred to a syringe filter and washed with DCM and MeOH (five alternating rinses with 5 mL each) and dried under vacuum for 45 minutes. The product was then weighed and transferred to a flame dried vial for future use.

Polyyne Capping Soluble alkyne (10 eq) was added to a flame dried vial containing the desired amine derivatized trityl resin (100 mg, 0.07 mmol, 1 eq) and tetrahydrofuran (2 mL). The copper catalyst (10 mg, 0.053 mmol, ~0.7 eq) and tetramethylethylenediamine (30 μ L) were added to a separate flame-dried vial then dissolved in tetrahydrofuran (2 mL). The catalyst mixture was then added to the resin in one portion and stirred at 60 °C for 16 h. The resin was transferred to a syringe filter and washed with DCM and MeOH (five alternating rinses with 5 mL each). The product was then cleaved from the resin by treatment with 2% TFA (DCM, 1 h) and filtered into a vial.

Octa-2,4,6-triyne-1,8-diamine (22). The previously described polyynes extension protocol was used to obtain the immobilized terminal alkyne diyne and was capped with propargyl amine (45 μ L, 0.70 mmol, 10 eq) using the previously described polyynes capping protocol. ^1H NMR (400 MHz; CDCl_3): δ 3.39 (s, 4H).

Deca-2,4,6,8-tetrayne-1,10-diamine (23). The previously described polyynes extension protocol was used to obtain the immobilized terminal alkyne triyne and was capped with propargyl amine (45 μ L, 0.70 mmol, 10 eq) using the previously described polyynes capping protocol. ^1H NMR (400 MHz; CDCl_3): δ 3.39 (s, 4H).

Dodeca-2,4,6,8,10-pentayne-1,12-diamine (24). The previously described polyynes extension protocol was used to obtain the immobilized terminal alkyne tetrayne and was capped with propargyl amine (45 μ L, 0.70 mmol, 10 eq) using the previously described polyynes capping protocol. ^1H NMR (400 MHz; CDCl_3): δ 3.39 (s, 4H).

7-(pyridin-2-yl)hepta-2,4,6-triyn-1-amine (25). The previously described polyynes extension protocol was used to obtain the immobilized terminal alkyne diyne and was capped with ethynyl pyridine (71 μ L, 0.70 mmol, 10 eq) using the previously described polyynes capping protocol. ^1H NMR (400 MHz; CDCl_3): δ 8.01 (d, $J = 7.5$ Hz, 1H), 7.65 (t, $J = 7.4$ Hz, 1H), 7.32 (t, $J = 7.5$ Hz, 1H), 6.91 (d, $J = 7.4$ Hz, 1H), 3.39 (s, 2H).

9-(pyridin-2-yl)nona-2,4,6,8-tetrayn-1-amine (26). The previously described polyynes extension protocol was used to obtain the immobilized terminal alkyne triyne and was capped with ethynyl pyridine (71 μ L, 0.70 mmol, 10 eq) using the previously described polyynes capping protocol. ^1H NMR (400 MHz; CDCl_3): δ 8.01 (d, $J = 7.5$ Hz, 1H), 7.65 (t, $J = 7.4$ Hz, 1H), 7.32 (t, $J = 7.5$ Hz, 1H), 6.91 (d, $J = 7.4$ Hz, 1H), 3.39 (s, 2H).

11-(pyridin-2-yl)undeca-2,4,6,8,10-pentayn-1-amine (27). The previously described polyynes extension protocol was used to obtain the immobilized terminal alkyne tetrayne and was capped with ethynyl pyridine (71 μ L, 0.70 mmol, 10 eq) using the previously described polyynes capping protocol. ^1H NMR (400 MHz; CDCl_3): δ 8.01 (d, $J = 7.5$ Hz, 1H), 7.65 (t, $J = 7.4$ Hz, 1H), 7.32 (t, $J = 7.5$ Hz, 1H), 6.91 (d, $J = 7.4$ Hz, 1H), 3.39 (s, 2H).

Preparation of Stock Solutions. Following synthesis, each compound was transferred to a pre-weighed, flame dried vial. The mass of each product was noted and dimethyl sulfoxide (DMSO) was added to create 50 mg/mL stock solutions of each product. Each solution was then transferred to eppendorf tubes and stored at -26 °C.

Preparation of Working Plate. A serial dilution of the stock solution for each product was performed in order to produce working solutions with concentrations of 5, 0.5, 0.05, and 0.005 mg/mL. For each product, the stock solution was transferred (15 µL) into the well of a 96-well microplate (Greiner Bio-One). DMSO (135 µL) was subsequently added to the well to create a 5 mg/mL solution of the product. The 5 mg/mL solution (15 µL) was then pipetted into a neighboring well and DMSO (135 µL) was added to create a 0.5 mg/mL solution. This process was repeated to form the 0.05 mg/mL and 0.005 mg/mL solutions, respectively. Similarly, a serial dilution of *fluconazole* (12 mg/mL) was plated as well as DMSO controls. The completed plate was stored at -26 °C.

High Density Plate Preparation for Initial Bacterial Screenings. Luria-Bertani (LB) media (10mL) was inoculated with *Escherichia coli* Novagen BL21 (DE3) strain of cells and then incubated for 16 h at 37 °C. Optical density measurements on a spectrophotometer at 600 nm (OD₆₀₀) was used to assess the density of the starter culture. In a new 96-well microplate (Greiner Bio-One), 5 mg/mL solutions of each compound were plated including chloramphenicol and DMSO (20 µL). The cell culture was not diluted (OD₆₀₀ of 4.8) and added directly to each of the wells in which compounds had been previously added. An initial absorbance was read using a Synergy HT Microplate Reader set to shake the plate for 10 seconds prior to reading the OD₆₀₀. An absorbance

reading was taken again at 2, 4, 6, 8, 12, and 24 h. Between OD₆₀₀ readings the microplate was allowed to shake at 37 °C.

Low Density Plate Preparation for Initial Bacterial Screenings. Luria-Bertani (LB) media (10 mL) was inoculated with *Escherichia coli* Novagen BL21 (DE3) strain of cells and then incubated for 16 h at 37 °C. Optical density measurements on a spectrophotometer at 600 nm (OD₆₀₀) was used to assess the density of the starter culture. The culture was diluted to an OD₆₀₀ of 1.0 (low density) by addition of fresh LB media. In a new 96-well microplate (Greiner Bio-One), 5 mg/mL solutions of each compound were plated including chloramphenicol and DMSO (20 µL). Subsequently, the low density cell solution was added to each well in which solution had been previously added. An initial absorbance was read using a Synergy HT Microplate Reader set to shake the plate for 10 seconds prior to reading the OD₆₀₀. An absorbance reading was taken again at 2, 4, 6, 8, 12, and 24 h. Between OD₆₀₀ readings the microplate was allowed to shake at 37 °C.

High Density Plate Preparation for Screening for Top Hits and Newly Synthesized Polyynes. Luria-Bertani (LB) media (10 mL) was inoculated with *Escherichia coli* Novagen BL21 (DE3) strain of cells and then incubated for 16 h at 37 °C. Optical density measurements on a spectrophotometer at 600 nm (OD₆₀₀) was used to assess the density of the starter culture. The culture was diluted to an OD₆₀₀ of 1.0 (high density) by addition of fresh LB media. In a new 96-well microplate (Greiner Bio-One), the solutions of varying concentration for each product from the working plate were plated including chloramphenicol and DMSO (20 µL). Subsequently, the low density cell solution was added to each well in which solution had been previously added. An initial absorbance was read using a Synergy HT Microplate Reader set to shake the plate for 10

seconds prior to reading the OD₆₀₀. An absorbance reading was taken again at 2, 4, 6, 8, 12, and 24 h. Between OD₆₀₀ readings the microplate was allowed to shake at 37 °C.

Low Density Plate Preparation for Screening for Top Hits and Newly Synthesized Polyynes.

Luria-Bertani (LB) media (10 mL) was inoculated with *Escherichia coli* Novagen BL21 (DE3) strain of cells and then incubated for 16 h at 37 °C. Optical density measurements on a spectrophotometer at 600 nm (OD₆₀₀) was used to assess the density of the starter culture. The culture was diluted to an OD₆₀₀ of 0.1 (low density) by addition of fresh LB media. In a new 96-well microplate (Greiner Bio- One), the solutions of varying concentration for each product from the working plate were plated including chloramphenicol and DMSO (20 µL). Subsequently, the low density cell solution was added to each well in which solution had been previously added. An initial absorbance was read using a Synergy HT Microplate Reader set to shake the plate for 10 seconds prior to reading the OD₆₀₀. An absorbance reading was taken again at 2, 4, 6, 8, 12, and 24 h. Between OD₆₀₀ readings the microplate was allowed to shake at 37 °C.

High Density Plate Preparation for Yeast Screenings. Yeast cultures were prepared in a 96-well microplate (Greiner Bio-One) and allowed to grow overnight at 30 °C. Subsequently, the solutions of varying concentration for each product from the working plate were added including fluconazole and DMSO (5 µL). An initial absorbance was read using a Synergy HT Microplate Reader set to shake the plate for 10 seconds prior to reading the OD₆₀₀. Absorbance readings were taken again at 2, 4, 6, 8, 12, and 24 h. Between OD₆₀₀ readings the microplate was allowed to shake at 30 °C.

Low Density Plate Preparation for Yeast Screenings. Yeast cultures were prepared in a 96-well microplate (Greiner Bio-One). Immediately following cell preparation, the solutions of varying concentration for each product from the working plate were added including fluconazole and DMSO (5 μ L). An initial absorbance was read using a Synergy HT Microplate Reader set to shake the plate for 10 seconds prior to reading the OD₆₀₀. An absorbance reading was taken again at 2, 4, 6, 8, 12, and 24 h. Between OD₆₀₀ readings, the microplate was allowed to shake at 30 °C.

Regrowth Plate Preparation for Yeast Screenings. In a new 96-well microplate (Greiner Bio-One) each well was plated with 200 μ L of yeast extract peptone dextrose (YPD). Immediately following the 24 h absorbance reading of the high density plate, 2 μ L of cell solution was transferred from the corresponding well on the new plate inoculating it. An initial absorbance was read using a Synergy HT Microplate Reader set to shake the plate for 10 seconds prior to reading the OD₆₀₀. Absorbance readings were taken again at 2, 4, 6, 8, 12, and 24 h. Between OD₆₀₀ readings, the microplate was allowed to shake at 30 °C.

Biofilm Screening Protocol. The previously published biofilm assay protocol by George O'Toole was translated to screening the polyynes compounds.⁹ *Pseudomonas fluorescens* was streaked and grown on blood agar overnight at 37 °C. One colony was then used to inoculate LB media (4 mL) and following overnight incubation at 37 °C was utilized according to the previously described protocol. The overnight culture was diluted into fresh M63 minimal media for biofilm assays (1:100) and 100 μ L of the diluted cell culture was added to each well of a 96-well plate to which 5 μ L of polyynes solution had already been added. Following overnight incubation, unattached cells not a part of the biofilm were dumped out and removed by submerging the plate in water. Then,

125 μ L of a 0.1% crystal violet solution in water was added to each well of the 96-well plate and incubated at room temperature for 10-15 minutes. The plate was then rinsed by submerging it in water and blotted on a stack of paper towels. The plate was then flipped upside down and left to dry overnight. To quantify the biofilm, 125 μ L of 30% acetic solution in water was added to solubilize the crystal violet and incubated for 10-15 minutes at room temperature. Then 125 μ L of the solubilized CV was transferred to a new 96-well plate and an optical density measure was taken at 550 nm (OD_{550}). The 30% acetic acid solution was also plated as a blank. Absorbance readings were standardized using the 30% acetic acid absorbance reading and compared relative to the DMSO control (negative control) and the chloramphenicol control (positive control).

References

1. Lampkowski, J. S., Uthappa, D. M., Halonski, J. F., Maza, J. C., & Young, D. D. *J. Org. Chem.*, **2016**, *81* (24), 12520–12524.
2. Lu, W.; Zheng, G.; Aisa, H.; Cai, J. *Tetrahedron Lett.* **1998**, *39*, 9521– 9522.
3. Nakayama, S.; Uto, Y.; Tanimoto, K.; Okuno, Y.; Sasaki, Y.; Nagasawa, H.; Nakata, E.; Arai, K.; Momose, K.; Fujita, T.; Hashimoto, T.; Okamoto, Y.; Asakawa, Y.; Goto, S.; Hori, H. *Bioorg. Med. Chem.* **2008**, *16*, 7705– 14.
4. Pan, Y.; Lowary, T.; Tykwinski, R. *Can. J. Chem.* **2009**, *87*, 1565– 1582.
5. Lee, Y.; Lim, C.; Lee, H.; Shin, Y.; Shin, K.; Kim, S. *Bioconjugate Chem.* **2013**, *24*, 1324–1331.
6. Bae, B. H.; Im, K. S.; Choi, W. C.; Hong, J.; Lee, C. O.; Choi, J. S.; Son, B. W.; Song, J. I.; Jung, J. H. *J. Nat. Prod.* **2000**, *63*, 1511– 4.
7. Lampkowski, J.S.; Durham, C.E.; Padilla, M.S.; Young, D.D.; "Preparation of Asymmetrical Polyynes by a Solid-Supported Glaser-Hay Reaction." *Org. Biomol. Chem.* **2015**, *13*, 424-427.
8. US Dept. of Health and Human Services. **2014**, *CDC. Atlanta, GA* .
9. O'Toole, George A. *J. Vis. Exp.* **2011**, *47*, 2437.
10. Bryers, J. D. *Biotechnology and Bioengineering.* **2008**, *100*(1), 1–18.